Chapter 6
Genetic Analysis of Main Physiological and Morphological Traits

Abstract Wheat physiological and morphological traits are the most important traits for wheat (*Triticum aestivum* L.) yield. In this chapter, quantitative trait loci (QTL) mapping for physiological traits including photosynthetic Characters, microdissection characteristics of Stem, heading date and cell membrane permeability of leaf, and for morphological traits of containing root-related traits and leaf-related traits were analyzed in different environments using the DH population, RIL population or natural population. Photosynthesis related traits of wheat were mapped under field and phytotron environments, respectively. Eight additive QTLs and three pairs of epistatic QTLs for chlorophyll were detected in field environments and 17 additive QTLs for conferring photosynthesis and its related traits were identified in phytotron environments. Furthermore, 18 additive loci for dry matter production (DMA) and Fv/Fm were detected. For microdissection characteristics of wheat stem, a total of 12 QTLs controlling anatomical traits of second basal internode on chromosomes 1B, 4D, 5B, 5D, 6A and 7D, and 20 additive QTLs for anatomical traits of the uppermost internode on chromosomes 1A, 1B, 2A, 2D, 3D, 4D, 5D, 6A, 6D and 7D were detected based on DH population. Two additive QTLs on chromosomes 1B and 5D in DH population, five additive QTLs on chromosomes 3B, 5B, 6A, 6B and 7D in RIL population derived from the cross of Nuomai 1 × Gaocheng 8901 and 12 additive QTLs on chromosomes 1A, 1B, 4B, 6A and 6B based on a RIL population derived from the cross of Shannong 01-35 × Gaocheng 9411 were identified for heading date. For cell membrane permeability of leaf, a total of 21 additive QTLs were detected on chromosomes 1B, 2A, 3A, 3B, 5B, 6A, 6B, 6D, 7B and 7D, respectively in three different environments based on a DH population. Seven additive QTLs and 12 pairs of epistatic QTLs for root-related traits were mapped on chromosomes 1A, 1D, 2A, 2B, 2D, 3A, 3B, 5D, 6D and 7D using IF_2 population derived from Huapei 3 × Yumai 57.31 additive QTLs and 22 pairs of epistatic QTLs conferring leaf morphology were detected based on a DH population. Finally, by genome-wide association analysis with a natural population derived from the founder parent Aimengniu and its progenies, 61 marker-trait associations (MTAs) involving 46 DArT markers distributed on 14 chromosomes (1B, 1D, 2A, 2B, 2D, 3A, 3B, 4A, 5B, 6A, 6B, 6D, 7A and 7B) for leaf-related traits were identified and the R^2 ranges from 0.1 to 16.4 %. These results provide a

J. Tian et al., *Genetic Analyses of Wheat and Molecular Marker-Assisted Breeding, Volume 1*, DOI 10.1007/978-94-017-7390-4_6

better understanding of the genetic factors for wheat physiological and morphological traits and facilitate marker-assisted selection strategy in wheat breeding.

Keywords Physiological traits · Morphological traits · Photosynthetic characters · Dry matter production · Microdissection characteristics · Heading date · Cell membrane permeability · Root traits · Leaf-related traits · QTL mapping

Wheat physiological and morphological traits are closely related to yield. From a physiological point of view, yield potential is the general performance for assimilates from unit photosynthesis furthest transfer to harvest organs. Final yield is formed by comprehensive coordination of source–sink translocation, that is to say the coordination among the accumulating rate of photosynthate, the distributing ability to grain, duration of distribution, and the turnover capacity of assimilates which stored in stem, leaf, and sheath. The production and transport of photosynthate product has direct relationships with aboveground plant type a leaf type and underground root. Therefore, for the improvement of wheat physiological trait, root, overground plant morphology, and plant anatomy features are considered in the first place, meanwhile several traits are related to photosynthetic characteristics, i.e., canopy structure, light-intercepting capability, photosynthetic capacity, and the storage and turnover capacity of carbohydrate. Hence, this chapter will connect physiological traits with morphological traits of wheat to discuss.

Most of the physiological traits are quantitative characters, which are controlled by multiple genes and easily affected by environmental conditions. So, genetic analyses of wheat physiological traits are started from QTL mapping and then discussed the number of genes, gene effect, and interaction effect. For example, for wheat root, researchers always focus on QTL analysis under abiotic stress; for photosynthetic characteristics, researchers always focus on QTL analysis of photoelectric energy conversion system, chlorophyll, fluorescence parameter, photosynthetic rate, stomatal conductance, flag leaf senescence, etc. Although QTL analysis of physiological traits has made good progress, but these results are difficult to be used for genetic improvement of wheat, because phenotypic determination of physiological traits has more difficulty in multi-year and multisite trails; moreover, mechanism of QTLs and those interaction effects are further complications when comparing to yield trait. These QTLs results have few direct applications in wheat genetic improvement. Hence, genetic analysis of physiological traits is needed to be deeper researched, in order to obtain molecular markers for improving wheat physiological traits, and then speed up the genetic improvement of physiological character and enhance yield and quality of wheat.

6.1 QTL Mapping of Photosynthetic Characters in Wheat

Photosynthesis is closely related to crop yield. The purpose of agricultural production is to enhance photosynthesis of crop, accumulate more organics, and then increase yield, according to various agricultural technical measures.

Hence, photosynthesis is the basis of enhancing crop yield, while breeding varieties with high photosynthetic efficiency is an important approach to improve crop yield. Researches related to QTLs analysis of physiological traits in rice (Nagata et al. 2002); soybean, sorghum (Ritter et al. 2008); barley (Guo et al. 2008); maize (Hund et al. 2005; Leipner et al. 2008; Pelleschi et al. 2006); cotton, and sunflower, etc., were conducted. However, similar researches for wheat (*Triticum aestivum* L.) are relatively few. The recent development of molecular markers and measuring technology related to photosynthesis, QTL analysis of wheat has started. However, it is difficult to precisely determine phenotype of photosynthetic property, especially photosynthetic property for population, because physiological traits are greatly influenced by environment and mechanism of photosynthesis is complex. Meanwhile, the determining methods have limitations. So far, most of the researches referenced QTL analyses of physiological traits were focused on chlorophyll content at seedling stage, dry matter accumulation, leaf photosynthetic rate, stomatal conductance, transpiration rate, inter-cellular CO_2 concentration, and leaf fluorescence parameters, etc. Further, QTL analysis of photosynthetic characters of population in field was few. Therefore, in this study, a set of double-haploid lines (DHLs) derived from a cross of two elite Chinese wheat cultivars were used to map QTLs for photosynthesis-related traits. And the purposes of this study were to obtain closely linked molecular markers that could be used for marker-assisted selection in wheat breeding programs.

6.1.1 QTL Mapping of Photosynthesis Characters of Wheat in Field

6.1.1.1 Materials and Methods

6.1.1.1.1 Materials

One hundred and sixty-eight DH lines derived from the cross of Huapei 3 (HP3)/ Yumai 57 (YM57) were used as materials.

6.1.1.1.2 Planting and Processing in Field Trails

The field trials were conducted on the experimental farm at Shandong Agricultural University (Tai'an, China, 36° 57′N, 116° 36′E) in 2005–2006 and 2006–2007, and in Suzhou Academy of Agricultural Sciences, (Anhui province) in 2006–2007, providing data for three environments. The experimental field consisted of a randomized block with two replications. In the autumn of 2005, all DH lines and parents were grown in a plot with three rows in 2-m length and 25 cm between rows. In the autumn of 2006, the lines were grown in a plot with four 2-m rows

spaced 25 cm apart. Crop management was carried out following the local practice. The soil was brown earth, in which the available N, P, and K contents in the top 20 cm were 40.2, 51.3, and 70.8 mg/kg, respectively. Before planting, 37,500 kg/hectare (ha) of farmyard manure or barnyard manure (nitrogen content, 0.05–0.1 %), 375 kg/ha of urea, 300 kg/ha of phosphorus diamine fertilizer, 225 kg/ha of potassium chloride, 15 kg/ha of zinc sulfate were added as fertilizers. Plots were irrigated in winter (December 1, 2006), and at jointing (April 3, 2007), anthesis (May 4, 2007), and grain filling (May 15, 2007). Topdressings of 300 and 75 g/ha urea were applied with the irrigation water at jointing and anthesis, respectively. In 2007–2008, all DH lines and parents were grown in a plot with five rows in 2-m length and 25 cm between rows. And two environments were set including environment I (2008 (+N)) and environment II (2008 (−N)). Moreover, base fertilizer, additional fertilizer, and irrigation in environment I were the same as 2006–2007, while there was no additional fertilizer in environment II, but base fertilizer and irrigation were the same as 2006–2007. Crop management was carried out following the local yield comparison trial.

6.1.1.1.3 Determining Methods

6.1.1.1.3.1 Determination of Wheat Chlorophyll Content at Grain Filling Stage in Field

For leaf chlorophyll content analyses, flag leaves were taken from five plants per plot at the grain filling stage (around 12 May) and saved in −80 °C ultra-low-temperature freezer. Samples of approximately 0.2 g of leaf tissue (taken from the middle of the leaves) were placed to 20 mL tubes and 10 mL 80 % acetone were added. All tubes were placed in dark at 4 °C for 24 h, and oscillated regularly till leaf tissue turned pale. And then OD was measured at 662 nm and 645 nm with a spectrophotometer UV-4802 (Unico instrument Co., Ltd, Shanghai, China). Chlorophyll a and b contents were estimated, adapting the procedure described by Porra et al. (1989).

6.1.1.1.3.2 Determination of Wheat Chlorophyll Fluorescence Parameters in Field

At jointing, anthesis, and grain filling stages, five uppermost leaves (fully expanded) of each line and the parents were sampled. And chlorophyll fluorescence was measured on the leaf using a portable fluorometer (Handy PEA; Hansatech Instruments, King's Lynn, UK) at ambient temperature after 20-min adaptation of leaves to dark conditions on the day of sampling. The fast chlorophyll a fluorescence transient (OJIP) was induced by pulsed light with 3000 μmol m^{-2} s^{-1}, and changes in fluorescence were registered during irradiation of 10 μs to 1 s with the initial rate of 105 data per second. The meaning and formula of each parameter for OJIP was as follows:

Fo, initial fluorescence, fluorescence level when plastoquinone electron acceptor pool (Qa) is fully oxidized;
Fm, maximum fluorescence, fluorescence level when Qa is transiently fully reduced;
Fv, variable fluorescence, Fv = Fm−Fo, maximum variable fluorescence, reflecting the reduction of Qa; and
Fv/Fm, maximum quantum efficiency of PSII, reflecting the maximum efficiency of PSII reaction center converting luminous energy.

6.1.1.2 Result and Analysis

6.1.1.2.1 QTL Mapping of Chlorophyll Content

6.1.1.2.1.1 Variation of Chlorophyll Content

Mean values of chlorophyll contents for the parents Huapei 3 and Yumai 57, as well as the 168 DH lines under three different environments are shown in Table 6.1. Male parent Yumai 57 had larger values than Huapei 3 for chlorophyll a and b contents, and the differences were visible. The distribution of chlorophyll a and b contents was continuous in the DH lines, showing their quantitative nature. Meanwhile, a transgressive separation was found from the DH lines (Figs. 6.1 and 6.2). Therefore, the distributive character of phenotypic data was suitable for QTL analysis. Correlation analysis showed that there was a highly positive correction between chlorophyll a and chlorophyll b, and the coefficient of correlation was 0.823**.

6.1.1.2.1.2 QTL Mapping and Effect Analysis for Chlorophyll Content

For chlorophyll, eight additive QTLs and three pairs of epistatic QTLs were detected (Tables 6.2 and 6.3). Among them, four additive QTLs and one pair of epistatic QTL had QTL × environment interaction effects.

Table 6.1 Phenotypic data of leaf chlorophyll content (mg g^{-1} FW)

Trait	Parent		DH population					
	Huapei 3	Yumai 57	Mean	Maximum	Minimum	SD	Skewness	Kurtosis
chlorophyll a content (mg g^{-1} FW)								
Suzhou 2006	25.42	31.01	27.94	32.16	21.44	2.24	−0.55	0.41
Tai'an 2006	24.33	32.56	25.20	34.84	17.42	2.79	0.20	0.36
Tai'an 2005	22.69	27.51	23.86	28.17	18.76	2.03	−0.05	−0.44
chlorophyll b content (mg g^{-1} FW)								
Suzhou 2006	9.59	10.24	10.21	11.76	7.84	0.82	−0.54	0.46
Tai'an 2006	7.98	10.96	9.22	12.74	6.37	1.02	0.18	0.35
Tai'an 2005	7.24	10.43	8.95	11.73	4.67	1.23	−0.27	0.65

SD Standard deviation

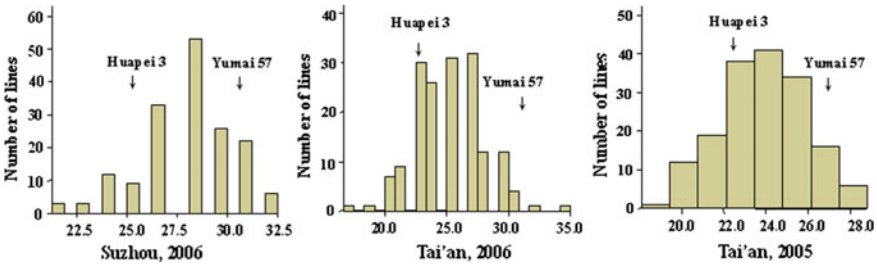

Fig. 6.1 Frequency distribution of chlorophyll a content

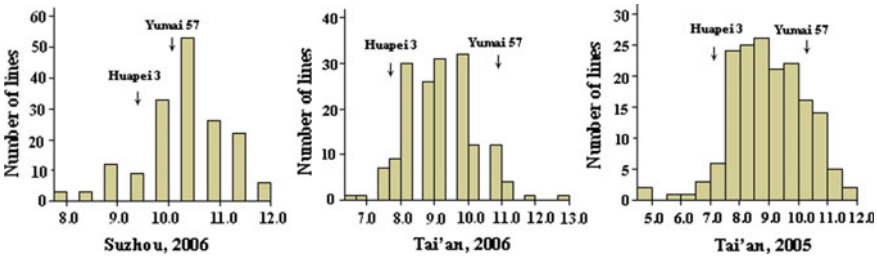

Fig. 6.2 Frequency distribution of chlorophyll b content

6.1.1.2.1.2.1 QTL Mapping and Effect Analysis for Chlorophyll a Content

Four additive QTLs controlled chlorophyll a content were detected on chromosomes 1B, 4A, 5D, and 7A, respectively. And the variance of chlorophyll a content explained by the QTLs ranged from 0.84 to 12.95 %. Among them, *qChla5D* had the highest phenotypic contribution, which could explain 12.95 % of total phenotypic variation, and its positive allele originated from Yumai 57. Environmental interaction effect was detected in *qChla5D*, explaining 21.27 % of total variation.

Three pairs of epistatic QTLs associated with chlorophyll a content were identified on chromosomes 2A-2B and 2A-3B(2), respectively. The pair of QTL (*qChla2Ab*/*qChla3B*) involved in environmental interaction and explained 1.62 % of total phenotypic variation.

6.1.1.2.1.2.2 QTL and Effect Analysis for Chlorophyll b Content

Four additive QTLs controlled chlorophyll a content were on chromosomes 2D, 4A, 5A, and 5D, respectively. And the variance of chlorophyll b content explained by the QTLs ranged from 1.37 to 23.29 %. Among them, *qChlb5D* had the highest phenotypic contribution, which could explain 23.29 % of total phenotypic variation, and its positive allele originated from Yumai 57. Further, *qChlb2D*, *qChlb4A,* and *qChlb5A* involved in environmental interaction, which explained 5.81 % of total variation. No pair of epistatic QTL for chlorophyll b content was detected in this study.

Table 6.2 Estimated additive (A) and additive × environment (AE) interactions of QTL for chlorophyll content

Trait	QTL	Flanking marker	Position (cM)	A	H^2 (%) d	A × E1		A × E2		A × E3	
						AE1	H^2 (%)	AE2	H^2 (%)	AE3	H^2 (%)
Chlorophyll a	*qChla1B*	Xbarc120.3–Xbarc008	38.6	0.34	1.89						
	qChla4A	Xwmc718–Xwmc262	3.0	−0.53	4.41						
	qChla5D	Xwmc215–Xgdm63	74.3	−0.90	12.95			−0.78	9.87	0.88	12.40
	qChla7A	Xwmc607–Xbarc049	74.6	0.23	0.84						
Chlorophyll b	*qChlb2D*	Xcfd53–Xwmc18	2.8	−0.14	1.70					−0.18	2.94
	qChlb4A	Xwmc718–Xwmc262	0.0	−0.26	6.15					−0.12	1.32
	qChlb5A	Xcfe026.1–Xcwem32.2	7.0	0.12	1.37					0.13	1.55
	qChlb5D	Xwmc215–Xgdm63	73.3	−0.51	23.29						

E1: Suzhou, 2006; E2: Tai'an, 2006; E3: Tai'an, 2005

Table 6.3 Estimated epistasis (AA) and epistasis × environment (AAE) interactions of QTL for chlorophyll content

Trait	QTL	Flanking marker	Position (cM)	QTL	Flanking marker	Position (cM)	AA	H^2 (%)	AA × E	
									AAE	H^2 (%)
Chl a	*qChla2Aa*	Xbarc296–Xcfa2263	69.0	qChla2B	Xbarc373–Xwmc477	77.6	0.57	3.97		
	qChla2Ab	Xbarc264–Xgwm448	75.1	qChla3B	Xcfe009–Xwmc3	51.8			−0.32	1.62
	qChla2Ac	Xwmc455–Xgwm515	104.9	qChla3B	Xcfe009–Xwmc3	51.8	−0.34	1.86		

6.1.1.2.2 QTL of Chlorophyll Fluorescence Parameters

6.1.1.2.2.1 Phenotypic Variations of Chlorophyll Fluorescence Parameters

Differences were found for chlorophyll fluorescence parameters between Huapei 3 and Yumai 57 (Table 6.4). The phenotypic value of PSII Fv/Fm for Huapei 3 was higher than Yumai 57 in all environments. In the environment of 2008 (−N), Fv/Fm for the two parents was higher than that in 2007 (+N) and 2008 (+N). The values of Chla/b were inconsistent in 2007 (+N) and 2008 (+N). No difference was found for Fo in nitrogen-deficiency environment and normal environment. The distribution of all parameters was continuous in the DH lines, and in accordance with normal distribution. Meanwhile, a transgressive separation was found from the DH lines.

6.1.1.2.2.2 QTL and Effect Analysis of Chlorophyll Fluorescence Parameters

A total of fourteen additive QTLs and five pairs of epistatic QTLs were identified for chlorophyll and fluorescence parameter, distributing on chromosomes 2A, 3A, 4A, 5A, 6A, 1B, 3B, 4B, 7B, 2D, 3D, 5B, 5D, and 6D, respectively (Table 6.5 and Fig. 6.3).

Five additive QTLs associated with Chl a, Chl b, and Chla/b were mapped on chromosomes 4A, 2D, and 5D, respectively. Among them, two major QTLs

Table 6.4 Phenotypic performance of chlorophyll content and chlorophyll a fluorescence of DH population in field test

Treatment	Trait	Parent			DH population					
		Ym57	Hp3	Mean	Max	Min	SD	Skewness	Kurtosis	CV (%)
2007 (+N)	Chl a	27.51	22.69	27.94	32.16	21.44	2.24	−0.55	0.41	0.08
	Chl b	10.43	7.24	10.21	11.76	7.84	0.82	−0.54	0.46	0.08
	Chla/b	2.64	3.13	2.73	2.76	2.71	0.01	0.5	0.77	0.01
	Fo	500	508	520	592	451	25.5	−0.14	0.36	0.05
	Fm	3103	2846	2809	3355	2124	233.0	−0.01	−0.23	0.08
	Fv	2603	2338	2286	2823	1587	229	−0.15	−0.13	0.1
	Fv/Fm	0.82	0.83	0.82	0.84	0.75	0.02	−0.9	1.22	0.25
2008 (+N)	Chl a	31.06	24.99	29.65	34.32	22.88	2.38	−0.43	0.36	0.08
	Chl b	10.98	9.06	8.54	13	5.46	1.26	0.36	0.43	0.15
	Chla/b	2.83	2.76	3.55	4.87	2.42	0.5	0.19	−0.5	0.14
	Fo	452	473	454	502	402	17.34	−0.12	0.52	0.04
	Fm	2458	2894	2710	3235	2378	161.2	0.16	−0.12	0.06
	Fv	2006	2421	2257	2747	1921	152.7	0.12	−0.16	0.07
	Fv/Fm	0.816	0.837	0.83	0.849	0.801	0.01	−0.82	0.95	0.01
2008 (−N)	Fo	452	448	453	503	315	44.1	−0.88	−0.55	0.01
	Fm	2382	2565	2552	3175	1761	296.3	−0.26	−0.49	3.47
	Fv	1930	2117	2007.3	2698	1414	263.1	−0.14	−0.44	0.13
	Fv/Fm	0.81	0.825	0.83	0.85	0.78	0.01	−0.58	0.57	0.01

Chl a chlorophyll a content; *Chl b* chlorophyll b content; *Chla/b* chlorophyll a/chlorophyll b; *Fo* initial fluorescence; *Fm* maximum fluorescence; *Fv* variable fluorescence; *Fv/Fm* maximum quantum efficiency of PSII

Table 6.5 Estimated additive (A) QTLs for wheat chlorophyll content and chlorophyll fluorescence of DH population in field test

Trait	QTL	Flanking marker	Site (cM)	A[a]	H^2 (A, %)[b]
Chl a	*qChla4A*	Xwmc718–Xwmc262	1.0	−0.70	8.24
	qChla5D	Xwmc215–Xbarc345	74.4	−0.97	16.12
					24.36
Chl b	*qChlb2D*	Xcfd53–Xwmc18	1.7	−0.44	11.59
	qChlb5D	Xbarc320–Xwmc215	67.3	−0.69	28.49
					40.08
Chl a/b	*qChla/b5D*	Xbarc320–Xwmc215	66.3	0.08	4.34
Fo	*qFo2A*	Xwmc455–Xgmw515	102.7	−9.00	11.08
	qFo5D	Xwmc215–Xbarc345	82.4	8.31	9.54
					20.62
Fm	*qFm3B*	Xgwm389–Xgwm533	15.6	−59.17	6.25
	qFm4B	Xwmc47–Xwmc413	4.2	48.78	4.25
					10.5
Fv	*qFv3B*	Xgmw389–Xgwm533	15.6	−57.77	6.18
	qFv4B	Xwmc47–Xwmc413	4.2	48.06	4.28
					10.46
Fv/Fm	*qFv/Fm5A*	Xgwm186–Xcfe223	58.8	0.0035	3.85
	qFv/Fm6A	Xcfe179.2–Xcfe179.1	84.1	−0.0031	4.23
	qFv/Fm6D	Xgwm55–Xgwm133.2	90.9	0.0047	9.38
					16.16

Note: [a]Additive effects, a positive value indicates that allele from Hp3 increases the trait, a negative value indicates that allele from YM57 increases the trait
[b]Contribution explained by additive QTL

(*qChla5D* and *qChlb5D*) flanked by Xwmc215 could explain 16.12 and 28.49 % of total variation, respectively. Other three additive QTLs (*qChla4A*, *qChlb2D,* and *qChla/b5D*) explained 8.24, 11.59, and 4.34 % of total variation, respectively.

Two additive QTLs controlling Fo were detected on chromosomes 2A and 5D, accounting for 20.62 % of total phenotypic variation. Further, the positive alleles of *qFo2A* and *qFo5D* came from Huapei 3 and Yumai 57, respectively, and which explained 9.54 and 11.08 % of phenotypic variation, respectively.

For Fm, two additive QTLs (*qFm3B* and *qFm4B*) were detected, whose positive alleles originated from Yumai 57, and could explain 7.86 and 7.38 % of phenotypic variation, respectively.

For Fv, two additive QTLs (*qFv3B* and *qFv4B*) were identified, jointly explaining 10.46 % of the total variation, whose location on chromosomes were as same as the two QTLs controlling Fm. However, their positive alleles came from Huapei 3.

Three additive QTLs (*qFv/Fm5A*, *qFv/Fm6A,* and *qFv/Fm6D*) associated with PSII Fv/Fm were detected, jointly explaining 16.16 % of phenotypic variation, and the positive alleles came from Huapei 3.

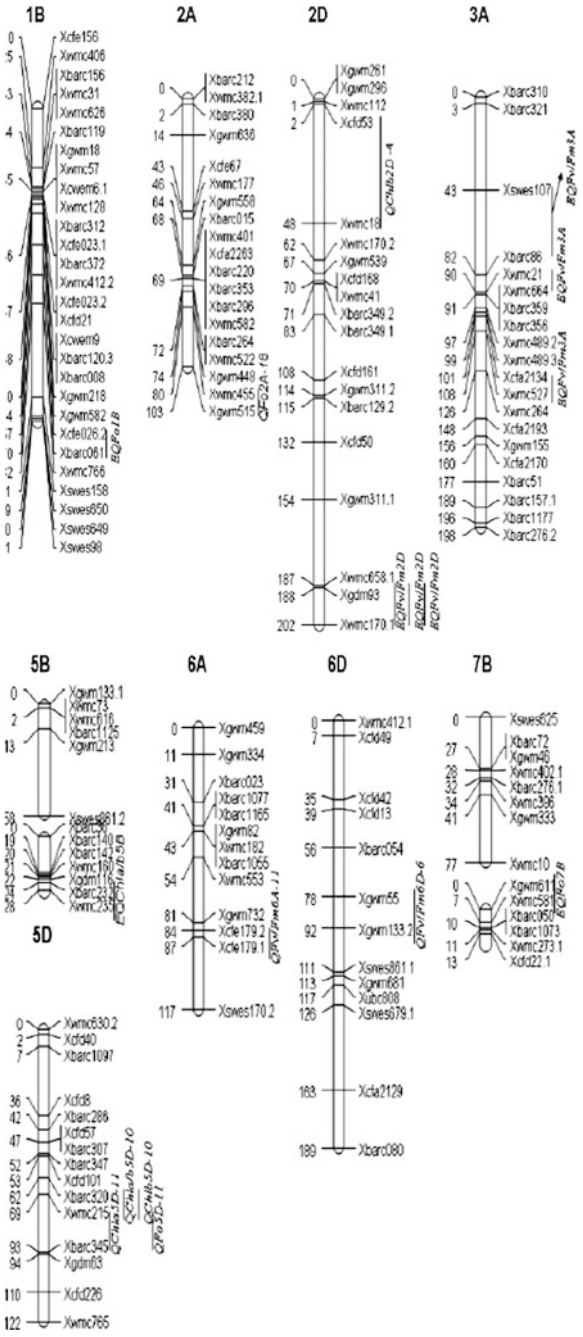

Fig. 6.3 The position of additive QTLs and epistatic QTLs conferring chlorophyll content and chlorophyll fluorescence of DH population in field test

Table 6.6 Estimated digenic epistatic (AA) effects of QTLs for wheat chlorophyll fluorescence of DH population in field test

Trait	QTL	Flanking marker	Site/cm	QTL	Flanking marker	Site/cM	AA[a]	H^2 (AA, %)[b]
Fo	*qFo1B*	Xcfe026.2–Xbarc061	68.3	qFo7B	Xgwm611–Xwmc581	5.0	9.36	12.1
Fv/Fm	*qFv/Fm2D*	Xgdm93–Xwmc170.1	201.8	qFv/Fm3A	Xcfa2134–Xwmc527	107	–	0.16
	qFv/Fm2D	Xgdm93–Xwmc170.1	201.8	qFv/Fm3A	Xwmc21–Xwmc664	90.3	−0.02	1.44
	qFv/Fm2D	Xgdm93–Xwmc170.1	201.8	qFv/Fm3A	Xswes107–Xbarc86	43.1	0.03	3.03
								4.63
Chla/b	*qChla/b3D*	Xbarc1119–Xcfd4	17.8	qChla/b5B	Xbarc232–Xwmc235	25.7	−0.01	3.54

Note: [a]Positive value indicates that the parental two-loci genotypes is greater than the recombinant-type effect, and the negative value means that the parent-type effect is less than the recombinant-type effect have a positive effect and that the recombinants have a negative effect
[b]Contribution explained by epistatic QTL

Five pairs of epistatic QTLs controlling Fo, Fv/Fm, and chl a/b were detected, distributing on chromosomes 1B-7B, 2D-3A, and 3D-5B, respectively (Table 6.6 and Fig. 6.3). And they could explain 12.1, 4.63, and 3.54 % of the phenotypic variation.

6.1.2 QTL Mapping of Photosynthesis of Wheat Seedlings in Phytotron

6.1.2.1 Planting and Determining Methods in Phytotron

6.1.2.1.1 Planting Trails

Two environment conditions including environment I (from September to October 2007) and environment II (from February to April 2008) were set in net room and phytotron in Shandong Agricultural University. A total of 168 lines and parents were planted in cultivate bowls (diameter for 10 cm and height for 8 cm) with homogeneous and fertile soils. Furthermore, each line and parent was planted for three bowls, and five plants were cultivated in a bowl. Under environment I, materials were sowed on September 5, 2007, while materials were sowed on February 28, 2008, under environment II. Materials management was carried out following the conventional potting trial and transforming the location of cultivate bowl once a week to reduce the difference in growing environment among lines and parents. After one month, all the materials were transferred to a phytotron (ACC-1, Hangzhou), and the upper two full extended leaves were sampled to determine the photosynthesis parameters after 7 days for adaptation. In phytotron, the day/might temperature was controlled in 24/18 °C, photon flux density 400 μmol m^{-2} s^{-1}, photoperiod 12 h/12 h, and relative humidity 60 %. In order to avoid the effect of circadian rhythms on determining of parameters, preliminary work was conducted, and multipoint photosynthesis and fluorescence parameters were determined on 5, 7, and 9 days after wheat in phytotron. It was found that photosynthesis and fluorescence parameters of leaf were basically stable in one day after 7 days.

6.1.2.1.2 Determining Methods

6.1.2.1.2.1 Determination of Leaf Gas Exchange Parameters at Seedling Stage

Net photosynthetic rate (Pn), stomatal conductance (Gs), inter-cellular CO_2 concentration (Ci) of the lines and parents were determined using portable photosynthesis system (CIRAS-2, PP Systems, UK) after 7 days stored in phytotron. Concentration of CO_2 was controlled in 380 μmol mol^{-1} by the system, and illumination intensity was controlled in 1000 μmol m^{-2} s^{-1} by LED red-white source.

6.1.2.1.2.2 Determination of Chlorophyll Fluorescence Parameters of Wheat Seedlings

After gas exchange parameters were determined, the same position of leaves were put in clip holders for a 20-min period of darkness adaptation and measuring the fast chlorophyll a fluorescence transient (OJIP) by using a Handy PEA (Hansatech instruments, Norfolk, UK) instrument, and the determination method was the same as that described above.

6.1.2.1.2.3 Determination of Chlorophyll Content of Wheat Seedlings

After determining photosynthetic character and fluorescence parameters, the samples of all lines and parents were taken according to the method described above. OD was measured at 662, 645, and 470 nm with a spectrophotometer UV-4802 (Unico instrument Co., Ltd, Shanghai, China). And then chlorophyll a, chlorophyll b, and carotenoid contents were estimated.

6.1.2.2 QTL Mapping and Effects Analysis of Photosynthetic Characters in Wheat Seedlings

QTL analyses were performed using QTL Network 2.0 software based on the mixed linear model approach. When $P < 0.005$, 17 additive QTLs and 20 pairs of epistatic QTLs conferring photosynthesis and its related traits were identified; furthermore, all additive QTLs and 16 pairs of epistatic QTLs involved in environmental interaction (Tables 6.7 and 6.8, Fig. 6.4).

Two additive QTLs (*QPn4D-11* and *QPn5D-11*) conferring Pn distributing on chromosomes 4D and 5D were detected, whose positive alleles came from Yumai 57 and Huapei 3, respectively, and could explain 2.47 and 7.15 % of phenotypic variation. Moreover, both the two additive QTLs involved in environmental interaction. Meanwhile, four pairs of epistatic QTLs, distributed on chromosomes 1B-3A, 1B-3A, 1B-3D, and 1D-5B, were also detected and could explain 2.17, 1.58, 1.09, and 3.22 % of phenotypic variation, respectively.

For Tr, one QTL (*QE4D-11*) accounting for 3.81 % of phenotypic variation was detected and involved in environmental interaction. Three pairs of epistatic QTLs, distributed on chromosomes 3A-4A, 3B-4D, and 3B-6D, were detected and could explain 2.59, 4.17, and 1.18 % of phenotypic variation. Moreover, all the three pairs of epistatic QTLs involved in environmental interaction, jointly accounting for 8.66 and 9.75 % of phenotypic variation in the two environments, respectively.

For Ci/Cr, two additive QTLs (*QGs4D-11* and *QGs5D-13*) were identified, accounting for 4.17 and 2.64 % of phenotypic variation. And both the two QTLs involved in environmental interaction. The phenotypic variations of *QGs4D-11* were larger in the two environments, which were 3.48 and 3.45 %, respectively. Five pairs of epistatic QTLs associated with Ci/Cr were also detected, distributing

Table 6.7 Additive effects of QTLs for photosynthesis and related physiological traits at seedling stage of wheat in two environments

Trait	Locus	Flanking marker	Site/cM	*A*	H^2 (%)	AE1	H^2 AE1 (%)	AE2	H^2 AE2 (%)
Chl a	*QCa5B-5*	Xgwm213–Xswes861.2	68.1	0.05	1.2	−0.03	0.6	0.20	0.6
	QCa5D-10	Xbarc320–Xwmc215	66.3	0.18	18.2	−0.15	12.5	0.17	12.3
Chl b	*QCb5B-5*	Xgwm213–Xswes861.2	68.1	0.02	1.8	−0.01	0.2	0.05	0.2
	QCb5D-10	Xbarc320–Xwmc215	66.3	0.04	10.4	−0.05	14.1	0.09	13.9
Car	*QCx5D-10*	Xbarc320–Xwmc215	66.3	0.04	27.3	−0.02	6.3	0.06	6.1
Pn	*QPn4D-11*	Xcfe254–Be293342	194.5	0.52	2.5	0.20	0.4	0.50	0.4
	QPn5D-11	Xwmc215–Xbarc345	79.4	0.89	7.2	−0.59	3.2	0.65	3.1
Tr	*QTr4D-11*	Xfe254–Be293342	194.5	0.12	3.8	0.05	0.6	0.30	0.6
Gs	*QGs4D-11*	Xcfe254–Be293342	194.5	13.24	4.2	12.12	3.5	12.38	3.5
	QGs5D-13	Xgdw63–Xcfd226	93.6	10.55	2.6	−5.81	0.8	6.74	0.8
Ci	*QCi5B-5*	Xgwm213–Xswes861.2	68.1	5.70	1.2	27.70	28.9	25.10	27.7
	QCi5D-9	Xcfd101–Xbarc320	58.6	2.71	0.3	–	–	2.05	0.2
Ci/Cr	*QCi/Cr4A-3*	Xbarc343–Xwmc313	16.3	0.01	0.6	−0.02	4.9	0.09	4.6
	QCi/Cr5B-5	Xgwm213–Xswes861.2	68.1	0.01	1.4	0.03	6.9	0.04	7.0
	QCi/Cr5D-9	Xcfd101–Xbarc320	58.6	0.02	5.1	0.02	2.8	0.07	2.6
Fm	*QFm1A-1*	Xgwm259–Xcwem32.1	4.0	140.90	1.4	−114.00	0.9	138.00	0.9
	QFm1A-17	Xwmc120–Xgwm498	64.5	126.44	1.2	53.60	0.2	55.80	0.2

A additive effect; H^2 contribution rate; E1: environment I (from September to October 2007); E2: environment II (from February to April 2008). P_n net photosynthetic rate; T_r transpiration rate; G_s stomatal conductance; C_i intercellular CO_2 concentration; C_i/C_r gas conductance; F_o initial fluorescence; F_m maximum yield of fluorescence in darkness; F_v variable fluorescence; F_v/F_m maximal photochemical efficiency of PSII; *Chl a* Chl a content; *Chl b* Chl b content; *Car* Carotinoid content. "–" data were not taken

Table 6.8 Epistatic effects of QTLs for photosynthesis and related physiological traits at seedling stage of wheat in two environments

Trait	QTL	Flanking markers	Site (cM)	QTL	Flanking markers	Site (cM)	AA	H^2 AA (%)	AAE1	H^2 AAE1 (%)	AAE2	H^2 AAE2 (%)
Chl a	*QCa3B-14*	Xwmc505–Xcfe282	52.6	*QCa5D-7*	Xbarc307–Xbarc347	48.6	0.04	0.9	−0.06	2.0	0.09	2.1
Chl b	*QCb3B-14*	Xwmc505–Xcfe282	52.6	*QCb5D-7*	Xbarc307–Xbarc347	46.6	0.01	0.2	−0.02	2.8	0.05	2.1
Car	*QCx1B-15*	Xcfe023.2–Xcfd21	37.3	*QCx4D-5*	Xcfa2173–Xcfe188	153.8	0.01	2.0	–	–	–	–
	QCx1B-21	Xgwm582–Xcfe026.2	44.6	*QCx4D-5*	Xcfa2173–Xcfe188	153.8	0.01	0.8	–	–	–	–
Pn	*QPn1B-24*	Xwmc766–Xswes158	92.9	*QPn3A-12*	Xwmc527–Xwmc264	120.8	0.49	2.2	−0.21	0.4	0.40	0.4
	QPn1B-27	Xswes649–Xswes98	130.1	*QPn3A-11*	Xcfa2134–Xwmc527	107.0	0.42	1.6	−0.16	0.2	0.24	0.2
	QPn1B-27	Xswes649–Xswes98	130.1	*QPn3D-6*	Xgwm52–Xgdm8	24.0	0.35	1.1	−0.47	2.0	0.50	2.0
	QPn1D-4	Xwmc429–Xcfd19	33.2	*QPn5B-1*	Xgwm133.1–Xwmc73	1.0	0.59	3.2	−0.86	6.7	1.04	8.5
Tr	*QTr3A-18*	Xbarc157.1–Xbarc1177	192.8	*QTr4A-10*	Xbarc327–Xbarc078	40.8	−0.10	2.6	0.11	3.0	−0.25	2.8
	QTr3B-1	Xbarc102–Xgwm389	6.0	*QTr6D-6*	Xgwm55–Xgwm133.2	77.9	0.13	4.2	−0.10	2.7	0.18	4.2
	QTr3B-3	Xgwm533–Xbarc251	23.0	*QTr6D-7*	Xgwm133.2–Xswes861.1	109.0	−0.07	1.2	0.11	3.0	−0.19	2.8
Gs	*QGs1A-11*	Xwmc278–Xbarc120.1	56.3	*QGs2B-18*	Xcwem55–Xbarc129.1	86.0	13.07	4.1	−5.55	0.7	4.99	0.6
	QGs1D-4	Xwmc429–Xcfd19	31.2	*QGs5B-2*	Xwmc73–Xwmc616	1.6	5.82	0.8	−5.99	0.9	0.62	5.1
	QGs2D-13	Xgwm311.2–Xbarc129.2	115.3	*QGs7D-12*	Xcfd175–Xwmc14	172.5	16.32	6.3	−18.59	8.2	18.83	8.4
	QGs4B-3	Xwmc413–Xcfd39.2	7.7	*QGs5B-2*	Xwmc73–Xwmc616	1.6	−9.74	2.3	–	–	–	–
	QGs4B-5	Xcfd22.2–Xwmc657	13.2	*QGs5B-5*	Xgwm213–Xswes861.2	68.1	−9.92	2.3	12.56	3.8	−12.27	3.6
Fm	*QFm1B-1*	Xcfe156–Xwmc406	0.0	*QFm2B-17*	Xbarc101–Xcwem55	77.4	120.10	1.0	61.24	0.3	−65.20	0.3
	QFm3B-21	Xwmc307–Xgwm566	63.0	*QFm7B-7*	Xgwm333–Xwmc10	68.2	118.80	1.0	45.80	0.2	−49.90	0.2
	QFm1B-9	Xcwem6.1–Xwmc128	34.9	*QFm1B-21*	Xgwm582–Xcfe026.2	47.6	168.00	2.0	–	–	–	–
	QFm5B-6	Xbarc232–Xwmc235	27.7	*QFm5D-10*	Xbarc320–Xwmc215	65.3	122.6	1.1	38.40	0.1	−39.40	0.1

AA epistatic effect. Other abbreviations are the same as in Table 6.7. "–" data are not taken

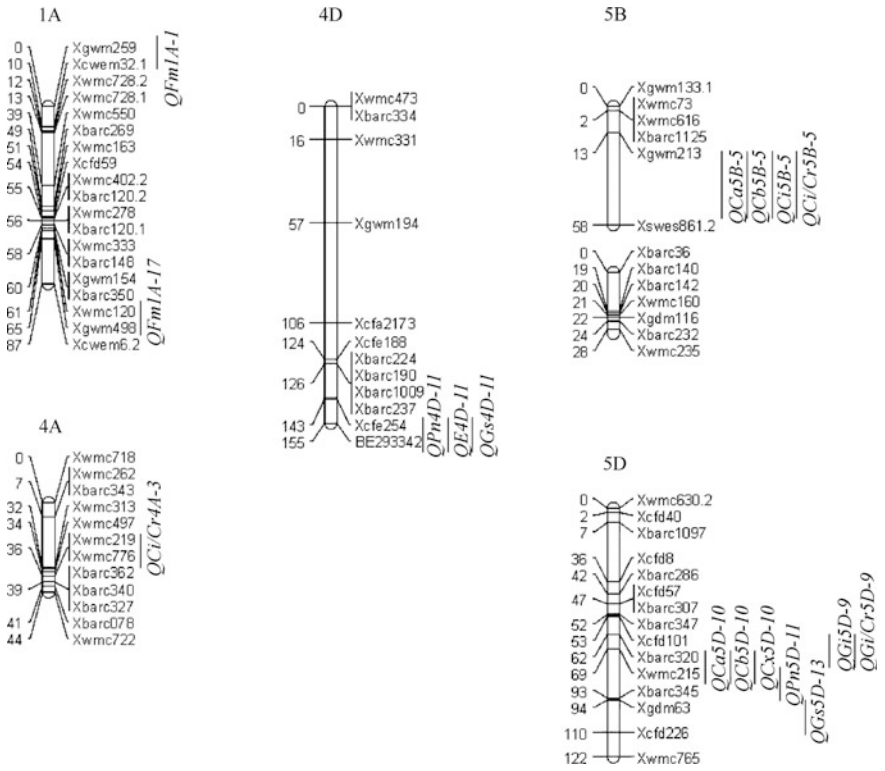

Fig. 6.4 Chromosome positions of additive QTLs for photosynthesis and related traits in 168 double-haploid lines derived from the cross of Huapei 3 × Yumai 57 at seedling stage of wheat

on chromosomes 1A-2B, 1D-5B, 2D-7D, 4B-5B, and 4B-5B, and explained 4.06, 0.81, 6.33, 2.25, and 2.33 % of phenotypic variation, respectively. In addition to *QGs4B-3/QGs5B-2*, other four pairs of QTLs involved in environmental interaction. Furthermore, *QGs2D-13/QGs7D-12* had the highest phenotypic contribution, accounting for 8.21 and 8.42 %, respectively, in the two environments.

Two additive QTLs conferring Ci, distributing on chromosomes 5B and 5D, were detected and explained 1.22 and 0.28 % of phenotypic variation. Among them, *QCi5B-5* had higher environmental interaction effect, accounting for 28.94 and 27.7 % of phenotypic variation in the two environments, respectively. In environment I, the parental effect was greater than recombinant effect, but that was opposite in environment II. No pair of epistatic QTL conferring Ci was detected.

Three additive QTLs for Ci/Cr (*QTL-QCi/Cr4A-3, QCi/Cr5B-5,* and *QCi/Cr5D-9*) were identified, accounting for 0.58, 1.37, and 5.07 %, respectively. The total variation of additive effect and environmental interaction effect were 14.69 and

14.21 %, respectively. No pair of epistatic QTL conferring Ci/Cr was detected (Tables 6.7 and 6.8, Fig. 6.4).

For chlorophyll a content, two additive QTLs (*QCa5B-5* and *QCa5D-10*) were detected, accounting for 1.2 and 18.23 % of phenotypic variation. And one pair of epistatic QTL on chromosome 3B-5D for chlorophyll a content involved in environmental interaction (Tables 6.7 and 6.8, Fig. 6.4).

Two additive QTLs (*QCb5B-5* and *QCb5D-10*) conferring chlorophyll b content were detected, accounting for 1.78 and 10.4 % of phenotypic variation, and their positive alleles came from Huapei 3, which was in accordance with Huapei 3 having the higher content of chlorophyll b. Both the two QTLs involved in environmental interaction, and *QCb5D-10* had the higher phenotypic contribution, explaining 14.12 and 13.9 % of phenotypic variation in two environments, respectively. One pair of epistatic QTL for chlorophyll b was detected, distributing on chromosomes 3B-5D, which involved in environmental interaction.

For carotenoid contents, only one additive QTL (*QCx5D-10*) was identified, accounting for 27.25 % of phenotypic variation, and whose positive alleles came from Huapei 3. Meanwhile, QE interaction could explain 6.3 and 6.12 % of phenotypic variation in the two environments, respectively. Two pairs of epistatic QTLs were also detected on chromosomes 1B-4D, accounting for 2.02 and 0.75 % of phenotypic variation; however, they did not involved in QE interaction (Tables 6.7 and 6.8, Fig. 6.4).

For Fm, two additive QTLs (*QFm1A-1* and *QFm1A-17*) were detected, accounting for 1.43 and 1.15 % of phenotypic variation, respectively. And both the two additive QTLs involved in QE interaction, but the contributions to phenotypic variation were small. Four pairs of epistatic QTLs on chromosomes 1B-2B, 3B-7B, 1B-1B, and 5B-5D, respectively, were detected, explaining 1.04, 1.02, 2.04, and 1.08 % of phenotypic variation, respectively. In addition to the pair of epistatic QTLs linked by Xcwem6.1–Xwmc128 and Xgwm582–Xcfe026.2 locating on chromosome 1B, other three pairs of epistatic QTLs all involved in QE interaction (Tables 6.7 and 6.8, Fig. 6.4).

6.1.3 QTL Mapping of Dry Matter Production (DMA) and Fv/Fm at Jointing and Anthesis Stage in Field

6.1.3.1 Materials and Methods

6.1.3.1.1 Planting Materials

Materials and Planting were same as one of the Sect. 6.1.1.1.1 in this chapter.

6.1.3.1.2 Determining Methods

6.1.3.1.2.1 Determining DMA at Jointing and Flowering Stage of Wheat in Field

Each genotype was tagged at jointing (first internode about 2 cm above the soil) and at flowering (anthers burst on more than 50 % of panicles). Five stems from each DHL were cut at the soil surface and then put in ice from both growth stages. Samples were treated at 105 °C for 30 min and further dried at 65 °C until reaching constant dry weight. The leaves were separated from the stem and the weights of each stem with the sheath and corresponding leaf were separately measured using a JA3003A electronic balance (Jingtian Instruments, Shanghai, China). The DM weight of each plant was the sum of the values of the stem and the leaf. The DMA of leaves, stems, and plants was calculated according to the difference in weight between the jointing and anthesis stages. The means of five replications from each plot were used for statistical analysis.

6.1.3.1.2.2 Determination of Fv/Fm at Jointing and Flowering Stage of Wheat in Field

The upper unfolded leaves at the jointing and anthesis stages were used to measure the maximum quantum efficiency (Fv/Fm), and the determining method as described above. Mean values of five replications per plot were taken for data analysis.

6.1.3.2 Result and Analysis

6.1.3.2.1 Phenotypic Variation Among DHLs

The phenotypic variation of DHLs and the parents for DMA of culms, leaves, total plants, and Fv/Fm at the jointing stage and anthesis stage in 2007 and 2008 are summarized in Table 6.9. HP3 and YM57 differed significantly in the measured traits and phenotypic values of HP3 for the majority of traits at both growth stages were much higher than those of YM57. However, the DMA of leaves for YM57 was higher than that of HP3 at the jointing stage. The mean values of DHLs were intermediate between the parents for most of the traits. Some lines had more extreme values than the parents, showing substantial transgress segregation. In addition, all target traits showed considerable phenotypic variation and continuous distributions, indicating their quantitative nature. The skewness and kurtosis of DMA were less than 1.0, implying polygenic inheritance and suitability of the data for QTL analysis, whereas the Fv/Fm values were often a little higher than 1.0, indicating the distribution of Fv/Fm was skewed to some extent.

Table 6.9 Phenotypic data for DMA and Fv/Fm in two developmental stages in the 2007 and 2008 crop seasons

Season growth stage	Trait	Parent		DH population					
		HP3	YM57	Mean	Max	Min	SD	Skew	Kurt
2007 Jointing	Culm (g·culm-1)	0.51	0.16	0.46	1	0.06	0.2	0.41	−0.27
	Leaves (g·culm-1)	0.11	0.14	0.07	0.4	−0.15	0.1	0.29	0.37
	Plant (g·culm-1)	0.62	0.30	0.54	1.34	0.1	0.23	0.73	0.64
	Fv/Fm	0.835	0.815	0.809	0.84	0.74	0.02	−1.1	2.26
2007 Anthesis	Culms (g·culm-1)	1.84	0.84	0.74	3.34	−1.53	0.79	0.45	0.91
	Leaves (g·culm-1)	0.08	−0.06	−0.02	0.17	−0.23	0.09	−0.1	−0.52
	Plant (g·culm-1)	1.92	0.78	0.87	3.46	−0.82	0.78	0.59	0.85
	Fv/Fm	0.82	0.82	0.82	0.84	0.75	0.02	−0.9	1.22
2008 Jointing	Culms (g·culm-1)	0.39	0.37	0.28	0.73	0.01	0.14	0.74	0.46
	Leaves (g·culms-1)	0.14	0.25	0.13	0.31	−0.08	0.07	−0.11	0.25
	Plants (g·culm-1)	0.53	0.62	0.4	0.87	−0.02	0.18	0.32	−0.14
	Fv/Fm	0.84	0.84	0.84	0.85	0.81	0.01	−1.15	2.6
2008 Anthesis	Culms (g·culm-1)	1.1	0.65	0.54	1.96	−0.9	0.49	−0.08	0.56
	Leaves (g·culm-1)	0.01	−0.07	−0.04	0.17	−0.22	0.08	−0.06	−0.3
	Plants (g·culm-1)	1.11	0.58	0.51	2.04	−1.09	0.55	0.04	0.43
	Fv/Fm	0.837	0.816	0.83	0.849	0.801	0.01	−0.82	0.95

Culms DMAs of culms; *Leaves* DMAs of leaves; *Plants* DMAs of plants; *Fv/Fm* maximum quantum efficiency of PSII; the same as below

6.1.3.2.2 Correlation Analysis for Identified Traits

Correlations among all the identified traits at the two growth stages in both years are given in Table 6.10. The correlations between DMA in culms and leaves at anthesis were much higher than those at the jointing stage in both years, with the exception of the highly significant correlations rA12 = 0.648**, rA22 = 0.737**, and rJ12 = 0.163, rJ22 = 0.378** (1, 2 represent the years 2007 and 2008, respectively). However, the DMAs of plants showed high positive correlations with those of both culms and leaves. In addition, the correlation coefficients between plants and culms (rG12 = 0.523**, rG22 = 0.996**, rJ12 = 0.943**, and rJ22 = 0.925**) were much higher than those between plants and leaves (rG12 = 0.344**, rG22 = 0.789**, rJ12 = 0.456**, and rJ22 = 0.699**) at the two growth stages in both years.

Table 6.10 Correlation coefficients for dry matter accumulation (DMA) and Fv/Fm at two developmental stages in the 2007 and 2008 crop seasons

Trait	Fv/Fm1 (n = 168)	Culms1 (n = 110)	Leaves1 (n = 110)	Plants1 (n = 110)	Fv/Fm2 (n = 168)	Culms2 (n = 168)	Leaves2 (n = 168)	Plants (n = 168)
Fv/Fm1 (n = 168)	–	0.077	0.015	0.03	0.129	0.141	0.115	0.142
Culms1 (n = 134)	−0.085	–	0.648**	0.523**	−0.006	−0.079	−0.063	−0.08
Leaves1 (n = 134)	−0.037	0.163	–	0.344**	0.081	−0.049	−0.095	−0.059
Plants1 (n = 134)	−0.082	0.943**	0.456**	–	−0.164	−0.098	−0.035	−0.093
Fv/Fm2 (n = 168)	0.032	−0.021	0.042	0	–	0.053	0.106	0.063
Culms2 (n-168)	−0.076	0.403**	−0.0164	0.312**	−0.201*	–	0.737**	0.996**
Leaves2 (n = 168)	−0.016	0.038	−0.092	−0.015	−0.083	0.378**	–	0.798**
Plants2 (n = 168)	−0.066	0.33**	−0.0162	0.239**	−0.19*	0.925**	0.699**	–

Numbers in the upper right segment apply to the anthesis stage; those at the lower left are for the jointing stage (*1* in 2007; *2* in 2008); significant at $*P = 0.05$ and $**P = 0.01$; other abbreviations are the same as in Table 6.9

This suggested that DMA in culms plays an important role in plant development. Fv/Fm was poorly correlated with the parameters for DMA.

6.1.3.2.3 QTL Mapping and Effect Analysis of DMA and Fv/Fm in Field

6.1.3.2.3.1 Additive QTLs and Additive QTL × Environment Interactions

A total of 18 additive loci affecting the measured traits were detected. Map locations and additive effects of the QTL and interaction effects between additive QTLs and environments are summarized in Table 6.11 and Fig. 6.5, respectively. It is interesting that all QTLs showing interacting effects with environments were identified at the jointing stage.

The three loci showing significant associations with DMA in culms explained from 7.02 to 14.02 % of the phenotypic variation. All loci derived their additive effects from favorable alleles of HP3. A major QTL, *Qculm5D-10*, was detected at the jointing stages, accounting for 14.02 % of the phenotype variation. The other two QTLs *Qculm1D-2* and *Qculm3B-21*, involved at the anthesis stage, explained 7.02 and 9.93 % of the phenotypic variation, respectively.

For DMA in leaves, seven additive QTLs, 4 at jointing and 3 at anthesis, were located on chromosomes 2A, 3A, 3B, 4A, 5A, 5B, and 5D. Five of these were conferred by favorable alleles from HP3. All QTLs with A-QEIs were identified at the jointing stage, explaining from 1.25 to 3.84 % of the phenotypic variation. No major loci were involved.

Five QTLs controlling DMA in plants were located on chromosomes 1D, 3B, 4B, 5D, and 6A, accounting for 0.37 to 9.34 % of the phenotypic variation. The favorable allele of *Qplant4B-7* came from YM57, and the other four favorable alleles were from HP3. Three QTLs with A-QEIs were identified at the jointing stage, explaining from 0.34 to 1.74 % of the phenotypic variation. No major loci were involved.

Three regions on chromosomes 5A, 6A, and 6D, associated with Fv/Fm, were detected at the anthesis stage. These loci accounted for 3.19–7.26 % of the phenotypic variation. Two of the favorable alleles were from HP3, and the other was from YM57. No loci were involved in additive and environmental interactions.

6.1.3.2.3.2 Epistatic QTL and Epistatic QTL × Environment Interactions

The 12 pairs of epistatic QTLs for DMA (Table 6.12 and Fig. 6.5) explained phenotypic variation ranging from 0.18 to 13.11 %. Among them, five pairs not only had epistatic effects, but also had E-QEI effects at jointing.

Three pairs of epistatic QTLs were detected for DMA in culms; one pair showed both epistatic effects and also E-QEI effects. Two epistatic pairs involved at the jointing stage had negative effects, which meant that recombinant types had higher effects than the parents. The single pair detected at anthesis showed positive effects, that is, parental effects were larger than recombinant effects.

Table 6.11 QTL detected in the HP3 × YM57 DH mapping population at two growth stages in 2007 and 2008

Trait	Locus	Flanking markers	Jointing site (cM)	A[a]	H^2 (A, %)	AE1	H^2 (AE1, %)	AE2	H^2 (AE2, %)	Anthesis site (cM)	A[a]	H^2 (A, %)[b]
Culmsc	*Qculm5D-10* *Qculm1D-2* *Qculm3B-21*	XBARC320–XWMC215	68.3	0.07	14.02							
		XWMC222–XGDM60								11.2	0.13	7.02
		XWMC307–XGWM566								64	0.16	9.93
					14.02							16.95
Leaves	*Qleaves3A-1* *Qleaves3B-2* *Qleaves5B-5* *Qleaves5D-9* *Qleaves2A-18* *Qleaves4A-10* *Qleaves5A-2*	XBARC310–XBARC321	1	0.0058	0.55	−0.0109	1.94	0.011	1.98			
		XGWM389–XGWM533	17.6	0.0073	0.86	−0.0094	1.45	0.0095	1.47			
		XGDM116–XBARC232	22	−0.00015	0.04	0.0153	3.84	−0.0153	3.81			
		XCFD101–XBARC320	53.6	−0.0151	3.74	−0.0088	1.26	0.0088	1.25			
		XWMC455–XGWM515								97.7	−0.0156	3.71
		XBARC327–XBARC078								38.8	−0.0043	0.28
		XCWEM32.2–XWMC59								12.6	0.014	2.97
					5.19							6.96
Plants	*Qplant4B-7* *Qplant5D-10* *Qplant6A-1* *Qplant1D-2* *Qplant3B-21*	XWMC48–XBARC1096	18.4	−0.0245	1.35	0.0141	0.45	−0.0137	0.43			
		XBARC320–XWMC215	64.3	0.0303	2.07	−0.0124	0.34	0.124	0.34			
		XGWM459–XGWM334	2	0.0127	0.37	0.0278	1.74	0.0278	1.74			
		XWMC222–XGDM60								12.2	0.1179	4.37
		XWMC307–XGWM566								65	0.1705	9.14
					3.79							13.51
Fv/Fm	*QFv/Fm5A* *QFv/Fm6A* *QFv/Fm6D*	XGWM186–XCFE223								58.8	0.0035	4.07
		XCFE179.2–XCFE179.1								84.1	−0.0031	3.19
		XGWM55–XGWM133.2								90.9	0.0047	7.26
												14.52

[a]Additive effects, a positive value indicates that the allele from HP3 increases the trait value; a negative value indicates that allele from YM57 increases the trait value
[b]Contribution explained by additive effect QTL; other abbreviations are the same as in Table 6.9

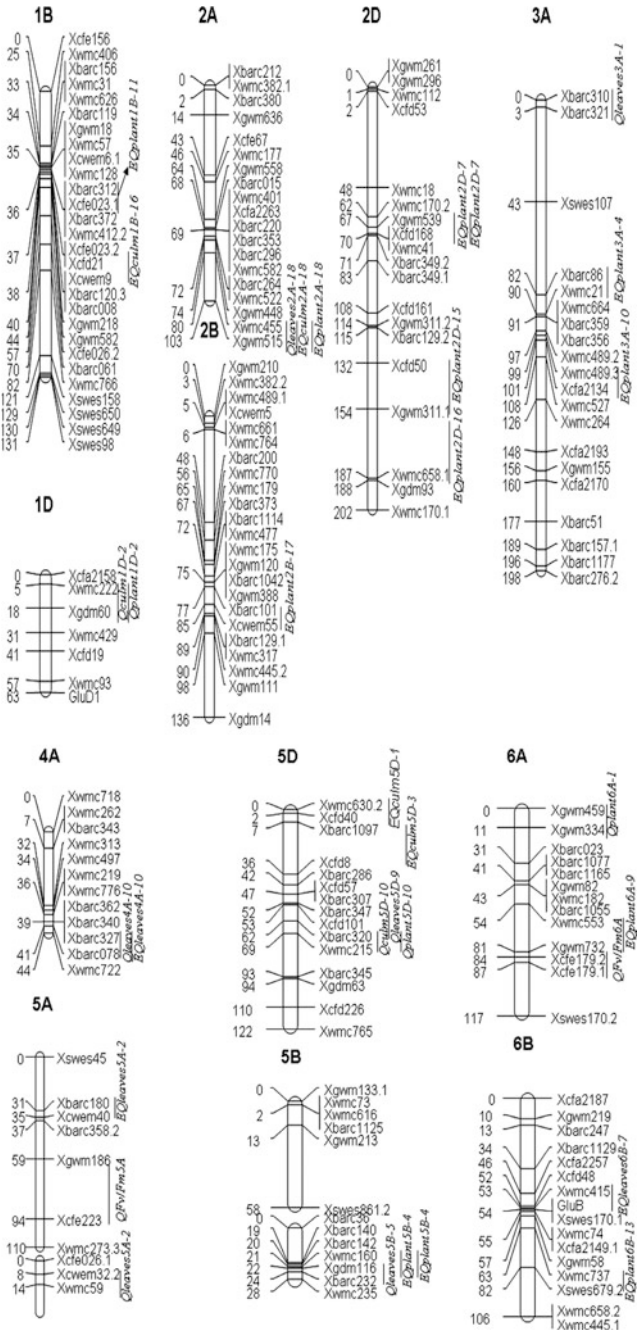

Fig. 6.5 The position of additive QTLs and epistatic QTLs conferring dry matter production and Fv/Fm at two developmental stages in 2007 and 2008

Table 6.12 Estimated digenic epistatic (AA) and epistasis × environment interaction (AAE) effects of QTLs for DMA at two developmental stages in 2007 and 2008

Trait	Locus						Jointing						Anthesis stage	
	Locus 1	Flanking markers	Site (cM)	Locus 2	Flanking markers	Site (cM)	AA[a]	H^2 (AA, %)[b]	AAE1	H^2 (AAE1, %)	AAE2	H^2 (AAE2)	AA[a]	H^2 (AA, %)
Culm	*Qculm5D-1*	*Xwmc630.2–Xcfd40*	0	*Qculm7B-2*	*Xwmc581–Xbarc050*	7.3	−0.01	0.52	−0.01	0.23	0.01	0.23		
	Qculm5D-3	*Xbarc1097–Xcfd8*	28.4	*Qculm7B-2*	*Xwmc581–Xbarc050*	7.3	−0.03	2.39						
	Qculm1B-16	*Xcfd21–Xcwem9*	37.4	*Qculm2A-18*	*Xwmc455–Xgwm515*	80.7							0.15	8.89
Leaves	*Qleaves5A-2*	*Xbarc180–Xcwem40*	30.6	*Qleaves7B-5*	*Xwmc273.1–Xcfd22.1*	12.7	0.01	0.53	−0.01	2.36	0.01	2.44		
	Qleaves4A-10	*Xbarc327–Xbarc078*	38.8	*Qleaves6B-7*	*Xwmc415-Glub*	53.2							0.03	13.11
Plant	*Qplant2D-7*	*Xgwm539–Xcfd168*	68.4	*Qplant3A-4*	*Xbarc86–Xwmc21*	86.5	0.01	0.18	−0.03	2.49	0.03	2.22		
	Qplant2D-7	*Xgwm539–Xcfd168*	68.4	*Qplant3A-10*	*Xwmc489.3–Xcfa2134*	98.7	−0.03	2.81	−0.01	0.28	0.01	0.28		
	Qplant2D-15	*Xcfd50–Xgwm311.1*	132.3	*Qplant5B-4*	*Xwmc160–Xgdm116*	21.4	−0.03	2.83						
	Qplant2D-16	*Xgwm311.1–Xwmc658.1*	186.5	*Qplant5B-4*	*Xwmc160–Xgdm116*	21.4	−0.02	0.59						
	Qplant6A-9	*Xwmc553–Xgwm732*	81.5	*Qplant6B-13*	*Xwmc737–Xswes679.2*	70.8	−0.02	1.05	−0.01	0.18	0.01	0.18		
	Qplant1B-11	*Xbarc312–Xcfe023.1*	36.1	*Qplant2A-18*	*Xwmc455–Xgwm515*	80.7							0.17	8.88
	Qplant2B-17	*Xbarc101–Xcwem55*	84.4	*Qplant7A-1*	*Xwmc593–Xbarc157.2*	4.0							0.17	9.27

[a]Positive value indicates that the effect of the parental two-loci genotype is greater than the recombinant, and a negative value means that the parental effect is less than the recombinant
[b]Contribution explained by epistatic QTL; other abbreviations are the same as in Table 6.9

Two pairs of epistatic QTLs affected DMA in leaves were detected (one at each growth stage). The *Qleaves4A-10/Qleaves6B-7* pair, with positive effects, explained 13.11 % of the phenotypic variation.

Seven pairs of epistatic QTLs affected DMA in plants. These included four pairs only for epistatic effects, and three pairs involved in both epistatic and E-QEI effects at jointing. Two pairs of epistatic QTL with positive effects explaining variation of 8.88 and 9.27 % were identified in the anthesis stage. No major loci were involved.

6.1.3.2.3.3 Distribution of the Additive and Epistatic QTLs

Overall, 16 chromosomes carried 18 additive QTLs for the four traits (Table 6.11, Fig. 6.5). An interesting feature was the highly concentrated distribution of additive QTLs in a few chromosomal regions, and the existence of QTL hot spots, namely chromosomal regions shared by multiple QTLs. For example, the additive QTLs involved in DMA in culms and plants, *Qculm1D-2* and *Qplant1D-2*, *Qculm3B-21* and *Qplant3B-2*, and *Qculm5D-10* and *Qplant5D-10*, were identified within the same chromosomal intervals, viz. XWMC222–XGDM60, XWMC307–XGWM566, and XBARC320–XWMC215, respectively. Some QTL clustering occurred in neighboring marker intervals, e.g., flanking markers XCFD101 to XWMC215 were shared by QTLs for DMA in culms, leaves, and plants on chromosome 5D. Similarly, clustered groups were also found for loci associated with the 12 pairs of epistatic QTLs (Table 6.12, Fig. 6.5), further increasing the locus densities in clustered regions.

6.1.4 Research Progress of Photosynthetic Characters QTL Mapping and Comparison of the Results with Previous Studies

6.1.4.1 Research Progress of Wheat Photosynthesis QTL Mapping

Cao et al. (2004) detected 16 QTLs for chlorophyll content under nitrogen (N) sufficient environment and N deficient environment. Yang et al. (2007) analyzed the QTL for chlorophyll fluorescence and related traits under conditions of rainfed and well-watered and reported that a total of 18 additive QTLs, including 11 QTLs detected under rainfed condition and seven QTLs detected under well-watered condition were located on eight chromosomes 1A, 5A, 6A, 7A, 1B, 3B, 4D, and 7D. The variance explained by the QTLs ranging from 7.27 to 72.72 % depended on the traits. Four QTLs controlling Chlorophyll b under two water regimes were located on chromosomes 1A, 5A, and 7A. Only one QTL for Fo was detected under rainfed condition and was located on chromosome 1B. One QTL of each water regime involved in Fm were identified and located separately on chromosomes 7A and 1B. Two QTLs for Fv under rainfed condition were detected and located on chromosomes 7A and 7D, respectively. No epistatic QTL was

identified for Chlorophyll b under two water regimes, for Fm under rainfed condition, as well as for Fo and Fv/Fo under the well-watered condition. In this research, there was no QTL controlling one given trait to be mapped on the same marker interval under two water regimes. Therefore, the results imply that there were different QTL expression patterns under different water conditions. More QTLs were revealed in stress conditions than in non-stressed conditions, suggesting that environmental stress can induce the expression of genes originally keeping silent under non-stressed conditions to alleviate plant damages from environmental stress. Cao et al. (2004), Li et al. (2013), Czyczyło-Mysza et al. (2013), Vijayalakshmi et al. (2010) and Ali et al. (2013) analyzed QTLs for some traits, i.e., chlorophyll, fluorescence, PS parameters, carotenoid, flag leaf senescence in wheat.

So far, scholars at home and abroad have studied wheat photosynthesis and related traits at different growth stages and that under different environments using RIL, DH, and other populations. QTL for about 11 traits related to photosynthesis and physiology were analyzed, and 224 QTLs were obtained conferring different traits. Among them, 101 QTLs whose effect is greater than 10 % were detected, furthermore, the highest contribution to phenotypic variation was 49.59 % (Table 6.13). Those QTLs referred to 21 chromosomes, especially 24 QTLs were found on chromosome 6B, which had the largest number of QTLs, followed by chromosome 5B (23 QTLs were detected) and chromosome 2D (19 QTLs). It can be seen, chromosomes 2D, 5B, and 6B were very important to traits related to photosynthesis and physiology of wheat.

6.1.4.2 Comparison of the Results with Previous Studies

QTL conferring Fm distributed on chromosome 1A, which were detected in this study, was nearby *QRaw.ipk-1A*, which also controlled Fm, detected by Börne et al. (2002). The QTL controlling Ci/Cr on chromosome 4A was near by the QTL associated with cereal protein content (Cao et al. 2004). The QTLs (*qCHO-5B* and *qCHN-5B*) conferring chlorophyll content detected in this study, which nearby *QTgwg.cgb-5B* controlling thousand seeds weight at grain filling stage. Meanwhile, QTLs for thousand seeds weight, yield, and protein content were also detected on the similar loci (Groos et al. 2003). *QPn4D-11*, *QE4D-11,* and *QGs4D-11* detected on chromosome 4D were adjacent to the QTL for Fv/Fo (Yang et al. 2007). Su et al. (2006) mapped major QTLs controlling grain yield on chromosome 3B in winter wheat, and in this study, *QCulmc.sau-3B*, *QLeavesc.sau-3B* and *QPlantc.sau-3B*, were detected on the same chromosome. In addition, the loci *QLeavesc.sau-2A*, *QPlantc.sau-4B,* and *QFv/fmc.sau-5A* coincided with loci for grain weight per ear and post-anthesis DMA per culm (Su et al. 2006; Huang et al. 2003; Quarrie et al. 2005). These indicate that most of the QTLs associated with photosynthesis and related traits were in accordance with the previous results. Meanwhile, many QTLs for some traits, which were not determined before, and QTLs, which were not identified, were also detected in this study (see the previous paper and Table 6.13).

Table 6.13 Summary of QTL of wheat photosynthetic physiology (PVE > 10 %)

Environment	Trait	QTL	Flanking markers	PVE (%)	Population	Reference
Nitrogen supply with 4.0 mmol/l	Chl	*qCHO-2Ba*	Xfbb62–Xfba272	10.85	RIL	Cao et al. (2004)
		qCHO-7D	Xfba8–Xbcd1872	13.45		
Nitrogen supply with 0.4 mmol/l	Chl	*qCHN-6A*	Xpsr312–Xfbb145	11.73		
	SOD activity	*QSod.sdau-2D*	Xissr859a–Xswes624e	16.64	RIL	Wei et al. (2007)
	POD activity	*QPod.sdau-4A*	Xissr23b–Xwmc308	49.56		
Normal	Fv/Fm	*QFv/Fm.csdh-2A**	gwm339	12	DH	Czyczyło-Mysza et al. (2013)
		*QFv/Fm.csdh-6A**	csb112(Dhn5)	13.8		
		*QFv/Fm.csdh-7A.2**	barc108a	12.8		
		*QFv/Fm.csdh-2D.3**	gwm349	17.7		
	PI	*QPI.csdh-3A.1**	cfa2234	12.8		
		*QPI.csdh-4A**	gwm30b	11.2		
		*QPI.csdh-5A**	psp3003b	13.3		
		*QPI.csdh-4B.1**	Rht-B1	18.4		
		*QPI.csdh-6B.1**	wPt-2424	11.4		
		*QPI.csdh-4D**	wPt-5809	24.6		
	ABS/CSm	*QABS.csdh-1A.1*	m51p65.5	10.7		
		*QABS.csdh-1A.2**	wPt-731617	10.9		
		*QABS.csdh-2B**	wPt-8776	12.2		
		*QABS.csdh-5B.2**	psp3037	13		
		QABS.csdh-5B.3	wPt-1548	10.9		

(continued)

Table 6.13 (continued)

Environment	Trait	QTL	Flanking markers	PVE (%)	Population	Reference
		*QABS.csdh-6B.1**	wPt-2424	14.3		
		*QABS.csdh-6B.3**	wPt-2564	13.1		
		QABS.csdh-3D	wPt-732092	10.5		
	TRo/CSm	*QTRo.csdh-1A.1**	wPt-731617	11.6		
		*QTRo.csdh-2B**	m65p64.5	12.1		
		QTRo.csdh-5B.2	psp3037	12.2		
		*QTRo.csdh-5B.3**	psr806.2	16		
		*QTRo.csdh-5B.4**	wPt-1548	15		
		*QTRo.csdh-6B.3**	wPt-2564	13.1		
	ETo/CSm	*QETo.csdh-6A**	wPt-667844	10.9		
		*QETo.csdh-6B.1**	wPt-2424	20.5		
		*QETo.csdh-6B.2**	wg232.4	21.7		
		*QETo.csdh-6B.3**	wPt-2564	20.2		
		*QETo.csdh-4D**	wPt-5809	23.8		
		*QETo.csdh-7D.1**	wPt-744354	14.3		
		*QETo.csdh-7D.2**	gwm37	10		
	DIo/CSm	*QDIo.csdh-5A*	Vrn-A1	10.9		
		*QDIo.csdh-5B.1**	wPt-5346	12.3		
		*QDIo.csdh-5B.2**	wmc73	15		
		QDIo.csdh-5B.3	wPt-5737	10.3		
		*QDIo.csdh-1D.3**	wPt-4671	18.5		
		*QDIo.csdh-7D.1**	wPt-744354	15.1		
	RC/CSm	*QRC.csdh-3A**	cfa2234	14.4		
		*QRC.csdh-4B**	Rht-B1	20.7		

(continued)

Table 6.13 (continued)

Environment	Trait	QTL	Flanking markers	PVE (%)	Population	Reference
		*QRC.csdh-5B**	wPt-5346	15.2		
		*QRC.csdh-7D**	barc154	17.6		
	chla + b	*Qchla + b.csdh-3B**	wPt-1682	11.5		
		*Qchla + b.csdh-2D.1**	wPt-6574	22.4		
		*Qchla + b.csdh-2D.2**	wPt-730613	16.7		
		*Qchla + b.csdh-2D.3**	gwm349	13		
	SPAD	*QSPAD.csdh-1B.1**	wPt-2389	15		
		*QSPAD.csdh-1B.2**	wPt-3451	11.6		
		*QSPAD.csdh-4B.1**	Rht-B1	15.6		
		*QSPAD.csdh-6B.2**	gwm191	13.6		
		*QSPAD.csdh-6B.3**	wPt-2564	13.5		
		*QSPAD.csdh-2D**	wPt-6574	17.4		
	Car	*QCar.csdh-3A.1**	wPt-2478	11		
		*QCar.csdh-3A.2**	wPt-4569	14.2		
		QCar.csdh-3D.1	dupw173	10		
		QCar.csdh-3D.2	wPt-4569	32		
		*QCar.csdh-4D**	psr375.1	12.3		
		*QCar.csdh-6D.1**	wPt-665675	13.4		
		*QCar.csdh-6D.3**	wPt-732626	13.8		
	DWP	*QDWP.csdh-5A**	wPt-668257	11.3		
		*QDWP.csdh-4B.2**	psp3030b	14.7		
		*QDWP.csdh-3D**	dupw173	11.6		
	Chl	*QcChl2.2*	HVM54	12.8/13.6	RIL	Guo et al. (2008) (Barley)

(continued)

Table 6.13 (continued)

Environment	Trait	QTL	Flanking markers	PVE (%)	Population	Reference
		QcChl4.1	p71m88-02	10.2/9.6		
	CFL	*qFC2.2*		20.2	DH	Xue et al. (2008) (Barley)
	MRS	*Qmrso.ksu-5A*	GTG.AGC-254- CGA. CGCT-485	12	RIL	Vijayalakshmi et al. (2010)
		Qmrso.ksu-6A	CAG.AGC-101- AGG. CTT-212	26		
		Qmrsh.ksu-2A	Xgwm356- CGT. TGCG-349	19		
		Qmrsh.ksu-2A	CGT.TGCG-349- CTCG. ACC-242	21		
	TMRS	*Qtmrso.ksu-3B*	CGT.CTCG-146- GTG. AGCT-206	18		
		Qtmrso.ksu-7B	Xbarc340–Xgwm43	12		
		QTmrsh.ksu-2A	Xgwm356-CGT. TGCG-349	17		
		QTmrsh.ksu-6A	CGT.GTG-343- CGA. CGCT-406	30		
	PGMS	*Qpgmso.ksu-4B*	Xgwm368-Xksum62	17		
	Fv/Fm	*QFv/Fmh.ksu-7A*	CGA.CGCT-272-Xbarc121	11		
	Chl at 4 DPA	*QChlc.tamu-1B*	Xbarc128	22.5		Ali et al. (2013)
	Chl at 8 DPA	*QChlc.tamu-1B*	Xbarc128	45.3		

Note: *Fv/Fm* the maximum photochemical efficiency; *PI* overall performance index of PSII photochemistry; *ABS/CSm* light energy absorption; *TR/CSom* amount of excitation energy trapped in PSII reaction centers; *ET/CSom* amount of energy used for electron transport; *DI/CSom* energy amount dissipated from PSII; *RC/CSm* number of active reaction centers; chl a+b The concentrations of total chlorophyll a + b; *SPAD* chlorophyll meter readings; *Car* carotenoids; *DWP* dry weight per plant at harvest; *CFL* chlorophyll content of flag leaf; *MRS* maximum rate of senescence; *TMRS* time to maximum rate of senescence; *PGMS* percent greenness at maximum senescence; *DPA* days post-anthesis

6.2 QTL Conferring Microdissection Characteristics of Wheat Stem

The structure of stem was closely related to lodging resistance of wheat and consists of epidermis, mechanical tissue, elementary tissue, vascular bundle, and pith. Furthermore, the vascular bundle plays an important role in transportation of photosynthetic products, mineral nutrients, and water. The number, size, and capacity of the vascular bundle influence the transportation ability, especially for photosynthetic products. The number and area of the vascular bundles are the basis of large sink and free flow. The growth of vascular bundle is affected by both variety and growing environment, and very complex. In wheat breeding practice with high yield, the relationship between structure of vascular bundle in stem, and size, and plumpness of grain becomes one of the important tissues for research. The capacity of the vascular bundle system transporting assimilates from the source to the sink may be one of the limiting factors for crop yield. Therefore, there is important significance for improving lodging resistance and yield in wheat by studying the structure of vascular bundle in stem.

6.2.1 QTL Mapping for Anatomical Traits of Second Basal Internode

6.2.1.1 Materials and Methods

6.2.1.1.1 Materials

Materials and Planting were same as one of the Sect. 6.1.1.1.1 in this chapter.

6.2.1.1.2 Field Trails

The field trials were conducted on the experimental farm at Shandong Agricultural University (Tai'an, China, 36°9′N, 117°9′E) and Jiyuan Agricultural Science Institute (Jiyuan, Henan province, 35°5′N, 112°38′E) in 2008–2009 and 2009–2010. And nine different environmental conditions were set, as follows:

2008–2009, one normal environmental condition was set in Jiyuan, and four environmental conditions (normal, rainfed, well-watered, and late-sowing) were set in Tai'an. While, in 2009–2010, one normal environmental condition was also set in Jiyuan, and three environmental conditions (normal, rainfed, and well-watered) were set in Tai'an.

In the autumn of 2008, the test materials were sowed on October 6–8 in the normal, rainfed, and well-watered conditions, and they were sowed on November

22 in the late-sowing condition. While in the autumn of 2009, the sowing date was October 4–7 in the normal, rainfed, and well-watered conditions.

All DH lines and parents were grown in a plot with four rows in 2-m length, 26.7 cm between rows and 2.2 cm between plants. And the basic seedling number was about 120,000.

For normal condition, crop management was carried out following the local practice. At jointing and anthesis stages, 225 and 75 kg/ha of urea were added, respectively. Meanwhile, plots were irrigated before winter and at jointing and anthesis. For rainfed condition, crop management was carried out following the normal practice. At jointing and anthesis, 225 and 75 kg/ha of urea were added, respectively. However, there was no irrigation during the whole growth period. For well-watered condition, crop management was also carried out following the normal practice. And plots were irrigated before winter and at jointing and anthesis. However, no fertilizer was applied at jointing and anthesis. For late-sowing condition, crop management was also carried out following the local practice, but the sowing date was delayed.

6.2.1.1.3 Determining Methods

6.2.1.1.3.1 Hanging Tag

At the beginning of May, main stems (flowered on the same day) in the center of every plot were marked.

6.2.1.1.3.2 Sampling

The transverse hand section was made for 2 cm in the middle of the second basal internode at milk-spike stage.

6.2.1.1.3.3 Fixing and Saving

The materials were put into carnoy's fluid, immediately and were extracted until no air bubbles were appeared. Then, carnoy's fluid was changed and air was extracted. After that, the materials were stored at 0–4 °C for use.

6.2.1.1.3.4 Section

Settled segment of stem was sectioned to slices with about 20 μm thickness (less than two layers of cells) by using thin razor.

6.2.1.1.3.5 Microscopy

Better sections were selected under the microscope and then dyed.

6.2.1.1.3.6 Dyeing

The selected sections were stained for 3 min using safranin, rinsed for 1 min, and again stained for 15 s using Fast Green, and then rinsed.

6.2.1.1.3.7 Microscopy

A drop of distilled water was taken on the glass slide, and the dyed sections were put on the glass slide and then observed using low power lens (Nikon YS100). Finally, the poorly dyed sections were rejected.

6.2.1.1.3.8 Photographing

Cover glass was put on the selected sections and photographed in DP71 high resolution by using microscope (Olympus BX51).

6.2.1.1.3.9 Statistics

The stem diameter (SD) for basal internode was measured, and matching parameter was set, and then the stem anatomical structure-related traits such as the number of large and small vascular bundle (LVB, SVB), culm wall thickness (CWT), and the pith diameter (PD) were measured by using the graphic program Image-pro Plus 6.0.

6.2.1.2 Result and Analysis

6.2.1.2.1 Variation of Phenotype

Five traits for anatomical structure of the second basal internode including the number of LVB, the number of SVB, SD, CWT, and PD were analyzed by using the DH population. The variations of phenotypic data of five traits related to the second basal internode in four environments for two years were summarized in Table 6.14.

Huapei 3 had the higher values of anatomical traits than Yumai 57 in Jiyuan and Tai'an (late-sowing condition) in 2008–2009, and in Tai'an (normal condition) in 2009–2010. However, Yumai 57 had the higher values in Tai'an (normal condition) in 2008–2009. The ranges of variation of the test traits were large, which was in accordance with normal distribution and the distribution was continuous. Meanwhile, a transgressive separation was found from the DH lines. Therefore, the phenotypic data were suitable for QTL analysis.

Table 6.14 Phenotypic values of the anatomical traits in the DH population

Env.	Trait	Parent		DH population					
		HP3	YM57	Min	Max	Average	SD	Skew	Kurt
E1	LVB	44.75	42.5	34.3	47	40.4	2.59	0.2	−0.04
	SVB	21	25	12.3	31.8	20.79	3.94	0.37	−0.07
E2	LVB	41.25	40.25	30	48	39.78	3.03	0.13	0.69
	SVB	22.5	19.25	11.75	33	20.81	3.99	0.38	−0.09
E5	LVB	33	35.75	26	41	32.9	2.94	0.04	−0.1
	SVB	16	25.25	13	26	18.25	2.6	0.17	−0.11
E7	LVB	37	39.57	31	45	37.27	2.59	0.06	0.05
	SVB	18.86	22.29	13	30	20.82	3.57	0.17	−0.38
E1	SD	4.79	5.06	3.52	5.71	4.63	0.39	0.31	0.26
	CWT	0.54	0.57	0.37	0.66	0.5	0.05	0.5	0.22
	PD	3.72	3.92	2.71	4.44	3.62	0.35	0.05	−0.29
E2	SD	4.56	4.36	3.52	5	4.12	0.3	0.42	−0.18
	CWT	0.41	0.41	0.34	0.52	0.4	0.03	0.77	0.61
	PD	3.75	3.55	2.73	4.16	3.32	0.28	0.35	−0.13
E5	SD	3.68	3.75	2.99	4.26	3.63	0.25	0.12	−0.17
	CWT	0.39	0.41	0.33	0.56	0.43	0.05	0.29	−0.14
	PD	2.91	2.92	2.21	3.37	2.77	0.22	0.3	0.22
E6	SD	4.31	4.11	3.36	4.94	4.15	0.27	0.03	0.33
	CWT	0.8	0.63	0.39	1.3	0.63	0.14	1.19	3.26
	PD	2.71	2.85	1.82	3.79	2.88	0.38	−0.19	0.2
E7	SD	3.75	4.49	3.39	5.11	4.17	0.31	0.4	0.09
	CWT	0.86	0.67	0.52	1.46	0.83	0.17	0.81	0.78
	PD	2.03	3.16	1.18	4	2.51	0.48	0.04	0.01
E8	SD	4.06	4.01	3.26	4.59	3.88	0.28	0.35	−0.32
	CWT	0.66	0.49	0.34	1.02	0.54	0.09	1.3	4.25
	PD	2.75	3.04	1.44	3.72	2.79	0.35	−0.26	1.19

LVB large vascular bundles; *SVB* small vascular bundles; *SD* stem diameter; *CWT* culm wall thickness; *PD* pith diameter; E1, Jiyuan, Henan province in 2008–2009 under normal environment; E2–E5, Tai'an, Shandong province in 2008–2009 under normal, rainfed, irrigation, late-sowing environment, respectively; E6, Jiyuan, Henan province in 2009–2010 under normal environment; E7–E9, Tai'an, Shandong province, in 2009–2010 under normal, rainfed, irrigation environment, respectively. The same as below

6.2.1.2.2 QTL Mapping and Effect Analysis of Anatomical Structure of the Second Basal Internode

A total of five QTLs conferring LVB on chromosomes 5D and 4D were detected in two years in four different environmental conditions (Table 6.15). Among them, the QTL on chromosome 5D detected in Jiyuan in 2008–2009 had the highest contribution, accounting for 13.69 % of phenotypic variation. A total of seven QTLs for SVB on chromosomes 1B, 5B, 6A, and 7D were identified, and the QTL detected in

Table 6.15 The additive effects for vascular bundle number of the second basal internode

Env.	Trait	Chromosome	Flanking marker	Site	Range	A	*P* value	h^2(a) %
E1	LVB	5D-11	Xwmc215–Xbarc345	77.3	63.2–84.3	−1.1724	0.0000	13.69
	SVB	1B-6	Xbarc119–Xgwm18	33.8	27.7–34.5	−1.6968	0.0000	17.12
		6A-4	Xbarc1077–Xbarc1165	41.2	35.5–42.2	−0.8242	0.0019	3.48
E2	LVB	4D-8	Xbarc190–Xbarc1009	165.5	156.7–172.4	−0.9156	0.0000	8.27
		5D-10	Xbarc320–Xwmc215	66.2	60.5–84.3	−1.1546	0.0000	11.37
	SVB	5B2-1	Xbarc36–Xbarc140	14.0	6.0–20.1	−1.5074	0.0000	10.87
E5	LVB	5D-2	Xcfd40–Xbarc1097	2.4	0.0–6.4	−0.8399	0.0000	10.39
	SVB	1B-7	Xgwm18–Xwmc57	34.5	25.7–34.9	−0.6899	0.0000	8.54
		1B-25	Xswes158–Xswes650	126.1	110.4–130.6	−0.7139	0.0001	7.80
		6A-8	Xbarc1055–Xwmc553	50.7	43.7–63.2	−0.9192	0.0000	9.28
E6	LVB	4D-10	Xbarc237–Xcfe254	169.4	164.3–177.4	−0.8101	0.0001	8.25
	SVB	7D-5	Xgwm676–Xgwm437	117.9	104.3–124.9	1.3033	0.0000	10.58

From E1 to E6 as the same as Table 6.14

Jiyuan condition in 2008–2009 had the highest contribution, accounting for 17.12 % of phenotypic variation. Meanwhile, the locus had the highest value of additive effect, which could increase the number of SVB by 1.69. In addition to the QTL controlling SVB on chromosome 7D, the positive alleles all came from Yumai 57.

The QTLs conferring LVB on chromosomes 5D and 4D and the QTLs conferring SVB on chromosomes 6A and 1B were detected twice in the four environmental conditions, accounting for 10.39–11.36, 8.25–8.27, 3.48–9.28, and 8.54–17.12 % of phenotypic variation, respectively. Other QTLs for the number of vascular bundle detected in this study were only one time and had poor reproducibility.

A total of seven QTLs controlling SD of the second basal internode on chromosomes 1A, 1B, 2D, 4B, and 5D were detected; furthermore, the QTL on chromosome 5D, which was detected in Jiyuan condition in 2008–2009, had the highest contribution, accounting for 15.49 % of phenotypic variation, and its additive effect was also the highest, which could increase SD by 0.19 mm (Table 6.16). In addition to the QTL conferring SD on chromosome 1A, the positive alleles of other QTLs all came from Yumai 57.

For CWT, seven QTLs on chromosomes 1B, 3D, 5B, and 6A were detected, and the QTL on chromosome 1B, detected in Jiyuan condition in 2008–2009, had the highest contribution, accounting for 13.41 % of phenotypic variation. Except for the QTL on chromosome 6A, positive alleles of other QTLs all originated from Yumai 57.

For PD, eight QTLs on chromosomes 1B, 2A, 2D, 3D, 4D, and 5D were detected, and the QTL detected in Jiyuan condition in 2008–2009 had the highest contribution, explaining 20.95 % of phenotypic variation. Except for the QTLs conferring PD on chromosomes 1B, 2D, and 5D, the positive alleles of other QTLs all came from Huapei 3.

The QTLs for SD and SWT on chromosome 1B stably express in all conditions in 2008–2009, but were not identified in all conditions in 2009–2010.

Table 6.16 Estimated the additive effect for SD, CWT, and PD in the DH population

Env.	Trait	Chromosome	Flanking marker	Site	Range	A	*P* value	h^2 (a) %
E1	SD	1B-6	Xbarc119–Xgwm18	33.8	33.0–34.5	−0.1167	0.0000	4.95
		2D-4	Xcfd53–Xwmc18	16.6	0.9–29.6	−0.1505	0.0000	8.12
		5D-10	Xbarc320–Xwmc215	64.2	58.5–69.2	−0.1910	0.0000	15.49
	CWT	1B-13	Xbarc372–Xwmc412.2	36.1	35.2–36.1	−0.0200	0.0000	13.41
	PD	2D-4	Xcfd53–Xwmc18	18.6	0.9–31.6	−0.1300	0.0000	6.91
		3D-11	Xwmc631–Xbarc071	86.0	77.3–93.9	0.0914	0.0002	11.33
		5D-10	Xbarc320–Xwmc215	66.2	62.2–76.3	−0.1655	0.0000	20.95
E2	SD	1B-2	Xwmc406–Xbarc156	28.7	24.0–33.0	−0.1111	0.0000	11.08
	CWT	1B-12	Xcfe023.1–Xbarc372	36.1	36.1–37.0	−0.0104	0.0000	9.65
	PD	1B-2	Xwmc406–Xbarc156	27.7	9.0–33.0	−0.0711	0.0006	9.48
		2D-3	Xwmc112–Xcfd53	0.9	0.0–22.6	−0.0714	0.0002	8.62
E5	SD	1B-9	Xcwem6.1–Xwmc128	34.9	33.8–35.2	−0.0852	0.0000	11.37
	CWT	1B-4	Xwmc31–Xwmc626	33.0	30.7–34.9	−0.0129	0.0000	6.79
		5B1-5	Xgwm213–Xswes861.2	68.1	53.1–68.1	−0.0144	0.0000	8.21
		6A-9	Xwmc553–Xgwm732	70.2	59.2–83.4	0.0166	0.0000	9.20
	PD	7A-4	Xbarc070–Xbarc250	23.5	18.8–36.5	0.0632	0.0001	8.08
E6	SD	1A-5	Xwmc550–Xbarc269	44.3	29.4–53.6	0.1109	0.0000	13.47
E7	SD	4B-7	Xwmc48–Xbarc1096	18.4	14.7–18.4	−0.0863	0.0002	7.92
	CWT	6A-8	Xbarc1055–Xwmc553	46.7	40.5–54.2	0.0152	0.0000	9.62
E8	CWT	3D-10	Xbarc323–Xwmc631	82.0	75.3–88.0	−0.0333	0.0000	12.84
	PD	2A-17	Xgwm448–Xwmc455	74.6	71.7–79.6	0.1035	0.0001	9.71
		4D-1	Xwmc473–Xbarc334	0.0	0.0–9.0	0.0881	0.0004	7.99

From E1 to E6 as the same as Table 6.14

For the QTLs conferring PD detected in 2009–2010, only the QTL on chromosome 2D was detected in the two environments, while other QTLs were detected only one time in different environmental condition.

6.2.2 QTL Mapping for Anatomical Traits of the Uppermost Internode

6.2.2.1 Materials and Methods

6.2.2.1.1 Materials

The test materials were the same as the previous paper for the second basal internode.

6.2.2.1.2 Field Trails

Field trials were conducted in 2006–2007 and 2007–2008 in Tai'an, Shandong province, China. The experimental field design consisted of a randomized block

design with two replications. One environment (environment I) was conducted in 2006. All lines and parents were grown in 2-m-long four-row plots (25 cm apart). Crop management was carried out following the local practices, which were irrigation in wintering, jointing, anthesis, and grain filling stages. An additional 225 and 75 kg/ha of urea were top-dressed at jointing and anthesis, with irrigation, respectively. The total water (millimeter) (rainfall 122.0 mm; irrigation 270.0 mm) and accumulated temperature days were 2605.1 °C day during the whole life of the wheat. Three environments (environment II–IV) were conducted in 2007 in the same soil conditions. The total water (mm) (rainfall 172.5 mm; irrigation 180.0 mm) and accumulated temperature days were 2362.5 °C day during the whole life of the wheat. The management of ground fertilizers, irrigation, and top-dressed fertilizers of environment II was the same as that of environment I; the management of ground fertilizers and irrigation of environment III was the same as that of environment I, but there was no top-dressed urea applied at the jointing and anthesis stages; the management of ground fertilizers and top-dressed urea of environment IV was the same as that of environment I, but there was no irrigation during the wheat's entire growing season.

6.2.2.1.3 Determining Methods

At anthesis stage, three main stems (flowered on the same day) in the center of every plot were selected. The lengths of uppermost internodes and the diameters at 2 cm below the neck of the spike were determining by using ruler and vernier caliper, respectively. Furthermore, 2 cm of uppermost internodes were put in stationary liquid (absolute ethyl alcohol/glacial acetic acid = 3/1) for 4–10 h, and then put in 70 % ethanol in the refrigerator. The numbers of large vascular bundles (LVB) located in the inner parenchyma of the stem (with diameters equal to or greater than 10 μm) were recorded, and the numbers of total vascular bundles (TVB) were counted with a Nikon YS100 (Nikon Co. Ltd, Nanjing, China) microscope (magnified 100×). According to TVB = LVB + SVB, the numbers of small vascular bundles (SVB) and the ratios of large to small vascular bundles (L/S) were calculated (Fig. 6.6). Mean values were used for the data analysis.

6.2.2.2 QTL Mapping for Anatomical Traits of the Uppermost Internode

6.2.2.2.1 Variation of Phenotypic Data of Uppermost Internode-Related Traits

Huapei 3 is a weak spring and precocity variety, while Yumai 57 is a semi-winterness and medium maturing variety. All lines and parents were planted in October 2006 and 2007 on experimental farm in Shandong Agricultural University. And four environmental conditions including environment I (normal

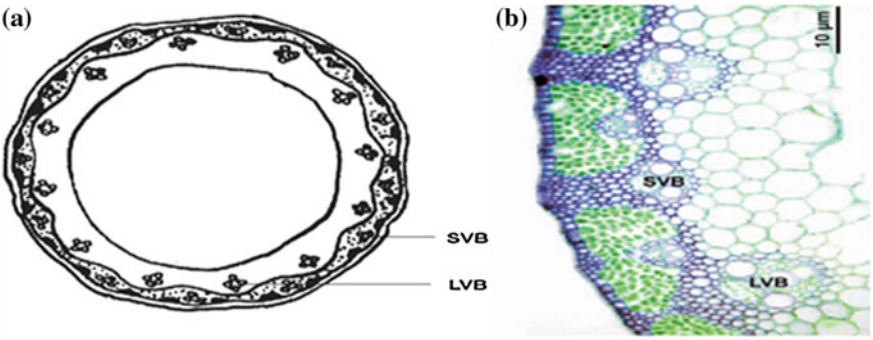

Fig. 6.6 The diagram and microscope structure of the internode in wheat **a** transverse section structure of wheat internode; **b** magnified structure of uppermost internode in wheat (magnified 200). *LVB* large vascular bundles; *SVB* small vascular bundles

irrigated and top-dressed urea in 2007), environment II (normal irrigated and top-dressed urea in 2008), environment III (normal irrigated but no top-dressed urea in 2008), and environment IV (no irrigated but top-dressed urea in 2008) were set. There were obvious differences in uppermost internode length (UIL), the number of total vascular bundles (TVB) and the number of small vascular bundles (SVB) between the parents. And the frequency distributions for eight traits (UIL, UID, CWT, CWA, TVB, LVB, SVB, and L/S) examined in the DH population of wheat exhibited continuous variations and more or less normal distributions with transgressive segregation, indicating that all the eight traits are quantitative traits controlled by polygenes (Table 6.17 and Fig. 6.7), and their quantitative nature which is suitable for QTL mapping.

6.2.2.2.2 QTL Mapping and Effect Analysis of Uppermost Internode-Related Traits

QTL conferring eight traits associated with morphological anatomy of uppermost internode were performed by using the software QTL Network 2.0 based on a mixed linear model. A total of 20 additive QTLs and one pair of epistatic QTL on chromosomes 1A, 1B, 2A, 2D, 3D, 4D, 5D, 6A, 6D, and 7D were detected (Table 6.18 and Fig. 6.7).

6.2.2.2.2.1 QTL Mapping for UIL

Three additive QTLs for UIL, located on chromosomes 1B, 4D, and 7D (Table 6.18 and Fig. 6.7) were detected and expressed differently in the four environments. In environment I, two QTLs on chromosomes 4D and 7D were detected; in environment

Table 6.17 Phenotypic performance of vascular bundle system under four environments

Trait	Env.	Hupei 3	Yumai 57	DH population					
				Mean	Max	Min	SD	Skewness	Kurtosis
UIL (cm)	EI	30.17	25.77	24.35	35.15	12.50	5.16	−0.11	−0.60
	E II	28.77	25.93	25.28	36.53	13.97	5.28	−0.00	−0.91
	E III	26.37	24.87	25.26	38.10	12.30	5.01	−0.14	−0.62
	E IV	27.97	25.30	23.96	33.83	12.50	4.88	0.00	−0.76
UID (mm)	E I	2.73	2.33	2.56	3.28	1.71	0.32	−0.07	−0.37
	E II	2.68	2.55	2.55	3.17	2.00	0.21	0.16	0.28
	E III	2.40	2.36	2. 42	3.35	1.85	0.25	0.60	0.90
	E IV	2.42	2.32	2. 24	3.18	1.67	0.23	0. 87	1.81
CWT (μm)	E I	390.0	368.3	406.8	560.0	290.0	50.05	0.27	−0.18
	E II	377.8	355.8	354.8	438.3	283.3	29.21	−0.00	−0.35
	E III	399.2	356.7	412.3	505.0	310.0	37.48	0.20	−0.31
	E IV	393.8	384.6	366.8	468.3	296.7	32.78	0.12	−0.15
CWA (mm^2)	E I	3.36	2.26	2.76	4.26	1.29	0.54	0.25	−0.06
	E II	2.74	2.45	2.44	3.36	1.57	0.33	0.15	−0.14
	E III	2.50	2.24	2.60	4.17	1.70	0.38	0.55	1.27
	EIV	2.50	2.00	2.16	3.45	1.41	0.32	0.71	1.33
TVB	E I	56	63	54	76	40	7.11	0.56	0.33
	E II	52	64	53	72	41	5.40	0.25	−0.04
	EIII	46	61	51	70	38	5.69	0.44	0.20
	E IV	46	60	53	73	38	5.74	0.68	0.75
LVB	E I	12	13	14	22	5	3.19	0.24	−0.05
	E II	12	14	13	20	6	2.49	0.35	0.50
	E III	11	12	12	18	7	2.28	0.30	0.08
	E IV	11	13	13	20	8	2.54	0.22	−0.20
SVB	EI	44	50	40	59	27	6.28	0.49	−0.03
	E II	40	50	41	59	29	4.90	0.23	0.28
	E III	35	49	39	57	26	5.50	0.49	0.24
	E IV	35	47	39	54	29	5.01	0.48	0.49
L/S	E I	0.27	0.26	0.36	0.67	0.11	0.10	0.50	0.12
	E II	0.30	0.28	0.31	0.53	0.16	0.07	0.50	0.19
	E III	0.31	0.24	0.31	0.59	0.13	0.08	0.54	0.40
	EIV	0.31	0.28	0.34	0.62	0.17	0.08	0.52	0.52

UIL uppermost internode length; *UID* uppermost internode diameter; *CWT* culm wall thickness; *CWA* culm wall area; *TVB* the number of total vascular bundles; *LVB* the number of large vascular bundles; *SVB* the number of small vascular bundles; *L/S* the ratio of large and small vascular bundles; *EI* normal irrigated and top-dressed urea in 2007; *EII* normal irrigated and top-dressed urea in 2008; *EIII* normal irrigated but no top-dressed urea in 2008; *EIV* no irrigated but top-dressed urea in 2008

II, three QTLs on chromosomes 1B, 4D and 7D were detected; in environment III, two QTLs on chromosomes 4D and 7D were detected; and in environment IV, the QTLs were detected on chromosomes 1B and 7D. The QTLs on chromosomes 4D and 7B were contributed by Huapei 3, and the contributions were 9.54 ∼ 22.04 %; while the

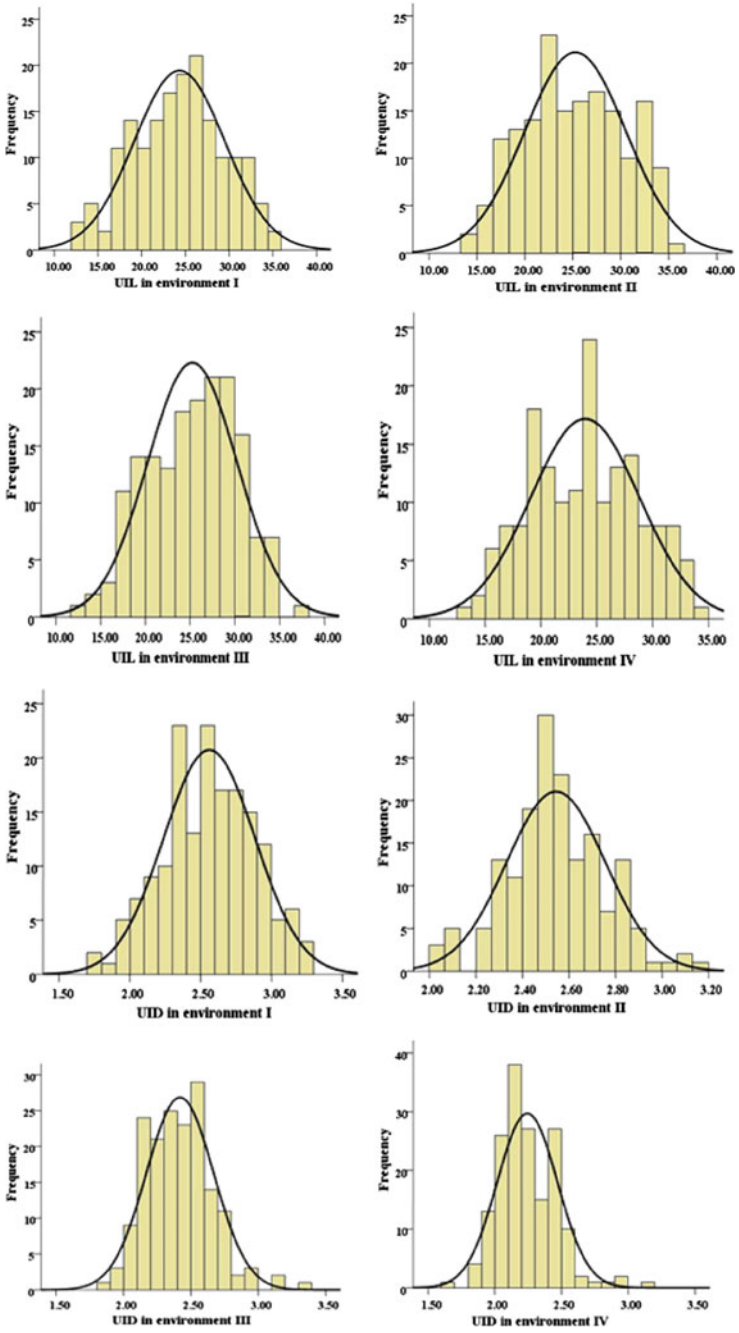

Fig. 6.7 Distribution of vascular bundle system and correlative traits of uppermost internode in DH population (environment and traits see Table 6.17)

Table 6.18 Main-effect QTL affecting TVB, LVB, SVB, and L/S in four environments

QTL Loci	Flanking marker	Position	A[a]	H^2 (A, %)[b]
QTL detected	Environment I			
q*UIL-4D*	XBARC334–XWMC331	2.1	2.21	17.19
qUIL-7D	XGWM676–XGWM437	120.9	1.84	11.97
qUID-5D	XWMC215–XBARC345	71.4	0.16	22.67
qCWA-5D	XWMC215–XBARC345	75.4	0.29	25.61
qTVB-5D	XWMC215–XBARC345	69.4	2.03	8.11
qLVB-5D	XWMC215–XBARC345	73.4	1.57	22.95
qSVB-5D-1	XCFD40–XBARC1097	2.4	−1.79	8.11
qL/S-5D	XWMC215–XBARC345	77.4	0.04	12.45
QTL detected	Environment II			
qUIL-1B	XWMC31–XWMC626	33.0	−1.43	7.08
qUIL-4D	XBARC334–XWMC331	5.1	1.66	9.54
qUIL-7D	XGWM676–XGWM437	118.9	2.05	14.49
qTVB-2D-1	XCFD53–XWMC18	1.7	−1.49	7.61
qTVB-7D	XGWM676–XGWM437	114.9	1.70	9.88
qSVB-7D	XGWM676–XGWM437	117.9	1.80	13.11
QTL detected	Environment III			
qUIL-4D	XBARC334–XWMC331	6.1	1.72	10.74
qUIL-7D	XGWM676–XGWM437	118.9	2.47	22.04
qCWT-3D	XWMC631–XBARC071	82.1	−10.97	8.52
qTVB-2D-2	XWMC112–XCFD53	1.0	−1.87	10.49
qSVB-2D	XWMC112–XCFD53	1.0	−1.52	8.96
qSVB-6A	XBARC1077–XBARC1165	41.2	−1.42	7.80
qSVB-7D	XGWM676–XGWM437	119.9	1.73	11.58
QTL detected	Environment IV			
qUIL-1B	XWMC31–XWMC626	33.0	−1.49	9.00
qUIL-7D	XGWM676–XGWM437	118.9	1.87	14.16
qTVB-1A	XWMC333–XBARC148	57.8	−2.04	12.76
qSVB-1A	XWMC333–XBARC148	57.8	−1.92	12.05
qSVB-5D-2	XBARC320–XWMC215	66.3	1.70	9.53
qSVB-7D	XGWM676–XGWM437	116.9	1.78	10.44
qL/S-7D	XGWM295–XGWM676	101.3	−0.03	15.17

Note: [a]Additive effects, a positive value indicates that allele from Hp3 increases the trait, a negative value indicates that allele from YM57 increases the trait

[b]Contribution explained by additive QTL

Environment I normal irrigated and top-dressed urea in 2007; *Environment II* normal irrigated and top-dressed urea in 2008; *Environment III* normal irrigated but no top-dressed urea in 2008; *Environment IV* no irrigated but top-dressed urea in 2008

QTLs on chromosome 1B were contributed by Yumai 57, the contributions were 7.08 ~ 9.00 %. The QTL located within XGWM676–XGWM437 on chromosome 7D had the most significant effect, explaining 22.04 % of phenotypic variation, and expressed stably in the four environments.

6.2.2.2.2.2 QTL Mapping for UID

Only one additive QTL conferring UID on chromosome 5D was detected in environment I, explaining 22.67 % of phenotypic variation. And its positive allele came from Huapei 3, increasing UID by 0.16 mm.

6.2.2.2.2.3 QTL Mapping for CWT

Only one additive QTL conferring CWT on chromosome 3D was detected in environment III, while its contribution to phenotypic variation was small. And its positive allele came from Yumai 57, increasing CWT by 10.97 μm.

6.2.2.2.2.4 QTL Mapping for CWA

Only one additive QTL for CWA on chromosome 5D was identified in environment I, explaining 25.61 % of phenotypic variation, and its additive effect was contributed by Huapei 3 alleles, increasing CWA by 0.29 mm^2.

6.2.2.2.2.5 QTL Mapping for TVB

A total of five additive QTLs for TVB were detected on chromosomes 1A, 2D (two regions), 5D, and 7D under four different environments (Table 6.18 and Fig. 6.8). Under environment I, one QTL on chromosome 5D was detected; under environment II, two QTLs on chromosome 2D and 7D were detected; under environment III, one QTL on chromosome 2D was detected; under environment IV, one QTL was detected on chromosome 1A. The additive effects of *qTVB-5D* and *qTVB-7D* were contributed by Huapei 3 alleles, and the rest were contributed by Yumai 57 alleles. The QTL detected under environment III and IV (*qTVB-1A* and *qTVB-2D-2*) had the most significant effects, explaining 12.76 and 10.49 % of the phenotypic variance, respectively.

One pair of epistatic QTL for TVB was detected on chromosome 2A and 6D (Fig. 6.9), accounting for 10.81 % of phenotypic variation and increasing by two TVBs. The epistatic QTL had no additive effect, was sensitive to environment, and only expressed in environment III.

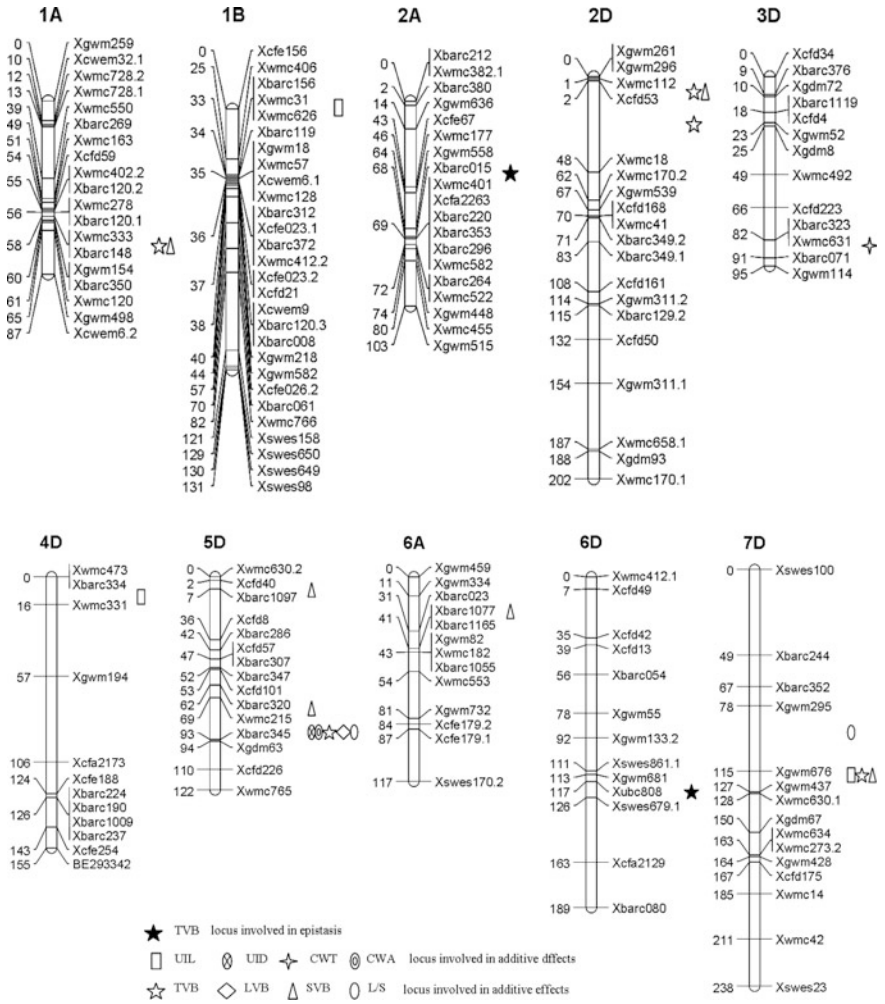

Fig. 6.8 QTL for the vascular bundle system and correlative traits of uppermost internode in SSR linkage map

6.2.2.2.2.6 QTL Mapping for LVB

Only one *qLVB-5D* for LVB was detected on chromosome 5D, contributed by Huapei 3 alleles. The *qLVB-5D* had a significant effect, accounting for 22.95 % of the phenotypic variance, and increased by two LVBs.

6.2.2.2.2.7 QTL Mapping for SVB

A total of six additive QTLs conferring SVB were detected on chromosomes 1A, 2D, 5D (2 regions), 6A, and 7D (Table 6.18 and Fig. 6.8). Under environment I,

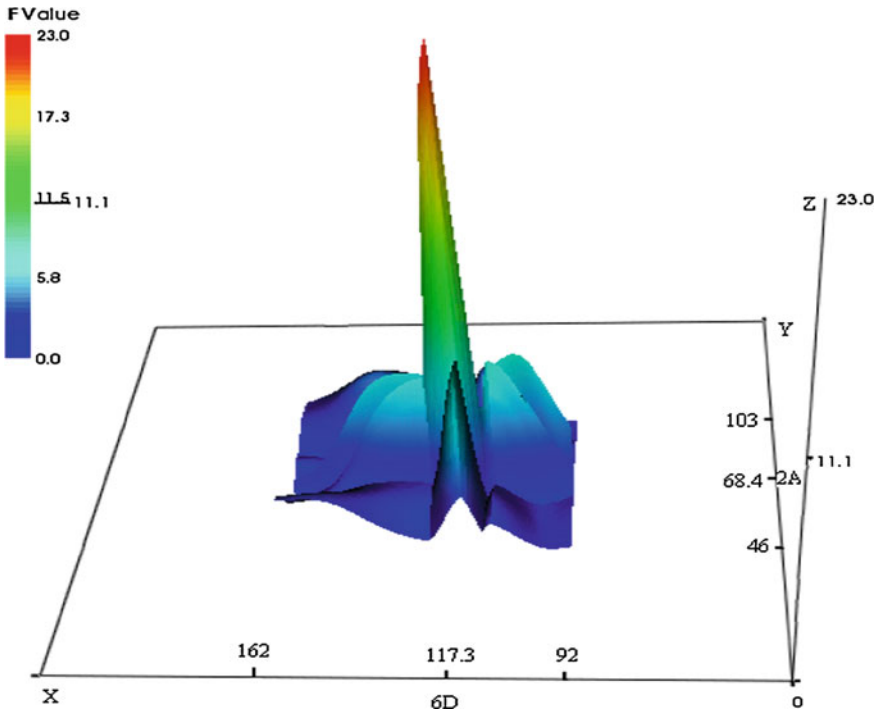

Fig. 6.9 3D visualization for the test statistics of genome scan for epistatic QTL associated with total vascular bundle under environment III (normal irrigated but no top-dressed urea in 2008) between 2A and 6D (F value is taken as height); AA: 1.9; H: 10.81 %

one QTL on chromosome 5D was detected; under environment II, one QTL on chromosome 7D were detected; under environment III, the QTLs on chromosome 2D, 6A, and 7D were detected; under environment IV, the QTLs on chromosomes 1A, 5D, and 7D were detected. Among them, the QTLs on chromosomes 1A, 2D, and 7D were main-effect QTLs.

6.2.2.2.2.8 QTL Mapping for L/S

Two QTLs affecting L/S were identified in environments I and IV and contributed by Huapei 3 and Yumai 57, explaining 12.45 and 15.17 % phenotypic variance, respectively.

In a word, after analyzing anatomical characteristics of the basal internode and uppermost internode, it was found that there were main-effect QTLs on chromosomes 5D and 7D, declaring that important gene and region confer the traits on these chromosomes. Meanwhile, some important genes were also found on chromosomes 1B, 4D, and 2D.

6.2.3 *Research Progress of Anatomical Traits of Culm QTL Mapping and Comparison of the Results with Previous Studies*

6.2.3.1 Research Progress of QTL Conferring Anatomical Traits of Culm and the Comparative Analysis with This Study

6.2.3.1.1 Research Progress of QTL Conferring Anatomical Traits of Culm

Because stem strength was closely related to lodging resistance of wheat, it will be of great significance for enhancing the lodging resistance of wheat by studying QTL for stem strength-related traits. Marza et al. (2006), Huang et al. (2006), and Zhang et al. (2008) conducted QTL analysis of lodging resistance of wheat by using DH population or RIL population. And a total of 16 QTLs, including four main-effect QTLs, were detected on chromosomes 1B, 1D, 2B, 4A, 4B, 4D, 5A, 6D, and 7D, and the highest contribution was 23 % of phenotypic variation.

Few researches related to QTL for anatomical traits of stem were conducted. Only Keller et al. (1999) in abroad and Guo et al. (2002) in domestic studied UIL, UID, CWT, culm wall strength, the length, and diameter of other internode; however, few studies associated with TVB, LVB, SVB, and L/S were conducted (Table 6.19).

Table 6.19 Summary of QTL of wheat stem microdissection traits (PVE > 10 %)

Trait	QTL	Flanking marker	PVE (%)	Population	Reference
Stem trait		Xpsr949–Xgwm18	12	RIL	Keller et al. (1999)
		Xpsr958–Xpsr566c	15		
		Xpsr933b–Xglk529a	15		
		Xpsr598–Xpsr570	21		
		Xgwm397–Xglk315	23		
		Xpsr918b–Xpsr1201a	31		
		Xpsr370–Xpsr580b	20		
Stem strength	*QSs-3A*	Xwmc527–Xwmc21	10.61	DH	Hai et al. (2005)
	QSs-3B	Xgwm108–Xwmc291	16.6		
PD	*QPd-1A*	Xgwm135–Xwmc84	10.72		
	QPd-2D	Xgwm311–Xgwm301	18.7		
LVB	*5A*	xgwml86–xgwm415	18	DH	Guo (2002)
	4B	xgwm368–xgwm276	38		
SVB	*2A*	xgwm294–xgwm356	14		
	5B	xgwm99–xgwml64	11		

Abbreviations are the same as in Table 6.14

6.2.3.2 Comparison of this Study with Previous Researchers

We researched QTL for anatomical traits of the second basal internode and the uppermost internode for the first time. A total of 62 QTLs, including 31 major QTLs (contribution is greater than 10 %), were detected on chromosomes 1B, 2D, 4D, 5D, and 7D, and the most significant QTL could explain 25.61 % of phenotypic variation. Further, some loci controlled multiple traits. In addition, it was found that LVB and SVB were controlled by different genes, and the locus (*Qlvb.sdau-5D*) on chromosome 5D, controlling LVB, was detected in several environments. Comparing with the results of spike yield, leaf morphology, and related traits studied by Zhang et al. (2008) using the same DH population, the QTLs for LVB and spike and leaf traits were on the same or near regions and tended to be co-located within the genome, which can be used as marker to polymerize multiple excellent traits in breeding program.

The main-effect QTLs conferring UID, CWA, TVB, LVB, and L/S were all located within the interval XBARC320–XWMC215–XBARC345 on chromosome 5D, and nearby the main-effect interval controlling grain yield and spike-correlated traits (kernels for spike, the total number of spikelets, density of spikelet) (Zhang et al. 2009). In addition, the QTLs conferring UIL, LVB, and SVB located within the interval of XGWM676–XGWM437 on chromosome 7D had high contribution and stably expressed in four different environments, which can be used in marker-assisted selection (MAS) to polymerize several traits and improve multiple traits simultaneously in wheat breeding.

In a word, the QTL conferring stem-correlated traits distributed on chromosomes 1B, 2A, 2D, 3D, 4D, 5D, 6A, 7A, and 7D. Comparing with previous researches, more loci were detected on genome D in this study; furthermore, QTL cluster controlling important physiology and yield-correlated traits was located on chromosome 5D.

6.3 QTL Mapping and Effect Analysis of Heading Date

Heading date is an important trait that is a major determinant of the regional and seasonal adaptation of wheat varieties. Appropriate heading date and anthesis are important target traits for breeding, which not only correlate with growth period, but also directly or indirectly affect some important agronomic traits such as yield, disease resistance, and stress resistance. According to the different signal response to the environment, there are three categories of genes influence heading date including the following: (1) vernalization response (Vrn), controlling winter wheat took on low temperature treatment for a certain time before ear differentiation; (2) photoperiod response (Ppd), decides the response to the length of sunlight; and (3) earliness per se (Eps), when vernalization and photoperiod are satisfied, the number of days for wheat to heading date is determined by Eps, which control developmental rate independently of the other two genes. Vrn-A1, Vrn-B1, and

Vrn-D1 were located on long arms of chromosomes 5A, 5B, and 5D, and Vrn-A1 had the highest effect, showing the vernalization insensitivity. Now, Vrn-A1 and Vrn-B1 have been successfully cloned (Yan et al. 2004). The genes Ppd-A1, Ppd-B1, and Ppd-D1 were located on chromosomes 2A, 2B, and 2D, respectively, and Ppd-D1 had the highest effect, followed by Ppd-B1. Furthermore, these genes were all insensitive to photoperiod. However, few research for Eps was conducted. While, Eps was located on chromosomes 2B, 3A, 4A, 4B, 6B, 6D, and 7B by using aneuploid of Chinese spring and chromosome substitution. Song et al. (2006) identified nine QTLs for wheat heading date on chromosomes 2D, 3B (2 regions), 3D, 4A, 5B, 6B, 6D, and 7D, explaining 3.97–22.91 % of phenotypic variation, by using two mapping populations (Hanxuan 10 × Lumai 14 and Wenmai 6 × Shanhongmai) in field and greenhouse. Since some researches regarding QTL analysis for wheat growth period were conducted, few could be used in MAS. Therefore, in this study, several populations were used to analyze the QTL for wheat growth period, in order to find reliable and stable markers that can be used in MAS in wheat breeding programs.

Heading date was recorded as the number of days from sowing to 50 % of spikes fully emerging in a plot. And heading was noted when 1/3 of spikes emerged from the flag leaves.

6.3.1 *QTL Analysis of Heading Date Based on a DH Population Derived from the Cross of Huapei 3 × Yumai 57*

6.3.1.1 Phenotypic Variation of Heading Date

The heading date for the DH population and the parents in three environments were described in Fig. 6.10. Huapei 3 headed significantly earlier than Yumai 57 in all

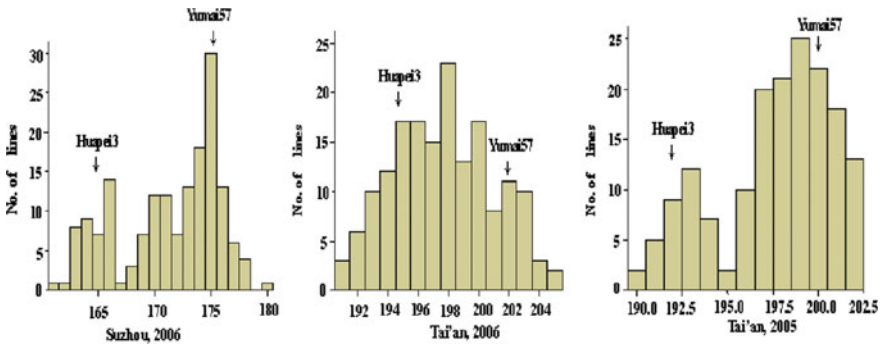

Fig. 6.10 Frequency distribution of heading date

three environments. Transgressive segregants were observed for heading date among DH lines in the three environments. The heading date of the DH population segregated continuously and followed a normal distribution, indicating its polygenic inheritance and suitability of the data for QTL analysis.

6.3.1.2 QTLs with Additive Effects and Additive × Environment (AE) Interactions

Two additive QTLs were detected for heading date on chromosomes 1B and 5D (Table 6.20). A highly significant QTL, designated as *Qhd5D*, was observed within the Xbarc320–Xwmc215 interval on the chromosome 5DL, accounting for 53.19 % of the phenotypic variance. The second QTL, *Qhd1B*, could explain 3.49 % of the phenotypic variance. The Huapei 3 alleles at the *Qhd5D* reduced days-to-heading by 2.77 days due to additive effects, but increased days-to-heading by 0.71 days at the *Qhd1B*. This suggested that alleles for reducing the heading date were dispersed within the two parents. This result was in accordance with the presence of a wide range of variation and transgressive segregations of wheat heading date in the DH population. The total additive QTLs for heading date accounted for 56.68 % of the phenotypic variance. The *Qhd5D* showed AE interactions in two environments, accounting for 3.81 and 1.51 % of the phenotypic variance, respectively. The general contribution of the two AE effects on wheat heading date was 5.32 %.

6.3.1.3 Epistasis and Epistasis × Environment (AAE) Interactions

Two pairs of digenic epistatic interactions were identified for heading date, located on chromosomes 2B–6D and 7A–7D (Table 6.21), explaining phenotypic variance from 2.45 to 3.44 %, respectively. The general contribution of digenic epistatic interactions to heading date was 5.90 %. The *Qhd2B/Qhd6D* was involved in AAE interactions in two environments, which explain 0.65 and 0.73 % of the phenotypic variance, respectively. The total contribution of AAE interactions was 1.38 %.

6.3.2 QTL Analysis of Heading Date Based on a RIL Population Derived from the Cross of Nuomai 1 × Gaocheng 8901

6.3.2.1 Phenotypic Variation of Heading Date

The heading date of the RIL population and the parents in three environments were described in Table 6.22 and Fig. 6.11. Nuomai 1 headed significantly earlier than Gaocheng 8901 in all three environments. Transgressive segregants were observed

Table 6.20 Estimated additive and additive × environment interaction of QTL for heading time

Trait	QTL	Flanking marker	Site (cM)	A	H^2 (A, %)	AE1	H^2 (AE1, %)	AE2	H^2 (AE2, %)	AE3	H^2 (AE3, %)
Heading date	*QHd1B*	Xwmc406–Xbarc156	26.7	0.71	3.49						
	QHd5D	Xbarc320–Xwmc215	67.2	−2.77	53.19	−0.74	3.81			0.47	1.51

E1: Suzhou, 2006; E2: Tai'an, 2006; E3: Tai'an 2005

Table 6.21 Estimated epistasis (AA) of QTL for heading time

Trait	QTL	Flanking marker	Site (cM)	QTL	Flanking marker	Site (cM)	AA	H^2 (AA, %)	AAE1	H^2 (AAE1, %)	AAE2	H^2 (AAE2, %)	AAE3	H^2 (AAE3, %)
Heading date	*qHd2B*	Xbarc129.1–Xgwm111	98.3	qHd6D	Xgwm133.2–Xgwm681	91.9	−0.59	2.45	−0.31	0.65	0.33	0.73		
	qHd7A	Xwmc603–Xwmc596	62.6	qHd7D	Xgwm295–Xgwm676	40.3	0.71	3.44						

E1: Suzhou, 2006; E2: Tai'an, 2006; E3: Tai'an 2005. AAE1: epistasis effect of Env.1 (Suzhou 2006); AAE1 H^2/%: H^2/% of Env.1 (Suzhou 2006); AAE2: epistasis effect of Env.2 (Tai'an 2006); AAE2 H^2/%: H^2/% of Env.2 (Tai'an 2006); AAE3: epistasis effect of Env.3 (Tai'an 2005); AAE3 H^2/%: H^2/% of Env.3 (Tai'an 2005)

Table 6.22 Phenotypic values for heading stage of two parents and the RIL population in three environments in wheat

Trait	Environment	Parent		RIL population			
		Nuomai1	Gaocheng8901	Range	Mean ± SD	Skewness	Kurtosis
Heading date (d)	E1	197	201	194 ~ 206	200.1 ± 2.22	0.38	0.44
	E2	199	202	197 ~ 207	202.4 ± 1.80	0.07	−0.66
	E3	205	208	203 ~ 211	206.4 ± 1.73	0.1	−0.80

E1: Tai'an, 2008; E2: Tai'an, 2011; E3: Tai'an, 2011

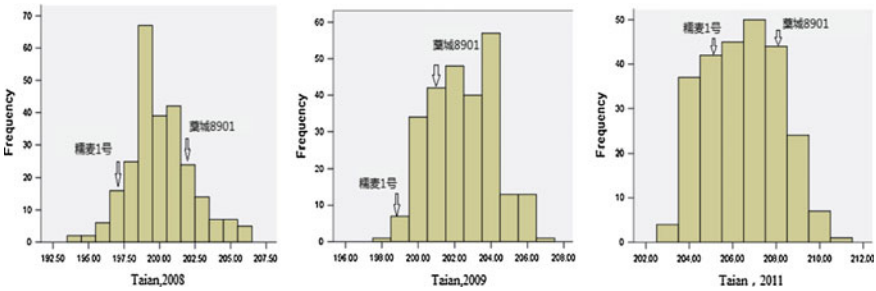

Fig. 6.11 The heading time distribution of the RIL population in three different environments

for heading date among RIL lines in the three environments. The heading date of the RIL population segregated continuously and followed a normal distribution, and both absolute values of skewness and kurtosis were less than 1.0, indicating its polygenic inheritance.

6.3.2.2 QTLs with Additive Effects and Additive × Environment (AE) Interactions

A total of five additive QTLs conferring heading date on chromosomes 3B, 5B, 6A, 6B, and 7D were identified (Table 6.23). *Qhs-6A* and *Qhs-6B* were detected four times in the three different environments and mixed environment and contributed by Gaocheng 8901, accounting for 16.16 ∼ 25.64 % and 5.75 ∼ 9.88 % of

Table 6.23 QTL with significant additive effects for heading stage detected in different environments

Trait	Env.	QTL	Chr.	Site (cM)	Interval marker	A	H^2 (A, %)
Heading date	E1	*Qhs-3B*	3B	58.00	wPt-9510-wPt-664393	0.53	5.65
		Qhs-6A	6A	41.00	xgpw-4085-wPt-667562	−0.89	16.16
		Qhs-6B	6B	17.00	xgpw-3241-wPt-0315	−0.55	5.75
	E2	*Qhs-6A*	6A	39.00	xgpw-4085-wPt-667562	−0.91	25.64
		Qhs-6B	6B	14.00	xgpw-3241-wPt-0315	−0.49	7.19
	E3	*Qhs-3B*	3B	57.00	wPt-9510-wPt-664393	0.44	6.55
		Qhs-6A	6A	44.00	xgpw-4085-wPt-667562	−0.87	25.44
		Qhs-6B	6B	12.00	xgpw-3241-wPt-0315	−0.53	9.22
	PD	*Qhs-3B*	3B	58.00	wPt-9510-wPt-664393	0.40	5.12
		Qhs-5B	5B	112.00	wPt-9454-wPt-3457	−0.38	4.57
		Qhs-6A	6A	43.00	xgpw-4085-wPt-667562	−0.75	18.03
		Qhs-6B	6B	15.00	xgpw-3241-wPt-0315	−0.57	9.88
		Qhs-7D	7D	90.00	wPt-730876-wPt-8343	0.85	22.67

E1: Tai'an, 2008; E2: Tai'an, 2011; E3: Suzhou, 2011; *PD* Pool data; Positive values indicate that Nuomai 1 alleles increase corresponding trait value; Negative values indicate that Gaocheng 8901 alleles increase corresponding trait value

phenotypic variation, respectively. And the contributions of *Qhs-6A* were all greater than 10 % in each environment. *Qhs-3B* was detected in E1, E3, and pool data (PD) three times and contributed by Nuomai 1, explaining 5.65, 6.55, and 9.22 % of phenotypic variation. In PD, *Qhs-7D* with a LOD value 15.49, located on chromosome 7D, accounted for 22.67 % of phenotypic variation. *Qhs-5B* was only detected on PD.

6.3.3 *QTL Analysis of Heading Date Based on a RIL Population Derived from the Cross of Shannong 01-35 × Gaocheng 9411*

6.3.3.1 Phenotypic Variation of Heading Date

There were smaller differences between two parents and bigger differences among lines in heading date and anthesis under the three environments. Furthermore, heading date varied from 194 to 206 in E1 and anthesis varied from 204 to 213. The heading time and flowering time of the RIL population segregated continuously and followed a normal distribution, and both absolute values of skewness and kurtosis were less than 1.0 (Table 6.24).

6.3.3.2 QTLs with Additive Effects and Additive × Environment (AE) Interactions

A total of 12 additive QTLs for heading time and four additive QTLs for flowing time were identified on chromosomes 1A, 1B, 4B, 6A, and 6B, respectively, using phenotypic data from E1, E2, and E3 and the mean value of the three environments (Table 6.25). The QTLs distributing on chromosomes 1A, 4B, and 6B were contributed by Gaocheng 8901, the rest were contributed by Shannong 01-35.

Four major QTLs for heading time, *QHt1A.1-54* (PD), *QHt1A.2-132* (E2, PD), *QHt1B.1-87* (E1, PD), and *QHt1B.2-44* (E2, E3) were detected, accounting for 10.75 ∼ 30.32 % of phenotypic variation. Furthermore, *QHt1A.2-132*, *QHt1B.1-87,* and *QHt1B.2-44* were detected by using both individual environment and average environment, which were stably major QTLs. In addition, *QHt1A.2-133* and *QHt1A.2-132* detected in E1 were located within the same interval.

The QTL for flowering time, designated as *QFt1B.1-87* (E2) and *QFt1B.1-105* (E3), were major QTLs, explaining 13.23 and 15.77 % of phenotypic variation, respectively. Meanwhile, *QFt1B.1-87* and *QHt1B.1-87*, controlling heading time, were located on the same locus; and *QFt6B.3-5* and *QHt6B.3-0* were within the same interval.

Table 6.24 Phenotypic values for heading time and flowering time of the RIL population and the parents in different environments

Trait	Environment	Parent		RIL population			
		Shannong 01-35	Gaocheng 9411	Mean ± SD	Range	Skewness	Kurtosis
Heading time (d)	E1	202	202	201.52 ± 1.96	194–206	−0.19	0.88
	E2	204	206	204.51 ± 1.66	201–208	−0.04	−0.90
	E3	205	206	205.49 ± 1.80	202–210	0.12	0.04
Flowering time (d)	E1	208	209	208.95 ± 1.30	204–213	0.21	1.31
	E2	209	210	210.3 ± 1.33	205–214	−0.20	0.79
	E3	209	210	210.84 ± 1.53	208–216	0.69	0.88

E1: 2008–2009 growing season at Tai'an site; E2: 2009–2010 growing season at Tai'an site; E3: 2010–2011 growing season at Tai'an site, the same as below

Table 6.25 Additive QTL for heading time and flowering time in different environments

Trait	Environment	QTL	Left marker	Right marker	A	LOD	PVE (%)
Heading time	E1	*QHt1A.2-133*	wPt-672089	wPt-730213	−0.60	5.03	9.32
		QHt1B.1-87	wPt-5562	wPt-8971	0.86	9.31	17.08
	E2	*QHt1A.2-132*	wPt-672089	wPt-730213	−0.51	5.52	9.46
		QHt1B.1-86	wPt-5562	wPt-8971	0.98	17.56	30.32
	E3	*QHt1B.1-104*	wPt-5363	wPt-1363	0.70	8.45	10.75
		QHt1B.2-44	wPt-4497	CFE026	0.56	7.45	9.54
		QHt4B.1-60	xcfd54-4D	Xgpw2172	−0.44	4.28	5.79
		QHt6A.1-61	wPt-5652	CFE041	0.48	5.67	6.95
	PD	*QHt1A.1-54*	wPt-6005	wPt-730172	−0.62	4.79	14.40
		QHt1A.2-132	wPt-672089	wPt-730213	−0.54	6.96	11.07
		QHt1B.1-87	wPt-5562	wPt-8971	0.90	17.24	26.58
		QHt1B.2-44	wPt-4497	CFE026	0.50	6.87	9.43
		QHt4B.1-66	Xgpw2172	wPt-1505	−0.47	4.96	8.09
		QHt6B.1-14	wPt-0259	wPt-2095	0.41	4.73	6.27
		QHt6B.3-0	wPt-1325	wPt-669607	−0.43	5.27	6.62
Flowering time	E2	*QFt1B.1-87*	wPt-5562	wPt-8971	0.51	6.18	13.23
	E3	*QFt1B.1-105*	wPt-1781	wPt-0974	0.71	9.35	15.77
		QFt6B.3-5	wPt-1325	wPt-669607	−0.49	5.11	9.92
	PD	*QFt1B.1-104*	wPt-5363	wPt-1363	0.36	4.73	6.71

Positive and negative values of additive effect (EstAdd) indicate that alleles to increase thousand-grain weight are inherited from Shannong 01-35 and Gaocheng 9411, respectively

6.3.4 Research Progress of Growth Period QTL Mapping and Comparison of the Results with Previous Studies

6.3.4.1 Research Progress of QTL Mapping for Growth Period of Wheat

Heading date is a quantitative trait controlled by multiple genes. The QTL expressed differently in different environment, because of the interaction between genotype and environment. Many researches regarding QTL for growth period of wheat have been conducted, and there were loci detected on each chromosome. However, there were differences in detected loci by using different test materials, linkage map, and environment. Song et al. (2005, 2006), Yao et al. (2010), Xu (2005), and Hanocq et al. (2004) analyzed QTL conferring heading date of wheat by using different DH and RIL population and identified 21 QTLs, including seven major QTLs, with the highest effect of 22.91 % (Table 6.26). Summary analysis showed that most of the researchers found QTLs for heading date on chromosomes 7B, 2D, and 3B.

Table 6.26 Summary of QTL of wheat heading date (PVE > 10 %)

Trait	QTL	Flanking marker	(PVE)/%	Population	Reference
Heading date	*QDH.CAAS-5D*	Vrn-D1-WMS212	24.40/49.80	RIL	Yao et al. (2010)
	QDH.CAAS-7B.2	wPt4230-wPt4660	19.53		
	3B	WMS299-M539.1	16.36	DH	Song (2005)
	5B	WMS371-WMS335	22.91		
	6B	A1142.1-A8166.1	11.09		
	4B	WMS265-WMC161	10.38		
	3B	A2478.1-WMC505.1	12.53		
	7D	WMS295-WMC346	12.68		
	5B	WMS371-WMS335		RIL	Hanocqet et al. (2004)
	Ht-2D1	xgwm261–xgwm349	20.77	RIL	Xu (2005)
	qHd 5D	Xbarc320–Xwmc215	53.19	DH	Zhang (2008)

6.3.4.2 Comparsion of the Results with One of the Previous Studies

The major QTL (*qHd5D*) for heading time detected in this DH population were located within Xbarc320–Xwmc215 interval on chromosome 5DL, explaining 53.19 % of phenotypic variation, and closely linked with Vrn-D1. And it was contributed by precocious parent Huapei 3. In addition, *qHd5D* was closely linked with Xwmc215, with the genetic distance of 2.1 cm. Therefore, it was more likely used in MAS and polymerizing breeding programs. Another additive QTL (*qHd1B*) located within the interval Xwmc406–Xbarc156 on chromosome 1BS explained 3.49 % of phenotypic variation and was not found in the previous studies. It may be allelic loci of *Ppd-H2* on chromosome 1B and that needed further research to prove.

QTLs conferring heading date were located on chromosomes 3B, 6A, and 6B in the RIL population derived from the cross of Nuomai 1 × Gaocheng 8901. And the most significant QTL (*Qhs-6A*) was located on chromosome 6A, which was not found in the previous studies, indicating that chromosome 6A was a main chromosome for controlling heading date. Song et al. (2006) also identified QTLs conferring heading date on chromosome 3B and 6B, but the loci were different with those detected in this study, which may be correlated with Eps.

QTL conferring growth period was identified on chromosomes 1A, 1B, 4B, 6A, and 6B in the RIL population derived from the cross of Shannong 01-35 × Gaocheng 9411. QTLs (*QHt1A.2-132*, *QHt1B.1-87,* and *QHt1B.2-44*) with stable expression were the new-found main-effect QTLs and could be used in MAS. In addition,

QTL identified on chromosome controlled heading time and flowering time simultaneously, that is *QFt1B.1-87* (controlling flowering time) and *QHt1B.1-87* (controlling heading time) was the same locus, which performed pleiotropic effects.

6.4 QTL Mapping of Cell Membrane Permeability of Wheat Leaf Treated by Low Temperature

Chilling injury and frost damage occur frequently in the most of the winter wheat growing areas. In northern winter wheat region of China, climate is cold, both frost damage in winter and late spring cold in spring cause large loss of yield. Therefore, chilling injury and frost damage is one of the highlights of researching stress resistance in wheat. Some physiological and biochemical changes will happen during cold resistance of wheat, and some physiological traits such as malondialdehyde (MDA) content, soluble protein content, and cell membrane permeability were all identification index for cold resistance. Too low temperature will damage the structure of cell membrane, and result in wheat tissue injury or death. Hence, cool tolerance of cell membrane closely correlated with cold resistance of wheat. Ju et al. (2012) determined cell membrane permeability of cold wheat leaf by using conductivity method, which was a relatively reliable method to determine cold resistance in wheat. Brube et al. (1988) showed that cold resistance of wheat was a quantitative trait, controlled by polygenes, and affected by environment easily. Furthermore, the genes those controlled cold resistance of wheat were a kind of modificator gene, which perform cold resistance only under low temperature and short day. Waldman et al. (1975) and Limin et al. (1997) located the gene for cold endurance of wheat on chromosomes 5A and 5D and deemed that wheat varieties with the gene from group D perform stronger cold resistance than that from group A. However, until now, no researches related to QTL for cold resistance of wheat were conducted. Therefore, in this study, the DH population derived from two parents with different cold resistance was used to analyze QTL for cold resistance by determining cell membrane permeability of leaf treated by low temperature. And the purpose was to identify molecular markers, closely linked with cold resistance, which were used in cold resistance breeding of wheat, furthermore, and lay a theoretical foundation for mining the genes controlling cold resistance in wheat.

6.4.1 QTL Mapping for Cell Membrane Permeability of Wheat Leaf

6.4.1.1 Test Materials

Materials and Planting were same as one of the Sect. 6.1.1.1.1 in this chapter.

6.4.1.2 Field Trails

All DH lines and parents were planted in Baoding (Hebei province, E1), Cangzhou (Hebei province, E2), and Handan (Hebei province, E3) on October 4, 2010. The experimental field consisted of a randomized block design with three replications. All DH lines and parents were grown in a plot with three rows in 2 m length, 26.7 cm between rows and 2.2 cm between plants. Crop management was carried out following the local practices.

6.4.1.3 Determining Method of Cell Membrane Permeability of Leaf

In late December 2010, five leaves (intermediate leaves of the plant) in the center of every plot were selected and washed by tap water and deionized water for three times successively, and then moisture was blotted on the surface of the leaves. Each sample of 0.2 g was cut into about 1 cm of small pieces, and put into two tubes, and then treated by room temperature (control) and low temperature (−18 °C), respectively. Cell membrane permeability was determined by using conductivity method.

A volume of 10 mL deionized water was added to each sample, including control and treatment, and then vacuumized for 15 min. After gently shaking, the tubes were put in room temperature for 10 min. Electrical conductivity of control (C) and treatment (R) was determined by using conductometer (DDS-11A) according to the method described by Shen et al. (modified slightly). And then, the tubes of treatment were put into the boiling water bath for 5 min, and the electrical conductivity (K) after cooling to room temperature was determined. The relative transuding rate of electrolyte (A, %) was used to show cell membrane permeability, whose value was calculated by using the formula: $A = (R - C)/(K - C) \times 100$.

6.4.1.4 Data Analysis

Analysis of phenotypic data was carried out using the SPSS program (version 17.0, SPSS, Chicago, USA). The inclusive composite interval mapping (ICIM) was applied by means of the QTL IciMapping 2.2 to identify QTLs for cell membrane permeability under three environments, based on the molecular genetic map constructed by Zhang et al. (2009). A logarithm of odds (LOD) of 2.5 and Sep of 1 cM were set to declare QTL as significant. QTL effects were estimated as the proportion of phenotypic variance (R^2) explained by the QTL. QTL was named referring to the method described by McIntosh et al.

Table 6.27 Variations of cell membrane permeability of leaf treated by low temperature (−18 °C) in parents and DH population in three environments

Environment	Parent		DH population				
	Huapei 3	Yumai 57	Mean ± SD	Range	CV (%)	Skewness	Kurtosis
E1	36.22	32.32*	30.11 ± 5.39	15.84–48.92	17.9	0.322	0.855
E2	29.45	20.34*	28.29 ± 4.07	18.04–40.60	14.4	0.106	−0.249
E3	33.73	31.09*	31.34 ± 4.37	20.42–42.48	13.9	0.092	−0.486

E1: Baoding site; E2: Cangzhou site; E3: Handan site

*Indicates significant difference between parents ($P < 0.05$) according to *t*-test

6.4.1.5 Results and Analysis

6.4.1.5.1 Analysis of Phenotypic Variation

In three different environments, significant difference was found in cell membrane permeability of leave treated by low temperature between parents and large range of variation was observed among DH lines. And the coefficients of variations were 17.9 % (E1), 14.4 % (E2), and 13.9 % (E3), respectively. The cell membrane permeability of the DH population segregated continuously and followed a normal distribution, and both absolute values of skewness and kurtosis were less than 1.0 (Table 6.27), indicating its polygenic inheritance and suitability of the data for QTL analysis.

6.4.1.5.2 QTL Analysis of Cell Membrane Permeability of Leaf in Wheat

A total of 21 additive QTLs conferring cell membrane permeability of leaf were detected on chromosomes 1B (three regions), 2A (two regions), 3A (three regions), 3B (three regions), 5B (five regions), 6A (one region), 6B (one region), 6D (one region), 7B (one region), and 7D (one region), respectively, in three different environments. Seven, nine, and five QTLs were found in E1, E2, and E3, respectively, and most of them were contributed by Huapei 3, which had stronger cold resistance (Table 6.28).

The QTLs located on chromosome 5B, including *qCMP-5B-1* (E1), *qCMP-5B-2* (E2), and *qCMP-5B-4* (E3), were located within the interval Xgwm213–Xswes861.2, were away from Xswes861.2 for 0.0 cM, and were detected in the three environments. The locus had most significant contribution in three environments, accounting for 17.5, 8.1, and 14.0 % of phenotypic variation.

In addition, *qCMP-1B-1*, *qCMP-3B-2*, *qCMP-5B-1,* and *qCMP-5B-4* were all main-effect QTLs, whose contributions were all greater than 10 %, accounting for 18.4, 17.7, 17.5, and 14.0 % of phenotypic variation. Except for *qCMP-3B-2*, their positive alleles were all came from Huapei 3. And other 17 additive QTLs were minor genes, whose contributions smaller than 10 %.

Table 6.28 Position, effect, and phenotypic contribution of additive QTL for cell membrane permeability of leaf treated by low temperature (−18 °C) in three environments

QTL	Site/cM	Marker interval	LOD	Additive effect	PVE (%)
Environment 1					
qCMP-2A-1	42	Xgwm636–Xcfe67	2.796	−2.395	7.4
qCMP-2A-2	102	Xwmc455–Xgwm515	2.652	10.113	4.3
qCMP-3A-1	188	Xbarc51–Xbarc157.1	2.691	2.313	6.6
qCMP-3B-1	90	Xgwm566–Xcfe009	2.636	−9.926	4.2
qCMP-5B-1	58	Xgwm213–Xswes861.2	10.046	21.176	17.5
qCMP-6B	83	Xswes679.2–Xwmc658.2	4.036	17.207	7.6
qCMP-7B	48	Xgwm333–Xwmc10	3.484	13.845	7.3
Environment 2					
qCMP-1B-1	23	Xcfe156–Xwmc406	8.073	2.846	18.4
qCMP-1B-2	39	Xbarc008–Xgwm218	2.828	−1.67	6.0
qCMP-3A-2	196	Xbarc157.1–Xbarc1177	2.828	−1.583	5.7
qCMP-3B-2	86	Xgwm566–Xcfe009	6.697	−3.450	17.7
qCMP-3B-3	50	Xgwm285–Xgwm685	3.817	2.658	9.8
qCMP-5B-2	58	Xgwm213–Xswes861.2	3.974	−1.966	8.1
qCMP-5B-3	1	Xgwm133.1–Xwmc73	2.580	1.519	5.2
qCMP-6A	19	Xgwm334–Xbarc023	2.726	1.834	7.6
qCMP-6D	118	Xubc808–Xswes679.1	2.651	−3.303	6.5
Environment 3					
qCMP-1B-3	22	Xcfe156–Xwmc406	3.420	−1.787	7.9
qCMP-3A-3	97	Xbarc356–Xwmc489.2	2.829	1.681	7.1
qCMP-5B-4	58	Xgwm213–Xswes861.2	6.452	2.477	14.0
qCMP-5B-5	1	Xbarc36–Xbarc140	2.700	−1.663	7.0
qCMP-7D	211	Xwmc14–Xwmc42	3.667	2.892	9.7

Positive and negative additive effects indicate that the positive alleles are from Huapei 3 and Yumai 57, respectively. *PVE* phenotypic variation explained

6.4.2 *Research Progress of Cell Membrane Permeability QTL Mapping and Comparison of the Results with Previous Studies*

6.4.2.1 Research Progress of QTL Conferring Cold Resistance of Wheat

Although Brube et al. (1988) and Waldman et al. (1975) found that genes related to cold resistance were on chromosomes 4D, 5A, 5D, and 7A, etc., but the specific locations were not clear. With the development of genetic map and QTL analysis, Båga et al. (2007), Galiba et al. (1995), Vágújfalvi et al. (2003), Sutka et al. (2001), Tóth et al. (2003), and Liu et al. (2005) studied the cold resistance and relative

Table 6.29 Summary of QTL of wheat resistance to cold (PVE > 10 %)

Trait	Site	Flanking marker	PVE (%)	Population	Reference
Cold resistance	1D	E37M60_(72); barc152_(145)	P = 0.001	DH	Båga et al. (2007)
	1D	barc169_122	P = 0.0005		
	2A	gwm296_177	P = 0.005		
	5A	wmc206_224; cfd2_326	P = 0.0001		
	6D	cfd76_153	P = 0.005		
	5A	Vrn1	LOD > 3	SCRL	Galiba et al. (1995)
		Xpsr426,	LOD > 3		
		Xwg644	LOD > 3		
		Xcdo504	LOD > 3		
		Frl	LOD > 3		
	5A	Xbcd508	49 %	RIL	Vágújfalvi et al. (2003)
		CBF3	Transcription factor		
		Vrn-A1/Xpsr426/Xwg644			Sutka (2001)
		Fr1			
	5D	Vrn-D1			
		Fr2			
	5B	Vrn-B1			Tóth et al. (2003)
		Fr-B1			
		Xgwm639			
	2A	Xgwm372–Xgwm249	10.45/15.61/17.14	DH	Liu et al. (2005)
	4B	Xwroe48–DuPw043	16.97		
	2A	BARC208–Xgwin95	19.8		

DH double haploid; *SCRL* single chromosome recombinant lines; *RIL* recombinant inbred lines

transuding rate of electrolyte under low temperature using DH, RIL, and SCRL (single chromosome recombinant lines) populations and identified 24 loci and their linking molecular markers, among them 19 QTLs, were major QTLs, including one transcription factor, three vernalization genes and two cold-resistant genes. Precious results showed that important QTLs conferring cold resistance distributed on chromosomes 2A, 5A, and 5D (Table 6.29).

6.4.2.2 Comparison of this Study with Previous Researchers

In this study, a total of 21 QTLs conferring cell membrane permeability of leaf treated by low temperature (−18 °C) were detected, including four major QTLs

(contribution greater than 10 %), which located on chromosomes 1B, 3B, and 5B, respectively. Furthermore, *qCMP-5B-1* (E1) and *qCMP-5B-4* (E3) were located within the interval Xgwm213–Xswes861.2, and a locus was also detected within this interval in environment 2, accounting for 8.1 % of phenotypic variation, and was away from Xswes861.2 for 0.0 cM. Hence, Xswes861.2 could be used in MAS in wheat breeding programs of cold resistance. In previous studies, QTLs conferring cold resistance were mainly located on chromosomes 1D, 2A, 2B, 5A, 6D, 7B, 4B, 5D, and 5B, while this study showed that the chromosomes 2A, 6B, 7B, 3A, 6A, 6D, and 7D were also related to cold resistance, except the chromosomes 1B, 3B, and 5B. Comparing with the previous results, it was found that the related QTLs on chromosomes 2A, 7B, 5A, 5B, and 5D were very important for cold resistance in wheat.

6.5 QTL Mapping of Root Traits in Wheat

Root is an important organ absorbing water and minerals, whose development directly affects the growth and development of overground parts and material production, and is the foundation of the high and stable yield for crop (Liu et al. 2002; Moudal and Kour 2004; Partha et al. 2004). Development of root is not only affected by environment and cultivating condition but also controlled by genes. Caradus (1995) indicated that the traits correlated with root size such as root weight, root volume, the number of root, root length, root surface area, and the ratio of root dry weight to shoot dry weight had higher heritability; furthermore, the traits correlated with root morphology such as root average diameter, root hair length, adventitious root grade, branch grade, root density, and density of root length also had higher heritability. These root traits were all quantitative traits. In addition, Jing et al. (1997) researched the heritability of root morphology and its relationship with drought resistance and showed that there was significant positive correlation between drought resistance of wheat seedling and root dry weight.

Now, most of the researches related to root traits in wheat were focused on mapping QTL under abiotic stress such as high temperature and drought, using efficiency of NPK, salt stress, water stress, and heavy metal stress; in addition, majority studied root traits at seedling stage. Zhang and Xu (2002) identified QTL and interaction QTL conferring the number of root, root diameter, root dry weight, the ratio of root dry weight to shoot dry weight, and growth rate of root using a RIL population in wheat. Zhou et al. (2005) analyzed QTL and interaction QTL for the number of root, maximum root length, root raw weight, root dry weight, the ratio of root raw weight to shoot raw weight and the ratio of root dry weight and shoot dry weight under two different environments including water stress and no stress conditions, by using a DH population containing 150 progeny lines derived from a cross between Hanxuan 10 and Lumai 14. Landjeva et al. (2010) identified QTL for

vigor located on the wheat D genome at seedling stage. Ibrahim et al. (2012) researched QTL conferring root morphology at wheat seedling stage under drought environment. Bai et al. (2013) researched the QTL for root traits at seeding stage and its relationship with plant height. Because wheat root is closely related to final yield and that it is difficult to improve wheat root by using traditional breeding method, we can use MAS to speed up the further improvement of wheat root. Hence, in this study, immortalized F_2 (IF_2) population of wheat derived from a DH population was used to analyze QTL for root traits at seedling stage, in order to find the markers, closely linking with root traits, to conduct molecular-assisted breeding.

6.5.1 QTL Mapping and Effects' Analysis of Root Traits

6.5.1.1 Experiment Designing

A total of 30 seeds of 168 single crossed derived from a DH population (Huapei 3 × Yumai 57) and parents were sampled, and soaked with 1 % H_2O_2 for 24 h. After washing for 2 ∼ 3 times by water, the samples were put in a light incubator (nighttime temperature was set as 12 ± 2 °C, while daytime temperature was 20 ± 4 °C) and cultured with deionized water until the first leaf emerged. Six excellent plants of each cross were sampled and cultured on foamed plastic with thickness of 0.5 cm (perforated with the diameter of 1 cm), and then fixed by disinfected sponge. At last, wheat seedlings were cultured with Hoagland's solution (An et al. 2006) in cultivating basins (with height of 30 cm) for three replicates. Furthermore, 1 L of Hoagland's solution consisted of 1 mmol $Ca(NO_3)2{\cdot}4H_2O$, 0.2 mmol KH_2PO_4, 0.5 mmol $MgSO_4{\cdot}7H_2O$, 1.5 mmol KCl, 1.5 mmol $CaCl_2$, 1 μmol H_3BO_3, 50 nmol $(NH4)6Mo_7O_{24}{\cdot}4H_2O$, 0.5 μmol $CuSO_4{\cdot}5H_2O$, 1 μmol $ZnSO_4{\cdot}7H_2O$, 1 μmol $MnSO_4{\cdot}H_2O$, and 0.1 mmol Fe^{3+}-EDTA, and the pH of the solution was 6.0. Meanwhile, cultivating basins were brushed by black paint to supply dark environment for the growth of root. Replacement of the nutrient solution was done every three days.

Three individuals with consistent growth of each cross were sampled when the fourth leaf emerged, washed with distilled water, and divided into stems and roots using scissor. The traits including root total length (RTL), root surface area (RSA), root average diameter (RAD), root volume (RV), root tip number (RT), and maximum root length (MRL) were measured using the WinRHIZO root analysis system. The fresh roots and shoots were killed out for 10 min under 105 °C and then dried to balance weight under 80 °C. Furthermore, shoot dry weight (SDW) and root dry weight (RDW) were weighed. Root–shoot ratio was the root dry weight to shoot dry weight.

6.5.1.2 Results and Analysis

6.5.1.2.1 Phenotypic Variation and Correlation of Root Traits in IF_2 Population

Big differences were found in nine root-related traits between parents. And the nine root traits of IF_2 population segregated continuously and followed a normal distribution, and both absolute values of skewness and kurtosis were less than 1.0, except for RDW/SDW (Table 6.30), indicating its polygenic inheritance and suitability of the data for QTL analysis.

In addition to RAD, RTL was significantly or extremely significantly positively correlated with other seven traits, and the correlation between RTL and RSA was the largest ($r = 0.981$, $P < 0.01$), while RAD was negatively correlated with RT and RTL ($r = 0.417$, 0.314, respectively, $P < 0.01$), and they both reached significant level (Table 6.31).

Table 6.30 Analysis of root traits at seedling stage in the IF_2 population derived from Huapei 3 × Yumai 57

Root trait	Parent		Immortalized F_2 population			
	Huapei 3	Yumai 57	Mean ± SD	Range	Skewness	Kurtosis
RTL (cm)	96.12	165.01	151.56 ± 4.47	35.19–365.00	0.65	1.86
RSA (cm^2)	9.48	13.29	12.05 ± 0.33	3.01–26.50	0.38	0.96
RAD (μm)	320.23	260.41	250.21 ± 0.00	210.12–290.31	0.17	−0.55
RV (mm3)	70.38	90.47	76.13 ± 0.00	20.31–0.15	0.14	0.26
RT	199	302	262.00 ± 7.43	61.00–528.00	0.49	0.37
MRL (cm)	16.71	17.48	19.88 ± 0.29	10.35–27.8	−0.36	0.14
SDW (mg)	19.77	24.60	18.13 ± 0.50	4.50–43.75	0.61	2.80
RDW (mg)	6.7	6.4	6.14 ± 0.15	1.60–11.95	0.09	0.52
RDW/SDW	0.34	0.26	0.34 ± 0.00	0.13–0.82	3.23	22.25

RTL root total length; *RSA* root surface area; *RAD* root average diameter; *RV* root volume; *RT* root tip number; *MRL* maximum root length; *SDW* shoot dry weight; *RDW* root dry weight

Table 6.31 Coefficients of pairwise correlations of mean values of root traits at seedling stage in the IF_2 population derived from Huapei 3 × Yumai 57

Traits	RTL	RSA	RAD	RV	RT	MRL	SDW	RDW
RSA	0.981**							
RAD	−0.314**	−0.136						
RV	0.916**	0.977**	0.067					
RT	0.831**	0.788**	−0.417**	0.708**				
MRL	0.846**	0.829**	−0.322**	0.773**	0.774**			
SDW	0.750**	0.786**	−0.033	0.791**	0.652**	0.683**		
RDW	0.870**	0.915**	0.015	0.924**	0.712**	0.768**	0.779**	
RDW/SDW	0.093	0.091	0.032	0.084	0.058	0.012	−0.344*	0.216*

*Significant at 0.05 probability level

**Significant at 0.01 probability level. Abbreviations are the same as in Table 6.30

6.5.1.2.2 QTL Mapping and Effect Analysis of Root Traits in the IF_2 Population

A total of seven additive QTLs (Table 6.32 and Fig. 6.12) and 12 pairs of epistatic QTLs (Table 6.33 and Fig. 6.13) for eight root traits were mapped on chromosomes 1A, 1D, 2A, 2B, 2D, 3A, 3B, 5D, 6D, and 7D. Additive (A), dominant (D) effects were observed across these QTLs, and the interactions between additive and

Table 6.32 Intervals, effects, and contributions of QTL for root traits at seedling stage in the IF_2 population derived from Huapei 3 × Yumai 57

Root trait	QTL	Flanking marker	Position (cM)	Additive		Dominance		Gene action
				A	H^2 (%)	D	H^2 (%)	
RTL	*QRtl2D*	XWMC41–XBARC349.2	69.5	−15.04	4.44	−19.07	8.88	OD
RSA	*QSa2D*	XWMC170.2–XGWM539	65.4			−2.50	8.18	
RAD	*QAd2A*	XBARC380–XGWM636	1.6	6.67	9.32			
RV	*QRv7D*	XGWM295–XGWM676	107.3	7.00	0.03	−20.00	11.91	OD
MRL	*QMrl6D*	XWMC412.1–XCFD49	0	−1.32	9.98	1.18	3.01	PD
RDW	*QRdw2D*	XWMC41–XBARC349.2	69.5	−0.63	3.53	−1.15	11.1	OD
	QRdw7D	XGWM295–XGWM676	101.3			−1.35	9.81	

For additive effect, a positive value indicates that the allele from Huapei 3 increases plant height. For dominant effect, a positive value indicates that the heterozygote has a higher phenotypic value than the homozygote. In the column of "Gene action," PD, D, and OD denote partial dominant ($D/A < 1.00$), dominant ($D/A = 1.00$), and overdominant ($D/A > 1.00$), respectively. Other abbreviations are the same as in Table 6.30

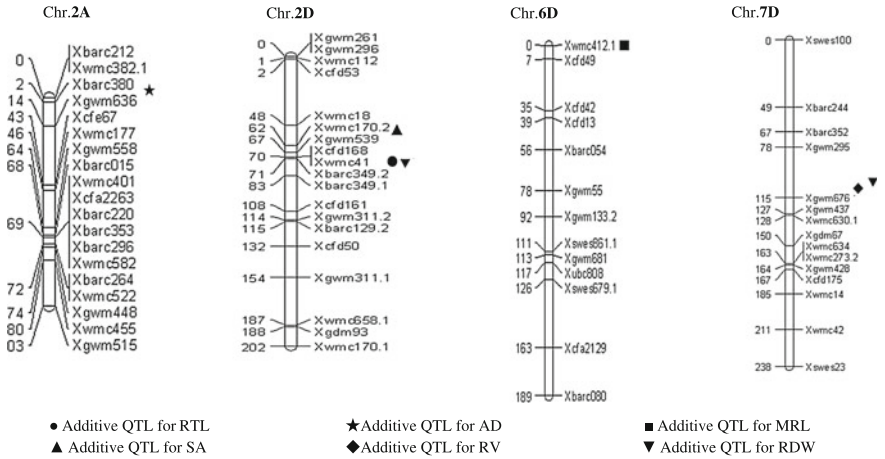

Fig. 6.12 Positions of additive QTL associated with root traits at seedling stage in the IF_2 population derived from Huapei 3 × Yumai 57

Table 6.33 Estimated epistasis and contributions of QTL for root traits at seedling stage in the IF_2 population derived from Huapei 3 × Yumai 57

Trait	QTL	Marker interval	Position (cM)	QTL	Marker interval	Position (cM)	AA	H^2 (%)	AD	H^2 (%)	DA	H^2 (%)	DD	H^2 (%)
RTL	*QRtl2D*	XCFD50–XGWM311.1-2A	141.1	QRtl5D	XBARC307–XBARC347	50.5	25.75	14.05			39.91	2.78	76.57	3.40
	QRtl3B	XCFE282–XGWM144	53.0	QRtl5D	XBARC1097–XCFD8	18.4	41.75	6.38			29.20	0.17	46.98	1.34
RSA	*QSa2D*	XCFD53–XWMC18	1.6	QSa7A	XBARC070–XBARC250	30.5					3.31	17.40		
	QSa2D	XCFD53–XWMC18	1.6	QSa7A	XWMC593–XBARC157.2	0							3.86	9.13
RV	*QRv1A*	XCFD59–XWMC402.2	54.0	QRv2A	XGWM558–XBARC015	65.4			20.90	0.04				
	QRv1A	XCFD59–XWMC402.2	54.0	QRv2A	XGWM448–XWMC455	73.6							20.30	1.43
	QRv1A	XBARC148–XGWM154	58.9	QRv2A	XGWM448–XWMC455	73.6								
	QRv1A	XGWM498–XCWEM6.2	80.8	QRv2A	XGWM448–XWMC455	73.6	14.30	5.46			10.40	0.20	10.7	0.83
	QRv1A	XGWM498–XCWEM6.2	80.8	QRv2A	XWMC455–XGWM515	89.1	12.10	2.95						
RT	*QRt1D*	XCFD19–XWMC93	40.9	QRt2B	XBARC200–XWMC770	52.7	7.23	0.20	69.63	7.2	72.40	7.02		
RDW	*QRdw1A*	XWMC402.2–XBARC120.2	55.1	QRdw2A	XGWM448–XWMC455	73.6	0.69	8.49						
	QRdw2A	XWMC382.1–XBARC380	1.0	QRdw3A	XWMC527–XWMC264	115.7	1.12	8.68	1.38	3.58			2.13	3.36

For the epistatic effect, the positive value means that the parent-type effect is greater than the recombinant-type effect, and the negative value means that the parent-type effect is less than the recombinant-type effect. Abbreviations are the same as in Table 6.30

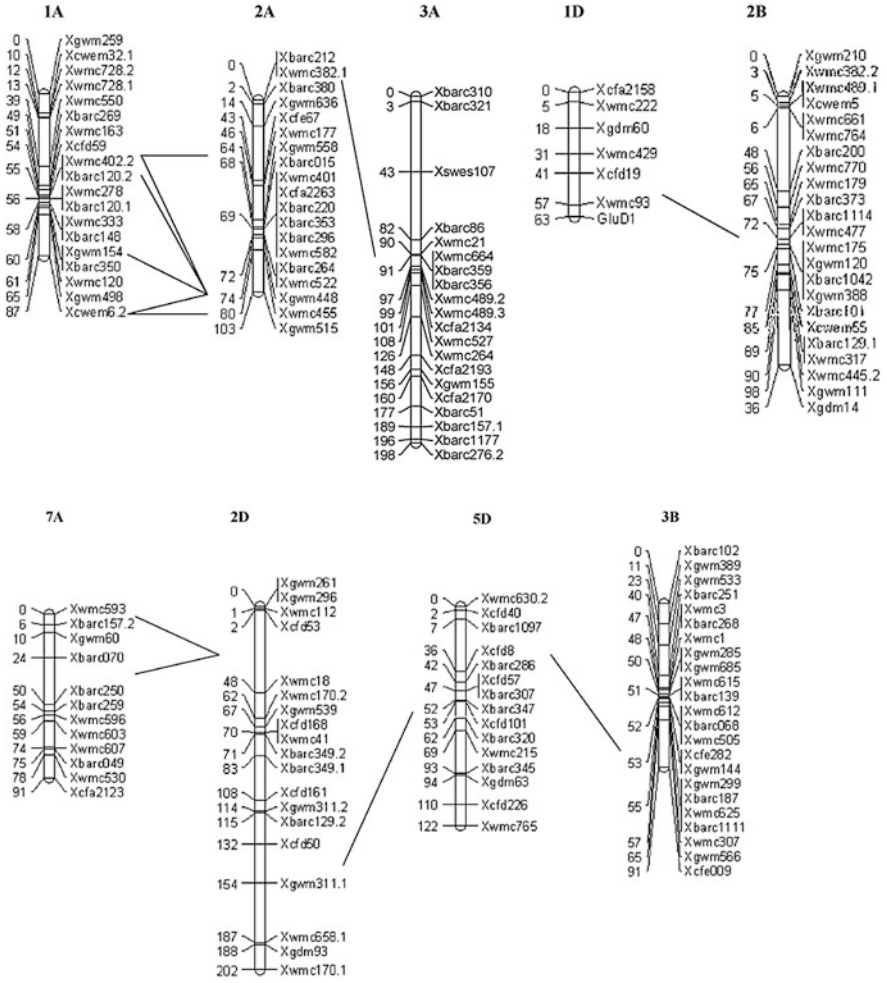

Fig. 6.13 Positions of epistatic QTL for root traits at seedling stage in the IF_2 population derived from Huapei 3 × Yumai 57

additive (AA), additive and dominance (AD), dominance and additive (AD), as well as dominance and dominance (DD) were also detected.

For RTL, one additive QTL and two pairs of epistatic QTLs were detected. The additive QTL on chromosome 2D was contributed by Yumai 57, accounting for 4.44 % of phenotypic variation, and performed overdominant effect. The two pairs of epistatic QTLs on chromosomes 2D-5D and 3B-5D explained phenotypic

variation from 0.17 to 14.05 % and performed AA, DA, and DD interactions. Meanwhile, the QTL designated as *QRtl2D* performed epistatic effect.

One additive QTL and two pairs of epistatic QTLs conferring RSA were identified. The additive QTL on chromosome 2D accounted for 8.18 % of phenotypic effect and performed dominant effect. The two pairs of epistatic QTLs on chromosomes 2D-5D and 3B-5D explained 14.05 and 6.38 % of phenotypic variation, respectively. Further, the epistatic QTL of 2D-5D performed AD interaction, while the epistatic QTL of 3B-5D performed DD interaction.

One additive QTL for RAD on chromosome 2A was detected, accounting for 9.32 % of phenotypic variation, and contributed by Huapei 3. No pair of epistatic QTL was identified.

One additive QTL and five pairs of epistatic QTLs conferring RV were detected. The additive QTL on chromosome 7D, explaining 0.03 % of phenotypic variation, was contributed by Huapei 3 and showed overdominant effect. Five pairs of epistatic QTLs were all mapped on chromosomes 1A and 2A and showed different effects of AA, DA, and DD, explaining phenotypic variation from 0.04 to 5.46 %.

One additive QTL for MRL was identified on chromosome 6D, accounting for 9.98 % of phenotypic variation, and contributed by Yumai 57. And it performed partial dominant effect.

One pair of epistatic QTL for RT was mapped on chromosomes 1D-2B, and showed AD, DA, and AD effects, accounting for 0.20, 7.20, and 7.02 % of phenotypic variation, respectively. No QTL with additive effect and dominant effect was identified.

One additive QTL, one dominant QTL, and two pairs of epistatic QTLs for RDW were detected. Further, the additive QTL on chromosome 2D was contributed by Yumai 57, accounting for 3.53 % of phenotypic variation, and showed overdominant effect. The dominant QTL explained 9.81 % of phenotypic variation. The two pairs of epistatic QTLs were mapped on chromosomes 1D-2A and 2A-3A, accounting for 8.49 and 8.68 % of phenotypic variation, respectively, and performed AA interactions.

Among the seven additive QTLs for root traits detected in this study, some loci only performed additive effects, and some loci only performed dominant effects, while only a few loci showed additive and dominant effects simultaneously. Furthermore, the loci with both additive and dominant effects gave priority to dominant effects, and only one locus was detected in this study. There were differences in effect size among different loci, and their directions were not consistent. Twelve pairs of epistatic QTLs detected in this study gave priority to AA and DD effects.

6.5.2 *Research Progress of Root Traits' QTL Mapping and Comparison of the Results with Previous Studies*

6.5.2.1 Research Progress of QTL Mapping Conferring Root Traits

Growth and development of root directly affects acquiring nutrient substance, thus affecting final yield of wheat because growth of wheat was affected by environment condition such as drought, water, N, P, K, heavy metal, and salt. Therefore, in recent years, researches regarding root traits were focused on QTL mapping for related traits under abiotic stress. It was found that Wu et al. (2007), Landjeva et al. (2010), Yang (2012), Xu et al. (2012), and Ren et al. (2012) detected QTL for wheat root traits under salt stress using DH and RIL populations, and a total of 26 QTLs were identified. Most of these QTLs distributed on chromosomes 3A, 5A, 5B, and 2D, among which 16 QTLs were major QTLs with the highest R^2 of 36.06 % (Table 6.34). Ibrahim et al. (2012) detected QTL for root traits in wheat using BC2F4-6 population under drought condition, and 32 QTLs were detected. Furthermore, multiple QTLs conferring root traits were distributed on chromosomes 1D, 2A, 2D, and 7D. Liu et al. (2013) detected QTL for root traits under water stress, and 46 QTLs including 20 major QTLs were detected with the highest effect of 24.31 %. An et al. (2006) mapped five QTLs for RDW under condition with different level of N fertilizer, and four major QTLs were found with the highest effect of 19.6 %. Bail et al. (2013), Liu et al. (2011), Ren et al. (2012), Jiang (2012), and Hamada et al. (2012) identified 69 QTLs conferring root-related traits of wheat seedlings on chromosomes 2A, 2B, 5D, 2D, 3B, 4D, 3A, 6A, and 7D, using different DH population and RIL population, and 29 of 69 QTLs were major QTLs with the highest effect of 68 % (Ren et al. 2012). Sharma et al. (2011) identified 15 QTLs for root-related traits using 1RS-1BS map, and the highest effect of single QTL was 56.0 %.

6.5.2.2 Comparsion of the Results with the Previous Studies

A total of seven QTLs for root-related traits of wheat seedlings were identified in this study. Among them, three QTLs were contributed by Yumai 57, while two QTLs were contributed by Huapei 3, and *QRtl2D*, *QRv7D,* and *QRdw2D* showed overdominant effects, indicating that the parents with strong advantage should be selected to configured crosses. Among the 12 pairs of epistatic QTLs detected in this study, some QTLs interacted with other two QTLs simultaneously. For example, *QRtl5D* interacted with *QRtl2D* and *QRtl3B*, controlling RTL; while the QTL located within the interval Xgwm448–Xwmc455 interacted with both *QRdw1A* and *QRv3A*, indicating that epistasis was very important for heredity of root-related traits in wheat seedlings, but the mechanism was very complicated (Xing et al. 2002; Li et al. 2001; Mei et al. 2005), which needed further research. Most of the additive QTLs for root traits, detected in this study, were mapped on

Table 6.34 Summary of QTL of wheat root traits (PVE > 10 %)

Env.	Trait	QTL	Flanking marker	PVE (%)	Population	Reference
Salt–tolerance	RDW/SDW	*QRsrc.ipk–5D*	Xgwm1122	18.6	DILs	Landjeva et al. (2010)
			Xgwm174	18.6		
			Xgwm182	18.6		
			Xgwm3063	18.6		
			Xgdm99	17.2		
	PRL	*qTL3A*	Xwmc527–Xwmc264	17.45	DH	Yang (2012)
		qTL3D–2	Xgdm72–Xbarc1119	23.72		
		qTL7D	Xwmc630.1–Xgdm67	13.9		
	RRW	*qFRW2D–1*	Xwmc170.2–Xgwm539	36.06		
		qFRW2D–2	Xbarc349.2–Xbarc349.1	19.39		
		qFRW5B	Xgwm213–Xswes861.2	10.33		
	RDW	*qDRW5B–4*	Xgwm213–Xswes861.2	12.98		
	RL	*QRl–7B*	Xgwm297–NP43	14.75	RIL	Xu et al. (2012)
	RDW	*QRdw.sqn–3A*	Xgwm497.1–Xcfa2193	10.2	RIL	Ren et al. (2012)
	MRL	*QMrl.sqn–3A*	Xgwm497.1–Xcfa2193	25.5		
	RRDW	*QRdwr.sqn–4A*	Xbarc78–Xgwm350.1	12.2		
Normal	TRL	*5BS*	gwm213.5B4D7B–barc74.5BLT	11.44	DH	Bai et al. (2013)
	TRSA	*2D*	gwm132–wPt–9997.2DS	10.1		
		5A	gwm293b.5ASM–gwm146a.5ASM	12.89		
	RDW/SDW	*4D*	RhtMrkD1.4D–wPt–0431. 4B4D/wPt–5809.4B4D	21.08		
	NR > 30 cm	*1RS–1BS*	Sec–1	34	RL	Sharma et al. (2011)
		1RS–1BS	Xurc–1–Pm8	26		
		1RS–1BS	Pm8	57		

(continued)

Table 6.34 (continued)

Env.	Trait	QTL	Flanking marker	PVE (%)	Population	Reference
		1RS–1BS	Sr31	47		
	LRLa	*1RS–1BS*	Xurc–8–Gli–1,Glu–3	18		
		1RS–1BS	Xurc–4	52		
	TRL	*1RS–1BS*	Pm8	56		
		1RS–1BS	Xurc–2–Pm8	24		
		1RS–1BS	Sr31	40		
	SRW	*1RS–1BS*	NOR–Xurc–4	15		
		1RS–1BS	Pm8–Gli–1,Glu–3	18		
	DRW	*1RS–1BS*	Pm8–Gli–1,Glu–3	31		
		1RS–1BS	NOR–Xurc–4	11		
	TRW	*1RS–1BS*	NOR–Xurc–4	14		
		1RS–1BS	Pm8–Gli–1,Glu–3	23		
	MRL	*QMRL.cgb–4A*	Xgwm610–Xgwm397	12.37	DH	Liu et al. (2011)
	RN	*QRN.cgb–2B*	Xgwm429–Xgwm388	11.9		
	RA	*QRA.cgb–3B*	P3622–400–P2076–147	12.16		
	MRL	*qMRL–2B*	Xgwm210–Xbarc1138.2	68	RIL	Ren et al. (2012)
	PRL	*qPRL–2B1*	Xgwm210–Xbarc1138.2	59		
	LRLb	*qLRL–6A*	Xgwm570–Xgwm169.2	30.5		
	TRL	*qTRL–2B*	Xgwm210–Xbarc1138.2	20.3		
	RN	*qRN–6A*	Xgwm570–Xgwm169.2	24.5		
		qRN–6D	Xgwm55.3–Xgdm14.6	10.3		
	RL	*QRl–7A*	wpt4637–barc121	12.26	RIL	Jiang (2012)
	RRW	*QFrw–4A*	wpt671707–barc70a	14.45		
		QFrw–6A	wpt668031–wpt4229	11.69		

(continued)

Table 6.34 (continued)

Env.	Trait	QTL	Flanking marker	PVE (%)	Population	Reference
	RDW	*QDrw–4A.1*	swes147–swes624c	10.63		
		QDrw–4A.2	wpt671707–barc70a	10.05		
	RV	*QV–1A*	wpt729788–wpt667395	11.57		
		QV–3A	wpt1562–wpt2587	10.21		
	RAD	*QRdm–3B*	ubc834a–wpt5906	12.71		
	RTN	*QRn–1B*	wpt668027–swes169a	13.29		
		QRn–3A	wpt730892–barc314	11.15		
		QRn–4A	issr23b–wmc308	15.4		
	RTN	*qRN*	wmc150a	11.63	DH	Hamada et al. (2012)
	DRR	*qDRR–2*	wmc97	11.49		
	ER	*qER–1*	cfd266	12.53		
		qER–2	wmc405	14.73		
	HR	*qHR–1*	wmc278	13.44		
Water stress	MRL	*QMRL.cgb–5D*	Xgwm205.2–Xgwm68	12.2	DH	Liu et al. (2013)
		QMRL.cgb–2D	WMC453.1–WMC18	12.22		
		QMRL.cgb–5B	WMC380–Xgwm540	11.95		
	RN	*QSRN.cgb–3B*	WMC3–P6934.380	14.98		
		QSRN.cgb–5A	P2470.2–Xgwm154	19.82		
	TRL	*QTRL.cgb–1B*	P3470.2–P4133.1	11.43		
		QTRL.cgb–1B	CWM65–P8222.5	16.13		
		QTRL.cgb–3B	WMC231–Xgwm284	10.43		
		QTRL.cgb–3B	Xgwm644.2–WMC3	10.42		
		QTRL.cgb–5D	Xgwm3–Xgwm43	10.3		
		QTRL.cgb–7D	Xgwm44–Xgwm121	10.69		

(continued)

Table 6.34 (continued)

Env.	Trait	QTL	Flanking marker	PVE (%)	Population	Reference
		QTRL.cgb–3B	WMC3–P6934.380	13.81		
		QTRL.cgb–3B	P3622.4–P2076.1	14.23		
		QTRL.cgb–5B	P8143.3–P2454.1	10.9		
	PRA	*QPRA.cgb–7D*	Xgwm44–Xgwm121	11.9		
		QPRA.cgb–5B	P8143.3–P2454.1	16.24		
	RSA	*QRSA.cgb–7D*	QRSA.cgb–7D	11.93		
		QRSA.cgb–5B	QRSA.cgb–5B	16.22		
	RA	*QSRA.cgb–7D*	Xgwm44–Xgwm121	10.46		
		QSRA.cgb–2B	WMC474–Xgwm374	10.66		
		QSRA.cgb–2B	WMC179.2–P6901.2	11.16		
		QSRA.cgb–3B	WMC3–P6934.3	24.31		
Using efficiency of N	RDW		CWM70–P3474–480	19.6	DH	An et al. (2006)
			Xgwm539–P4233–175	11		
			P8422–170–CWM539.2	10.4		
			EST25–CWM88	11		

Note: RDW/SDW the ration of root dry weight to shoot dry weight; *PRL* primary root length; *RRW* root raw weight; *RDW* root dry weight; *RL* root length; *MRL* maximum root length; *RRDW* relative root dry weight; *TRL* total root length; *TRSA* total root surface area; *RN* root number; *RA* root angle; *RV* root volume; *RAD* root average diameter; NR > 30 cm, number of roots greater than 30 cm; *LRL*[a] longest root length; *SRW* shallow root weight; *DRW* deep root weight; *TRW* total root weight; *LRL*[b] lateral root length; *RTN* root tip number; *DRR* Deep root ratio; *ER* elongation rate of the primary seminal root; *HR* hydrotropic response of root; *PRA* primary root area

chromosomes 2D and 7D, which were also found in the previous researches, indicating that important QTLs or genes confer root traits in wheat distributed on D genome.

6.6 QTL Mapping Conferring Leaf-Related Traits in Wheat

Leaf is the main photosynthetic organ. Among them, flag leaf of wheat, with the highest photosynthetic efficiency at late growth stage and the highest contribution to formation of grain and yield, is the main source of carbohydrates in wheat grain and can contribute to yield for one-third. At home and abroad, lots of researches related to effects of wheat flag leaf on photosynthetic efficiency and yield were conducted, but few researches focused on genetic loci conferring flag leaf. Keller et al. (1999) identified eight QTLs for flag leaf width on chromosomes 1A, 1B, 2A, 3B, 5A, 5B, and 6A, respectively, which could account for 59.5 % of phenotypic variation, using a RIL population derived from Forno/spelt Oberkulmer including 226 lines. Lohwasser et al. (2004) detected 23 QTLs for length and width of the three basal leaves by using a RIL population including 114 lines under greenhouse conditions. Identifying molecular markers closely linked with leaf morphology on the base of previous studies is very important for improving photosynthetic efficiency and yield at the molecular level.

6.6.1 QTL Mapping for Leaf Morphology of Wheat Based on a DH Population

6.6.1.1 Materials and Methods

Five plants of each line were sampled on 10 days after heading to measure the included angle between flag leaf of main stem and stem designed as flag leaf angle (FLAN). While five main stems of each line were sampled at filling stage (20 days after anthesis) to measure length and width of the upper three leaves (flag leaf, second leaf, and third leaf). And leaf area was obtained by using the formula as follows: leaf area = (leaf length × leaf width)/1.2.

6.6.1.2 QTL Mapping and Effect Analysis of Leaf-Related Traits

Leaf morphology included the traits such as FLAN, and the length, width, and area of the upper three leaves. Furthermore, 31 additive QTLs and 22 pairs of epistatic QTLs confer leaf morphology, and seven of the 31 additive QTLs involved in QTL × environment interaction (Tables 6.35 and 6.36).

Table 6.35 Estimated additive (A) and additive × environment (AE) interactions of QTL for leaf morphology

Trait	QTL	Flanking marker	Position (cM)	A	H^2 (%)	A × E1		A × E2		A × E3	
						AE1	H^2 (%)	AE2	H^2 (%)	AE3	H^2 (%)
FLAN	*qFLAn2B*	Xgwm120–Xbarc1042	75.1	−3.08	5.15						
	qFLAn2D	Xcfd53–Xwmc18	1.7	2.00	2.17						
	qFLAn4D	Xcfe254–BE293342	192.5	−5.17	14.47						
	qFLAn5Ba	Xbarc36–Xbarc140	13.0	−3.18	5.48						
FLL	*qFLLe3Aa*	Xbarc86–Xwmc21	86.5	−0.54	13.82						
	qFLLe5D	Xbarc320–Xwmc215	64.3	−0.38	6.87						
	qFLLe6D	Xcfd42–Xcfd13	35.0	0.33	5.28			0.31	4.67	–0.17	1.32
FLW	*qFLWi3A*	Xwmc264–Xcfa2193	141.9	0.11	9.19						
	qFLWi4B	Xwmc48–Xbarc1096	18.4	−0.10	7.26						
	qFLWi4D	Xbarc334–Xwmc331	2.1	0.10	8.64						
	qFLWi7D	Xgwm676–Xgwm437	123.9	0.08	5.45						
FLAR	*qFLAr2Aa*	Xbarc380–Xgwm636	1.7	−0.95	2.02						
	qFLAr3Aa	Xswes107–Xbarc86	71.1	−1.10	2.74						
	qFLAr3Ac	Xwmc264–Xcfa2193	141.9	1.82	7.47						
	qFLAr4B	Xwmc48–Xbarc1096	18.4	−1.51	5.14						
	qFLAr4D	Xwmc473–Xbarc334	0.0	1.48	4.94						
	qFLAr7D	Xgwm676–Xgwm437	122.9	0.72	1.17						
SLL	*qSLLe2A*	Xwmc401–Xcfa2263	68.9	0.52	2.66						
	qSLLe2D	Xgwm261–Xgwm296	0.0	−1.18	13.74						
	qSLLe5D	Xwmc215–Xgdm63	72.4	−1.16	13.28			–0.67	4.37	0.85	7.12
SLW	*qSLWi5D*	Xcfd101–Xbarc320	58.6	−0.06	5.29			–0.04	2.30	0.06	5.83
SLAR	*qSLAr2D*	Xcfd53–Xwmc18	1.7	8.06	2.24						
	qSLAr5D	Xbarc320–Xwmc215	66.3	32.69	12.31			–0.84	7.45	–1.98	10.33

(continued)

Table 6.35 (continued)

Trait	QTL	Flanking marker	Position (cM)	A	H^2 (%)	A × E1		A × E2		A × E3	
						AE1	H^2 (%)	AE2	H^2 (%)	AE3	H^2 (%)
TLL	*qTLLe2D*	Xcfd53–Xwmc18	13.7	−0.40	3.55					–0.52	5.91
	qTLLe4A	Xwmc718–Xwmc262	0.0	−0.48	5.12						
	qTLLe5D	Xwmc215–Xgdm63	73.4	−1.00	21.91						
TLW	*qTLWi2D*	Xwmc170.2–Xgwm539	65.5	0.04	3.46						
	qTLWi5D	Xbarc320–Xwmc215	66.3	−0.07	8.38			–0.09	15.90	0.08	13.50
TLA	*qTLAr2D*	Xwmc170.2–Xgwm539	65.5	0.62	1.94						
	qTLAr4B	Xwmc657–Xwmc48	15.7	0.27		0.80	3.33			–0.80	3.33
	qTLAr5D	Xbarc320–Xwmc215	67.3	−1.88	18.0			–1.45	10.69	1.04	5.55

E1: Suzhou, 2006; E2: Tai'an, 2006; E3: Tai'an, 2005

FLAN Flag leaf angle; *FLL* Flag leaf length; *FLW* Flag leaf width; *FLAR* Flag leaf area; *SLL* Second leaf length from the top; *SLW* Second leaf width from the top; *SLAR* Second leaf area from the top; *TLL* Third leaf length from the top; *TLW* Third leaf width from the top; *TLAR* Third leaf area from the top

Table 6.36 Estimated epistasis (AA) and epistasis × environment (AAE) interactions of QTL for leaf morphology

Trait	QTL	Flanking marker	Position (cm)	QTL	Flanking marker	Position (cm)	AA	H^2 (%)	AA × E1		AA × E2		AA × E3	
									AAE1	H^2 (%)	AAE2	H^2 (%)	AAE3	H^2 (%)
FLAN	*qFLAn1Ba*	Xbac312–Xcfe023.1	36.1	qFLAn6D	Xgwm55–Xrwm133.2	77.9	−1.31	0.92						
	qFLAn1Bb	Xgwm218–Xgwm582	43.2	qFLAn6D	Xgwm55–Xrwm133.2	77.9	−1.06	0.61						
	qFLAn2Aa	Xgwm636–Xcfe67	40.1	qFLAn5D	Xbac1097vXcfd8	14.4	−1.66	1.50						
	qFLAn2Ab	Xgwm448–Xwmc455	80.2	qFLAn3D	Xbac1119–Xcfd4	17.8	2.13	2.45						
	qFLAn4D	Xcfe254- BE293342	192.5	qFLAn7Bb	Xbarc276.1–Xwmc396	33.5	2.26	2.77						
	qFLAn5Bb	Xbarc232–Xwmc235	23.7	qFLAn7D	Xgwm428–Xcfd175	163.7	3.10	5.22						
FLL	*qFLLe2B*	Xwmc317–Xwmc445.2	89.3	qFLLe3D	Xwmc631–Xbarc071	90.1	0.34	5.42						
	qFLLe2D	Xbarc349.2–Xbarc349.1	76.0	qFLLe5Ab	Xcfe026.1–Xcwem32.2	2.0	0.40	7.43						
	qFLLe3Ab	Xbarc1177–Xbarc276.2	196.3	qFLLe4B	Xwmc125–Xwmc140	0.0	0.33	5.08						
	qFLLe5Aa	Xbarc180–Xcwem40	31.6	qFLLe5B	Xbarc36–Xbarc140	0.0	0.33	5.27						
FLW	*qFLWi1D*	Xgdm60–Xwmc429	17.5	qFLWi6D	Xcfd49–Xcfd42	7.4	−0.07	3.41						
	qFLWi2Ba	Xbarc1042–Xgwm388	75.2	qFLWi6Ba	Xcfd48–Xwmc737	51.7	−0.05	2.04						
	qFLWi2Bb	Xcwem55–Xbarc129.1	85.0	qFLWi6Bb	Xgwm58–Xwmc737	61.3	−0.04	1.21						
	qFLWi2Bb	Xcwem55–Xbarc129.1	85.0	qFLWi4B	Xwmc48–Xbarc1096	18.4	0.05	2.23						
FLA	*qFLAr1B*	Xgwm18–Xwmc57	34.5	qFLAr4A	Xbarc078–Xwmc722	41.0	0.85	1.62						
	qFLAr2Ab	Xgwm455–Xgwm515	82.7	qFLAr7B	Xwmc396–Xgwm333	40.8	1.57	5.51						
	qFLAr2Ab	Xgwm455–Xgwm515	102.7	qFLAr3Ab	Xwmc21–Xwmc664	90.3	0.87	1.71						
	qFLAr5A	Xcfe223–Xwmc273.3	103.0	qFLAr6A	Xgwm334–Xbarc023	12.5	−1.42	4.50						
	qFLAr7Aa	Xgwm60–Xbarc070	9.8	qFLAr7Ab	Xgdm67–Xwmc634	152.5	−1.89	7.98						
SLL	*qSLLe6A*	Xwmc553–Xgwm732	56.5	qSLLe6B	Xcfa2187–Xgwm219	0.0	0.83	6.82						
SLW	*qSLWi4B*	Xwmc657–Xwmc48	17.7	qSLWi7D	Xwmc42–Xswes23	211.3	0.04	3.26	0.06	6.87			−0.04	3.07
TLL	*qTLLe2A*	Xbarc264–Xwmc522	72.2	qTLLe6A	Xgwm459–Xgwm334	5.0	−0.33	2.39						

Abbreviations are the same as in Table 6.35

6.6.1.2.1 QTL Mapping and Effect Analysis of Flag Leaf Angle (FLAN)

A total of four additive QTLs for FLAN were mapped on chromosomes 2B, 2D, 4D, and 5B, accounting for 5.15, 2.17, 14.47, and 5.48 % of phenotypic variation, respectively (Table 6.35), among which qFLAn4D had the highest R^2 value, explaining 14.47 % of phenotypic variation. Furthermore, in addition to qFLAn2D, the other three additive loci were contributed by Yumai 57. And no AE was detected.

Six pairs of epistatic QTLs for FLA distributed on chromosomes 1B-6D (2 regions), 2A-5D, 2A-3D, 4D-7B, and 5B-7D, respectively, were identified, accounting for phenotypic variation from 0.61 to 5.22 % (Table 6.36). However, no interactions between epistasis and environment were detected.

6.6.1.2.2 QTL Mapping and Effect Analysis of Flag Leaf Length (FLL)

Three additive QTLs conferring FLL on chromosomes 3A, 5D, and 6D were detected, accounting for 13.82, 6.87, and 5.28 % of phenotypic variation, respectively (Table 6.35). Among them, the QTL named as *qFLLe3Aa* had the highest contribution, explaining 13.82 % of phenotypic variation. In addition to *qFLLe6D*, other two QTLs were contributed by Yumai 57. Meanwhile, *qFLLe6D* involved in AE interactions and contributed 5.99 % of phenotypic variation.

Four pairs of epistatic QTLs for FLL on chromosomes 2B-3D, 2D-5A, 3A-4B, and 5A-5B were detected, explaining 5.42, 7.43, 5.08, and 5.27 % of phenotypic variation, respectively (Table 6.36), and no AAE was detected. The total contribution of epistasis was 23.20 % of phenotypic variation.

6.6.1.2.3 QTL Mapping and Effect Analysis of Flag Leaf Width (FLW)

Four additive QTLs for FLW on chromosomes 3A, 4B, 4D, and 7D were detected, accounting for 9.19, 7.26, 8.64, and 5.45 % of phenotypic variation, respectively (Table 6.35). Among them, *qFLWi3A* had the highest contribution, explaining 9.19 % of phenotypic variation. In addition, the four loci were all contributed by Huapei 3. No AE was detected.

Four pairs of epistatic QTLs conferring FLW on chromosomes 1D-6D, 2B-6B (2 regions), and 2B-4B were detected, accounting for 3.41, 2.04, 1.21, and 2.23 % of phenotypic variation, respectively (Table 6.36). And, no AAE was detected.

6.6.1.2.4 QTL Mapping and Effect Analysis of Flag Leaf Area (FLAR)

A total of six QTLs for FLAR on chromosomes 2A, 3A (2 regions), 4B, 4D, and 7D were detected, accounting for phenotypic variation from 1.17 to 7.47 % (Table 6.35), and the QTL (*qFLAr3Ac*) had the highest contribution, accounting for

7.47 % of phenotypic variation. The three QTLs, *qFLAr3Ac*, *qFLAr4D,* and *qFLAr7D,* were contributed by Huapei 3, while other QTLs were contributed by Yumai 57. And, no AE was detected.

A total of five pairs of epistatic QTLs for FLAR on chromosomes 1B-4A, 2A-7B, 2A-3A, 5A-6A, and 7A-7A were detected, explaining 1.62, 5.51, 1.71, 4.50, and 7.98 % of phenotypic variation, respectively (Table 6.36). And, no AAE was detected.

6.6.1.2.5 QTL Mapping and Effect Analysis of Second Leaf Length (SLL)

For SLL, three additive QTLs on chromosomes 2A, 2D, and 5D were identified, explaining 2.66, 13.74, and 13.28 % of phenotypic variation, respectively (Table 6.35), and *qSLLe2D* had the highest contribution, explaining 13.74 % of phenotypic variation. In addition to *qSLLe2A*, other QTLs were contributed by Yumai 57. The QTL (*qSLLe5D*) involved in AE, explaining 11.49 % of phenotypic variation.

Only one pair of epistatic QTL for SLL on chromosomes 6A-6B was identified (Table 6.36), explaining 6.82 % of phenotypic variation, and no AAE was detected in this study.

6.6.1.2.6 QTL Mapping and Effect Analysis of Second Leaf Width (SLW)

Only one additive QTL for SLW on chromosome 5D was mapped, explaining 5.29 % of phenotypic variation (Table 6.35), whose positive alleles originated from Yumai 57. Furthermore, the QTL involved in AE, and the total contribution of additive effect was 12.42 %.

One pair of epistatic QTL for SLW was also mapped on chromosomes 4B-7D (Table 6.36), explaining 3.26 % of phenotypic variation, and showed AAE.

6.6.1.2.7 QTL Mapping and Effect Analysis of Second Leaf Area (SLAR)

For SLAR, a total of two additive QTLs on chromosomes 2D and 5D were detected (Table 6.35), accounting for 2.24 and 12.31 % of phenotypic variation. Among them *qSLAr5D* had the highest contribution, with the value of 12.31 %, and involved in AE, explaining 17.78 % of phenotypic variation. The total contribution of additive effect was 32.23 %. Furthermore, no epistatic QTL for SLAR was mapped.

6.6.1.2.8 QTL Mapping and Effect Analysis of Third Leaf Length (TLL)

A total of three additive QTLs on chromosomes 2D, 4A, and 5D were identified, accounting for 3.55, 5.12, and 21.91 % of phenotypic variation (Table 6.35), and *qTLLe5D* had the highest contribution, accounting for 21.91 % of phenotypic variation. All of the three QTLs were contributed by Yumai 57. And no AE was detected.

Only one pair of epistatic QTL for TLL was detected on chromosome 2A-6A (Table 6.36), explaining 2.39 % of phenotypic variation, and no AAE for TLL was detected.

6.6.1.2.9 QTL Mapping and Effect Analysis of Third Leaf Width (TLW)

For TLW, two additive QTLs on chromosomes 2D, 4B, and 5D were detected, accounting for 3.46 and 8.38 % of phenotypic variation, respectively (Table 6.35). Meanwhile, *qTLWi2D* was contributed by Huapei 3, while *qTLWi5D* was contributed by Yumai 57. Furthermore, *qTLWi5D* involved in AE, and the interactive effect was 29.40 %.

No AAE was detected for TLW in this study.

6.6.1.2.10 QTL Mapping and Effect Analysis of Third Leaf Area (TLAR)

A total of three additive QTLs for TLAR were identified on chromosomes 2D and 5D, respectively. And the QTL (*qTLAr5D*) had the highest contribution, explaining 18.0 % of phenotypic variation, and whose positive alleles originated from Huapei 3. Meanwhile, both *qTLAr4B* and *qTLAr5D* involved in environmental interactions, accounting for 22.92 % of phenotypic variation (Table 6.35). And no epistasis was detected for TLAR.

6.6.2 Association Analysis for Leaf Morphology Based on a Natural Population Derived from the Founder Parent Aimengniu and Its Progenies

6.6.2.1 Materials and Methods

6.6.2.1.1 Materials

A total of 109 wheat accessions including sister lines, parents, and derived lines of the founder parent Aimengniu. Among which, the three parents and seven sister lines were provided by Tai'an subcenter of national wheat improvement, and the others were provided by Institute of Crop Sciences, Chinese Academy of Agricultural Sciences.

6.6.2.1.2 Field Trial and Determining Phenotypic Data

Field trial was conducted continuously for four years in 2007–2010 in farm of Shandong Agricultural University (Tai'an, Shandong province). The experimental

design followed a completely randomized block design with three replications in each environment. In autumn, each year, all varieties were planted in 2-m-long three-row plots (25 cm apart). Management was in accordance with local practices. At filling stage (20 days after anthesis), five flag leaves of main stems of each line were sampled to measure leaf length and width, and leaf area was calculated by the formula as follows: Leaf area = Leaf length × Leaf width ÷ 1.2. And the average value of each trait was used to analysis.

6.6.2.1.3 Analysis of DArT Marker

DNA of the 109 wheat accessions was extracted from adult plant leaves of five individuals using the cetyl trimethyl ammonium bromide (CTAB) method and then genotyped by DArT markers at the Diversity Arrays Technology Pty Limited (Canberra, Australia; http://www.triticarte.com.au). The concentration and purity of DNA were determined using 0.8 % agarose (final concentration of EB was 0.5 μg mL^{-1}).

A total of 7000 DArT markers, exploited on wheat, were used to scan all of the DNA samples by Triticarte Pty. Ltd. (Canberra, Australia). The known map including Cranbrook × Halberd (339 DArT markers) (Akbari et al. 2006), Arina × NK93604 (189 DArT markers) (Semagn et al. 2006), Avocet × Saar (112 DArT markers) (Lillemo et al. 2008), Colosseo × Lloyd (392 DArT markers) (Mantovani et al. 2008), the map consisted of 779 DArT markers (Wenzl et al. 2004), 3B physics map (Paux et al. 2008), and the information from nine populations were integrated by Triticarte Pty. Ltd. (http://www.triticarte.com.au/). Wheat DArT marker genetic map was constructed using the software of Mapchart 2.1 (Voorrips et al. 2002).

6.6.2.1.4 Analysis of Population Structure

A total of 42 DArT markers (one marker was selected on long arm and short arm of each chromosome) were used to analyze the population structure among wheat accessions using the software Structure 2.0 (Pritchard et al. 2000) with the admixed model. Five independent runs were performed setting the number of populations (K) from 2 to 12, burn-in period 100,000, and iterations 100,000. The maximum likelihood score corresponding to the setting K as target to select appropriate K value as subgroup number was taken.

6.6.2.1.5 Analysis of Linkage Disequilibrium

LD between mapped DArT loci was calculated by the squared allele frequency correlation coefficient (r^2) implemented in TASSEL 2.0.1 (http://www.maizegenetics.net). The pairwise significance was computed by 1000

permutations after removal of loci with rare alleles ($f < 0.10$). LD was calculated separately for unlinked loci and loci on the same chromosome.

6.6.2.1.6 Association Analysis

Significant marker–trait associations were identified using a mixed linear model (MLM) in TASSEL 2.1 (http://www.maizegenetics.net/). The population structure was inferred by program Structure 2.0 and kinship matrix was calculated by software TASSEL 2.1. The significance of associations between a marker locus and a trait was indicated by the p value. And it was considered that there were associations between them, when $P \leq 0.001$.

6.6.2.2 Analysis of Marker–Trait Associations

6.6.2.2.1 Phenotypic Data

The flag leaf length (FLL), flag leaf width (FLW), and flag leaf area (FLAR) of the population under the four environments were summarized in Table 6.37. There were significant differences in flag leaf traits among different individuals, while the differences were smaller among different environments. The mean percentages of phenotypic variation explained by population structure for FLL, FLW, and FLAR were 25.43, 9.78, and 25.73 %, respectively. And broad-sense heritability for FLL, FLW, and FLAR were 76.3, 80.1, and 72.8 %, respectively.

Table 6.37 Descriptive statistics and percentage of phenotypic variation explained by population structure for flag leaf length, width, and area (FLL, FLW, FLAR)

Trait	Environment	Min	Max	Mean	SD	R^{2a} (%)	H^{2b} (%)
FLL	E1: Tai'an (2007)	14.83	35.23	21.15	4.06	30.9	76.3
	E2: Tai'an (2008)	10.55	40.55	19.31	4.60	25.1	
	E3: Tai'an (2009)	13.38	29.96	18.82	3.13	22.6	
	E4: Tai'an (2010)	11.58	29.33	18.13	2.70	23.1	
FLW	E1: Tai'an (2007)	1.33	2.40	1.72	0.21	10.6	80.1
	E2: Tai'an (2008)	1.00	2.15	1.59	0.21	9.8	
	E3: Tai'an (2009)	1.33	2.24	1.68	0.17	9.5	
	E4: Tai'an (2010)	1.10	1.97	1.52	0.17	8.9	
FLAR	E1: Tai'an (2007)	18.07	69.27	30.61	8.47	31.2	72.8
	E2: Tai'an (2008)	11.94	72.65	25.95	8.65	18.9	
	E3: Tai'an (2009)	17.04	47.44	26.41	5.86	25.6	
	E4: Tai'an (2010)	13.32	46.44	22.97	4.87	27.2	

[a]Percentage of phenotypic variation explained by population structure
[b]Broad-sense heritability; abbreviations are the same as in Table 6.35

6.6.2.2.2 Association Analysis

The associations between DArT markers and FLL, FLW, and FLAR were tested through the mixed linear model. Percentage of phenotypic variation explained by individual-associated marker and significance of association was summarized in Table 6.38. Based on the critical p value less than 0.01, we identified 61 marker-trait associations (MTAs) involving 46 DArT markers distributed on 14 chromosomes (1B, 1D, 2A, 2B, 2D, 3A, 3B, 4A, 5B, 6A, 6B, 6D, 7A, and 7B) for the three traits and the R^2 ranges from 0.1 to 16.4 % (Fig. 6.14).

A total of 13 significant MTAs for FLL were detected on chromosomes 1B, 2B, 3A, 3B, 4A, 5B, 6A, 6B, and 6D, explaining phenotypic variation from 0.1 to 14.49 %. And wPt-3109 (2B) had the highest R^2.

Thirty eight significant MTAs involving 31 markers distributed on chromosomes 1D, 2A, 2B, 2D, 3A, 4A, 5B, 6A, 6B, 7A, and 7B for FLW were identified and the R^2 ranged from 1.03 to 16.4 %. And wPt-9422 had the highest R^2 (3A, 49.3 cM). Meanwhile, several MTAs were repeatedly detected in two environments, for example, wPt-665037 (1D, 11.7 cM), wPt-664989 (1D, 12.1 cM), wPt-665204 (1D, 12.1 cM), wPt-6711 (2A), wPt-1902 (2D), wPt-3130 (6B, 39.6 cM), wPt-9990 (6B, 39.6 cM), which explained phenotypic variation 11.28, 13.21, 12.18, 10.88, 5.45, 8.77, and 7.77 %, respectively.

A total of 10 significant MTAs distributed on chromosomes 2D, 3B, 4A, 5B, 6A, and 7B for FLAR were identified, and R^2 ranged from 1.1 to 13.97 %. Meanwhile, wPt-6043 (3B) had the highest R^2.

It is worth noting that some markers associated with several traits. For example, wPt-3457 (5B, 92.3 cM) simultaneously associated with both FLL and FLW, wPt-5836 (3B, 71.6 cM) and wPt-4270 (6A) associated with both FLL and FLAR, while wPt-730744 (2D, 61.4 cM), wPt-667476 (2D, 62.3 cM), wPt-1902 (2D), wPt-5737 (5B, 69.9 cM), and wPt-5737 (7B, 56.6 cM) associated with both FLW and FLAR.

6.6.3 Research Progress of Leaf Morphology QTL Mapping and Comparison of the Results with Previous Studies

6.6.3.1 Research Progress of Leaf Morphology QTL Mapping

Few researches related to QTL for physiological characteristic of leaf morphology in wheat. Keller et al. (1999) identified eight QTLs for FLW on chromosomes 1A, 1B, 2A, 3B, 5A, 5B, and 6A, explaining up to 59.5 % of phenotypic variation, by using a RIL population consisted of 226 lines derived from Forno/spelt Oberkulmer. Lohwasser et al. (2004) detected 23 QTLs for length and width of the third basal leaf by using a RIL population including 114 lines under greenhouse conditions. Zhang et al. (2012) used a RIL population to identify QTLs for FLL,

Table 6.38 The marker loci associated with flag leaf and corresponding explained phenotypic variation

Chr.	Marker	Position	R^2 (%)		
			FLL	FLW	FLAR
1B	wPt-9605	–	7.2* (E2)		
1D	wPt-665037	11.7		9.85* (E1) 12.7* (E2)	
	wPt-664989	12.1		11.45* (E1) 14.96** (E2)	
	wPt-665204	12.1		10.79* (E1) 13.56** (E2)	
	wPt-3855	–		10.69* (E2)	
2A	wPt-669355	281.9		10.69* (E1)	
	wPt-6711	–		9.16* (E1) 12.59* (E3)	
	wPt-0568	–		9.5* (E1)	
2B	wPt-2106	22.8		13.38** (E2)	
	wPt-3109	–	14.49* (E3)		
2D	wPt-1554	7.6		10.19* (E1)	
	wPt-730744	61.4		11.43* (E1)	7.47* (E4)
	wPt-667476	62.3		9.7* (E1)	10.11* (E4)
	wPt-668120	62.3		9.9* (E1)	
	wPt-731134	62.3		9.9* (E1)	
	wPt-1902	–		9.76* (E1) 1.03* (E4)	6.58* (E4)
	wPt-3692	–		14.1* (E3)	
	wPt-6704	–		10.67* (E1)	
3A	wPt-9422	49.3		16.4* (E3)	
	wPt-0398	146.4	8.71* (E1)		
	tPt-0519	–		9.91* (E2)	
3B	wPt-5836	71.6	6.49* (E1)		11.54* (E1)
	wPt-10186	–			12.17* (E3)
	wPt-2491	–	1.27** (E1)		
	wPt-6043	–			13.97* (E3)
4A	wPt-8091	180.1	9.16* (E2)		
	wPt-2985	–			1.11* (E1)
	wPt-6900	–		14.00* (E3)	
	wPt-6757	–	8.83* (E2)		
5B	wPt-5737	69.9		10.06* (E1)	5.84* (E1)
	wPt-3457	92.3	10.66* (E3)	11.86* (E1)	
	wPt-0819	–		6.75* (E4)	
	wPt-1548	–		10.33* (E1)	

(continued)

Table 6.38 (continued)

Chr.	Marker	Position	R^2 (%)		
			FLL	FLW	FLAR
6A	wPt-666988	39.8	0.9* (E2)		
	wPt-667618	142.4		6.67* (E4)	
	wPt-4270	–	10.19* (E2)		12.63* (E2)
6B	wPt-3130	39.6		8.89* (E1) 8.64* (E2)	
	wPt-9990	39.6		8.89* (E1) 8.64* (E2)	
	wPt-0959	57.7		10.14* (E1)	
	wPt-8183	92.5		9.97* (E1)	
	wPt-2424	96.1		8.56* (E1)	
	wPt-0171	172.1	0.2** (E3)		
	wPt-3581	–	0.1** (E4)		
6D	wPt-664719	134.9	10.18* (E2)		
7A	tPt-1755	–		11.28* (E2)	
7B	wPt-5737	56.6		10.06* (E1)	5.84* (E1)

Marker position "–" indicates that this marker has no definite genetic distance. Markers with significant marker–trait associations are listed ($P < 0.001$), and the phenotypic variation explained (R^2) is marked with single asterisk (*) or double asterisks (**) denotes the p value ranging from 0.0001 to 0.0010 or smaller than 0.0001, respectively. Abbreviations are the same as in Table 6.35

FLW, FLAR, SLL, SLW, SLAR, TLL, TLW, TLAR, and 29 QTLs were detected, and none of 29 QTLs were major QTLs, with the highest effect of 13.87 %. Meanwhile, several QTLs controlling leaf morphology were found on chromosomes 4B and 4D.

6.6.3.2 Comparsion of the Results with the Previous Studies

In this study, a total of 31 additive QTLs for leaf morphology-related traits were identified, mainly distributing on chromosomes 2D, 4D, 5D, and 7D, and six of 31 QTLs were major QTLs with the highest effect of 21.91 %. Meanwhile, the QTLs for leaf morphology were mainly mapped on chromosomes 2D, 4A, 4B, 4D, 5D, and 7D based on association analysis, and within the linked marker intervals of leaf morphology, some QTLs for yield-related traits, quality traits, and important agronomic traits were also mapped. There were similar results between the partial results of this paper and those of Keller et al. (1999) and Zhang et al. (2012), indicating that important QTLs or genes controlling leaf morphology of wheat were distributed on D genome. Moreover, some associations were repeatedly detected in several environments, which could be considered to be relatively stable, and linked molecular makers with higher contribution to phenotypic variation could be used in MAS breeding programs. For example, several markers distributing on

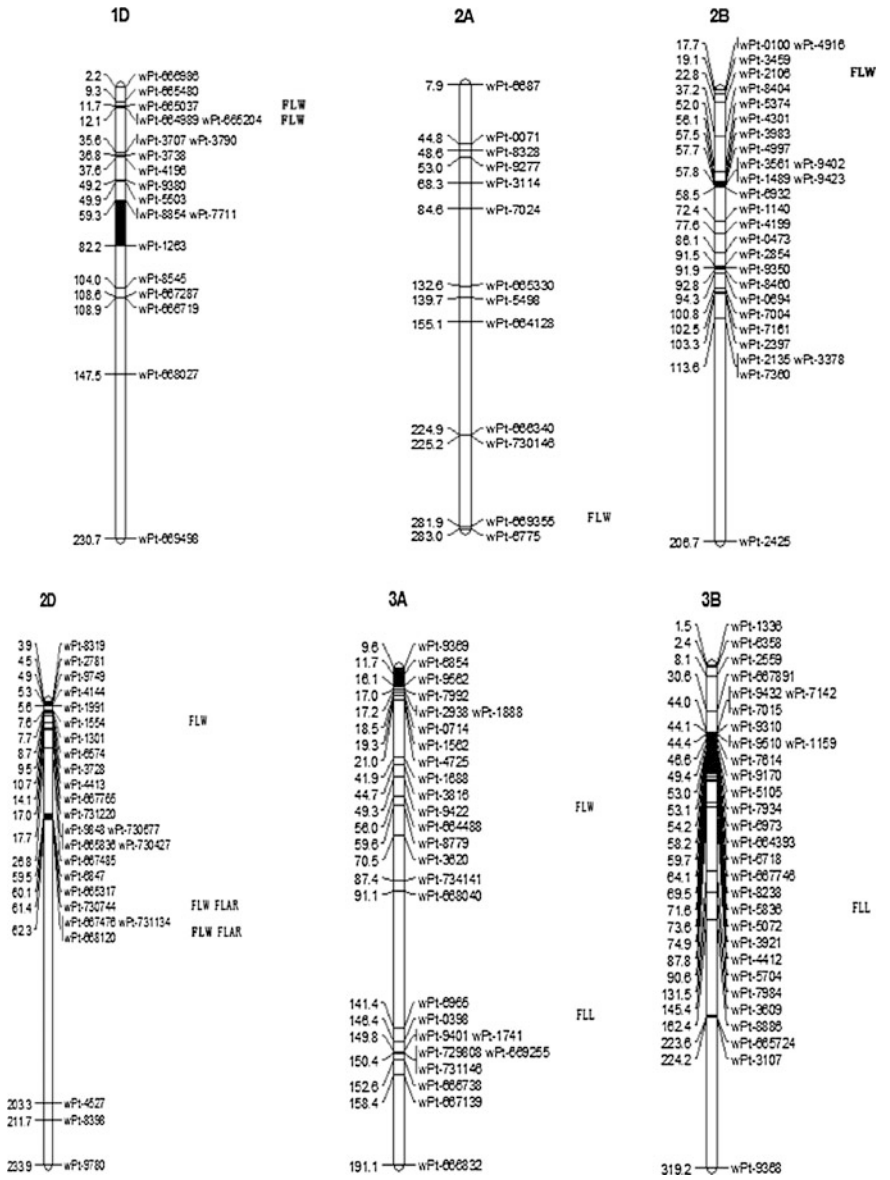

Fig. 6.14 Genetic linkage map for DArT markers significantly associated with flag leaf in bold, markers significantly associated with more than three environments

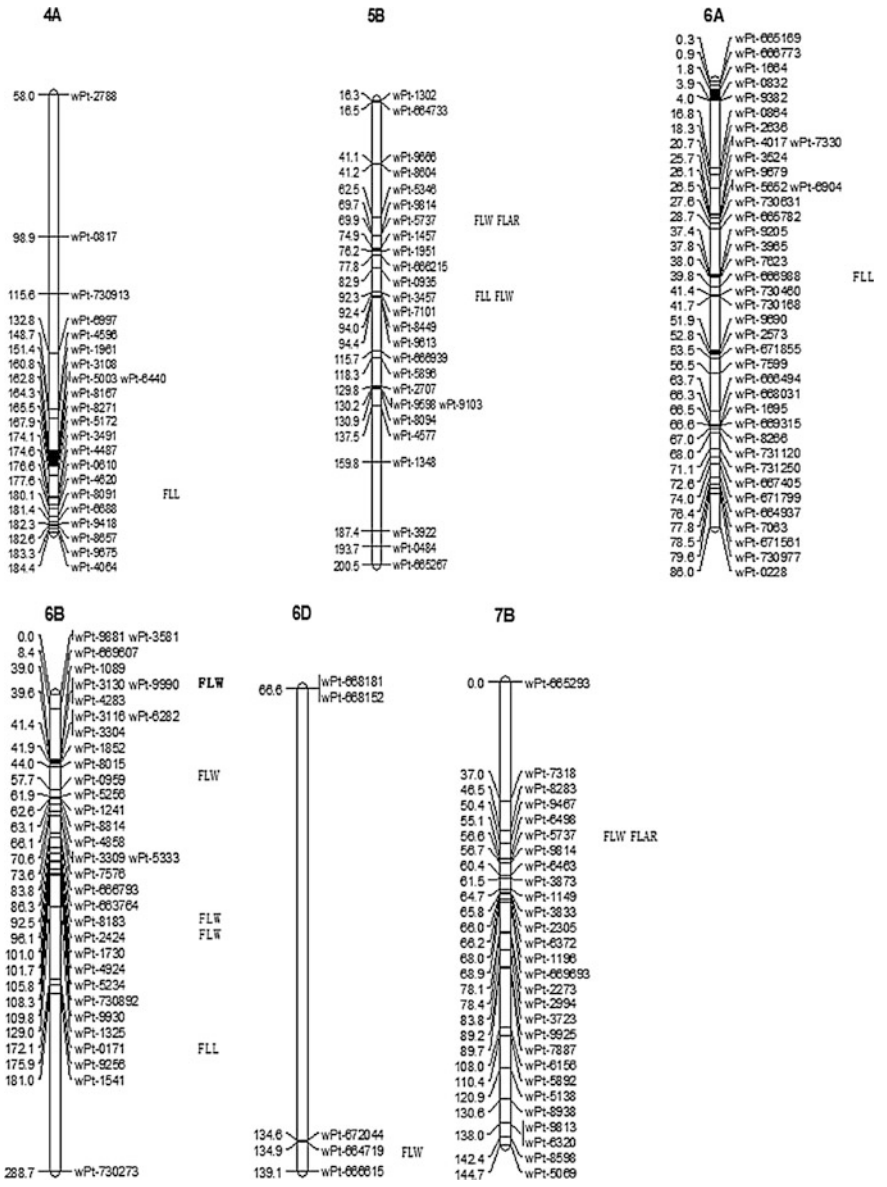

Fig. 6.14 (continued)

chromosomes 1D and 6B were associated with FLW and had the higher contributions to phenotypic variation.

The big ranges of variation of flag leaf in different varieties were in favor of mapping more key intervals linked with flag leaf traits. For example, several markers distributing on chromosomes 1D, 2D, and 6B were associated with some traits, which may be enrichment regions of genes controlling flag leaf traits, and that needs to be studied in further research.

References

Akbari M, Wenzl P, Caig V, Carling J, Xia L, Yang S, Uszynski G, Mohler V, Lehmensiek A, Kuchel H, Hoyden MJ, Howes N, Sharp P, Vaughan P, Rathmell B, Hutter E, Kilian A. Diversity arrays technology (DArT) for high-throughput profiling of the hexaploid wheat genome. Theor Appl Genet. 2006;113:1409–20.

Ali MB, Ibrahim AMH, Malla S, Rudd J, Hays D. Family-based QTL mapping of heat stress tolerance in primitive tetraploid wheat (*Triticum turgidum* L.). Euphytica. 2013;192:189–203.

An D, Su JY, Liu QY, Zhu YG, Tong YP, Li JM, Jing RL, Li B, Li ZS. Mapping QTLs for nitrogen uptake in relation to the early growth of wheat (*Triticum aestivum* L.). Plant Soil. 2006;284:73–84.

Båga M, Chodaparambil SV, Limin AE, Pecar M, Fowler DB, Chibbar RN. Identification of quantitative trait loci and associated candidate genes for low-temperature tolerance in cold-hardy winter wheat. Funct Integr Genomics. 2007;7:53–68.

Bai CH, Liang YL, Hawkesford MJ. Identification of QTLs associated with seedling root traits and their correlation with plant height in wheat. J Exp Bot. 2013;64:1745–53.

Börner A, Schumann E, Fürste A, Cöster H, Leithold B, Röder MS, Weber WE. Mapping of quantitative trait loci determining agronomic important characters in hexaploid wheat (*Triticum aestivum* L.). Theor Appl Genet. 2002;105:921–36.

Brube-Bable AL, Fowler DB. Genetic control of cold hardiness and venalization requirement in winter wheat. Crop Sci. 1988;28:879–84.

Cao WD, Jia JZ, Jin JY. Identification and interaction analysis of QTL for chlorophyll content in wheat seedlings. Plant Nutr Ferti Sci. 2004;10(5):473–8 (in Chinese with English abstract).

Caradus JR. Genetic control of phosphorus uptake and phosphorus status in plants. In: Genetic manipulation of crop plants to enhance integrated nutrient management in cropping system. Patancheru: ICRISAT Asia Centre; 1995. pp. 55–67.

Czyczylo-Mysza I, Tyrka M, Marcińska I, Skrzypek E, Karbarz M, Dziurka M, Hura T, Dziurka K, Quarrie SA. Quantitative trait loci for leaf chlorophyll fluorescence parameters, chlorophyll and carotenoid contents in relation to biomass and yield in bread wheat and their chromosome deletion bin assignments. Mol Breed. 2013;32(1):189–210.

Galiba G, Quarrie SA, Sutka J, Morgounov A, Snape JW. RFLP mapping of the vernalization (Vrn1) and frost resistance (Fr1) genes on chromosome 5A of wheat. Theor Appl Genet. 1995;90:1174–9.

Groos C, Robert N, Bervas E, et al. Genetic analysis of grain protein-content, grain yield and thousand-kernel weight in bread wheat. Theor Appl Genet. 2003;106(6):1032–40.

Guo HJ. QTL analysis for stem strength and its correlated traits in wheat. Master's thesis of Chinese Academy of Agricultural Sciences; 2002 (in Chinese with English abstract).

Guo PG, Baum M, Varshney RK, Graner A, Grando S, Ceccarelli S. QTLs for chlorophyll and chlorophyll fluorescence parameters in barley (*Hordeum vulgare* L.) under post-flowering drought. Euphytica. 2008;163:203–14.

Hai L, Guo HJ, Xiao SH, Jiang GL, Zhang XY, Yan CS, Xin ZY, Jia JZ. Quantitative trait loci (QTL) of stem strength and related traits in a doubled-haploid population of wheat (Triticum aestivum L.). Euphytica. 2005;141:1–9.

Hamada A, Nitta M, Nasuda S, Kato K, Fujita M, Matsunaka H, Okumoto Y. Novel QTLs for growth angle of seminal roots in wheat (*Triticum aestivum* L.). Plant Soil. 2012;354(1–2): 395–405.

Hanocq E, Niarquin M, Heumez E, Rousset M, Le GJ. Detection and mapping of QTL for earliness components in a bread wheat recombinant inbred lines population. Theor Appl Genet. 2004;110:106–15.

Huang XQ, Cöster H, Ganal MW, Röder MS. Advanced backcross QTL analysis for the identification of quantitative trait loci alleles from wild relatives of wheat (*Triticum aestivum* L). Theor Appl Genet. 2003;106:1379–89.

Huang XQ, Cloutier S, Lycar L, Radovanovic N, Humphreys DG, Noll JS, Somers DJ, Brown PD. Molecular detection of QTLs for agronomic and quality traits in a doubled haploid population derived from two Canadian wheats (*Triticum aestivum* L.). Theor Appl Genet. 2006;113:753–66.

Hund A, Frascaroli E, Leipner J, Jompuk C, Stamp P, Fracheboud Y. Cold tolerance of the photosynthetic apparatus: pleiotropic relationship between photosynthetic performance and specific leaf area of maize seedlings. Mol Breed. 2005;16:321–31.

Ibrahim SE, Schubert A, Pillen K, Léon J. QTL analysis of drought tolerance for seedling root morphological traits in an advanced backcross population of spring wheat. International Journal of Agri Science. 2012;2(7):619–29.

Jiang P. QTL mapping for related traits of wheat germination, Master's thesis of Shandong Agricultural University, 2012 (in Chinese with English abstract).

Jing RL, Hu RH, Zhu ZH, Chang XP. A study on heritabilities of seedling morphological traits and drought resistance in winter wheat cultivars of different genotype. Acta Bot Boreal-Occident Sin. 1997;17(2):152–7 (in Chinese with English abstract).

Ju W, Yang CF, Zhang SH, Tian JC, Hai Y, Yang XJ. Mapping QTL for cell membrane permeability of leaf treated by low temperature in Winter Wheat. Acta Agronomica Sinica. 2012;38(7):1247–52 (in Chinese).

Keller M, Karutz C, Schmid JE, Stamp P, Winzeler M, Keller B, Messmer MM. Quantitative trait loci for lodging resistance in a segregating wheat × spelt population. Theor Appl Genet. 1999;98:1171–82.

Landjeva S, Lohwasser U, Börner A. Genetic mapping within the wheat D genome reveals QTL for germination, seed vigour and longevity, and early seedling growth. Euphytica. 2010;171:129–43.

Leipner J, Jompuk C, Camp KH, Stamp P and Fracheboud Y. QTL studies reveal little relevance of chilling-related seedling traits for yield in maize (*Zea mays* L.). Theor. Appl. Genet, 2008, 116: 555–562.

Li ZK, Luo LJ, Mei HW, Shu QY, Tabien R, Zhong DB, Ying CS, Stansel JW, Khush GS, Paterson AH. Overdominance epistatic loci are the primary genetic basis of inbreeding depression and heterosis in rice: I. Biomass and grain yield. Genetics. 2001;158(4):1737–53.

Li SP, Chang XP, Wang CS, Jing RL. Mapping QTL for heat tolerance at grain filling stage in common wheat. Scientia Agricultura Sinica. 2013;46(10):2119–29 (in Chinese with English abstract).

Lillemo M, Asalf B, Singh RP, Huerta-Espino J, Chen XM, He ZH, Biornstad A. The adult plant rust resistance loci Lr34/Yr18 and Lr46/Yr29 are important determinants of partial resistance to powdery mildew in bread wheat line Saar. Theor Appl Genet. 2008;116:1155–66.

Limin AE, Danyluk J, Chauvinl LP, Fowler DB, Sarhan F. Chromosome mapping of low-temperature induced Wcs120 family genes and regulation of cold-tolerance expression in wheat. Mol Gen Genet. 1997;253:720–7.

Liu YY. Cold-resistance-index screening and QTL analysis of wheat. Master's thesis of Henan Agricultural University, 2005 (in Chinese with English abstract).

Liu TJ, Qi CH, Tang JJ. Studies on relationship between the character parameters of root and yield formation in Rice. Scientia Agricultura Sinica. 2002;35(11):1416–9 (in Chinese with English abstract).

Liu XL, Chang XP, Li RZ, Jing RL. Mapping QTLs for seminal root architecture and coleoptile length in wheat. Acta Agronomica Sinica. 2011;37(3):381–8 (in Chinese with English abstract).

Liu XL, Li RZ, Chang XP, Jing RL. Mapping QTLs for seedling root traits in a doubled haploid wheat population under different water regimes. Euphytica. 2013;189:51–66.

Lohwasser U, Röder MS, Börner A. QTL mapping of vegetative characters in wheat (*Triticum aestivum* L.). Genetic variation for plant breeding. Proceedings of the 17th EUCARPIA General Congress, Tulln, Austria, 8–11 September 2004 pp. 195–198.

Mantovani P, Maccaferri M, Sanguineti MC, Tuberosa R, Catizone I, Wenzl P, Thomson B, Carling J, Huttner E, DeAmbrogio E, Kilian A. An integrated DArT-SSR linkage map of durum wheat. Mol Breed. 2008;22:629–48.

Marza F, Bai GH, Carver BF, Zhou WC. Quantitative trait loci for yield and related traits in the wheat population Ning7840 × Clark. Theor Appl Genet. 2006;112(4):688–98.

Mei HW, Li ZK, Shu QY, Guo LB, Wang YP, Yu XQ, Ying CS, Luo LJ. Gene actions of QTL affecting several agronomic traits resolved in a recombinant inbred rice population and two backcross population. Theor Appl Genet. 2005;110:649–59.

Moudal S K, Kour K. Genetic variability and correlation coefficients of some root characteristics and yield components in bread wheat (*Triticum aestivum* L.) under rainfed condition. Environ Ecol, 2004, 22: 646–648.

Nagata K, Shimizu H, Terao T. Quantitative trait loci for nonstructural carbohydrate accumulation in leaf and culms of rice (*Oryza sativa* L.) and their effects on grain filling. Breeding Sci, 2002, 52: 275–283.

Partha DAS, Ali MN, Sarkar HK. Genetical studies on roots in bread wheat. J Interacademicia. 2004;8:166–8.

Paux E, Sourdille P, Salse J, Saintenac C, Choulet F, Leroy P, Korol A, Michalak M, Kianian S, Spielmeyer W, Lagudan E, Somers D, Kilian A, Alaux M, Vautrin S, Berges H, Eversole K, Appels R, Safar J, Simkova H, Dolezel J, Bernard M, Feuillet C. A physical map of the 1-Gigabase bread wheat chromosome 3B. Science. 2008;322:101–4.

Pelleschi S, Leonardi A, Rocher JP, Cornic G, Vienne D de, Thévenot C, Prioul JL. Analysis of the relationships between growth, photosynthesis and carbohydrate metabolism using quantitative trait loci (QTLs) in young maize (*Zea mays* L.) plants subjected to water deprivation. Mol Breeding, 2006, 17: 21–39.

Porra RJ, Thompson WA, Kriedemann PE. Determination of accurate extinction coefficients and simultaneous equations for assaying chlorophylls a and b extracted with four different solvents: verification of the concentration of chlorophyll standards by atomic absorption spectroscopy. Biochimica et Biophysica Acta (BBA)-Bioenergetics, 1989, 975 (3): 384–394.

Pritchard JK, Stephens M, Donnelly P. Inference of population structure from multilocus genotype data. Genetics. 2000;155:945–59.

Quarrie SA, Steed A, Calestani C, Semikhodskii A, Lebreton C, Chinoy C, Steele N and Pljevljakusić D. A high-density genetic map of hexaploid wheat (*Triticum aestivum* L.) from the cross Chinese Spring 9 SQ1 and its use to compare QTLs for grain yield across a range of environments. Theor Appl Genet, 2005, 110: 865–880.

Ren YZ, He X, Liu DC, Li JJ, Zhao XQ, Li B, Tong YP, Zhang AM, Li ZS. Major quantitative trait loci for seminal root morphology of wheat seedlings. Mol Breeding. 2012a;30:139–48.

Ren YZ, Xu YH, Gui XW, Wang SP, Ding JP, Zhang QC, Ma YS, Pei DL. QTLs analysis of Wheat seedling traits under salt stress. Scientia Agricultura Sinica. 2012b;45(14):2793–800 (in Chinese with English abstract).

Ritter KB, Jordan DR, Chapman SC, Godwin ID, Mace ES, Lynne MC. Identification of QTL for sugar-related traits in a sweet × grain sorghum (*Sorghum bicolor* L. Moench) recombinant inbred population. Mol Breed, 2008, 22: 367–384.

Semagn K, Bjornstad H, Skinnes AG, Marφy Y. Tarkegne, William M. Distribution of DArT, AFLP and SSR markers in a genetic linkage map of a double haploid hexaploid wheat population. Genome. 2006;49:545–55.

Sharma S, Xu SZ, Ehdaie B, Hoops A, Close TJ, Lukaszewski AJ, Waines JG. Dissection of QTL effects for root traits using a chromosome arm-specific mapping population in bread wheat. Theor Appl Genet. 2011;122(4):759–69.

Song YX, Jing RL, Huo NX, Ren ZL and Jia JZ. Detection of QTLs for heading in common wheat (*T. aestivum* L.) using different populations. Scientia Agricultura Sinica, 2006, 39(11): 2186–2193 (in Chinese with English abstract).

Song YX. QTLs analysis of heading date and other agronomic traits in wheat. Doctoral thesis of Sichuan Agricultural University, 2005 (in Chinese with English abstract).

Su JY, Tong YP, Liu QY, Li B, Jing RL, Li JY, Li ZS. Mapping quantitative trait loci for post-anthesis dry matter accumulation in wheat (*Triticum aestivum* L.). J Integr Plant Biol. 2006;48:938–44.

Sutka J. Genes for frost resistance in wheat. Euphytica. 2001;119(1–2):169–77.

Tóth B, Galiba G, Fehér E, Sutka J, Snape JW. Mapping genes affecting flowering time and frost resistance on chromosome 5B of wheat. Theor Appl Genet. 2003;107:509–14.

Vágújfalvi A, Galiba G, Cattivelli L, Dubcovsky J. The cold-regulated transcriptional activator Cbf3 is linked to the frost-tolerance locus Fr-A2 on wheat chromosome 5A. Mol Gen Genomics. 2003;269:60–7.

Vijayalakshmi K, Fritz AK, Paulsen GM, Bai GH, Pandravada S, Gill BS. Modeling and mapping QTL for senescence-related traits in winter wheat under high temperature. Mol Breeding. 2010;26(2):163–75.

Voorrips RE. MapChart: software for the graphical presentation of linkage maps and QTLs. J Hered. 2002;93:77–8.

Waldman M, Rikin A, Dovrat A, Richmond AE. Horironal regulation of morphogenesis and cold resistance. J Exp Bot. 1975;26:853–9.

Wei XY, Li SS, Jiang FS, Guo Y, Li RJ. QTL mapping for premature senescence and related physiological traits in Wheat. Acta Bot Boreal-Occident Sin. 2007;27(3):485–9 (in Chinese with English abstract).

Wenzl P, Carling J, Kudrna D, Jaccoud D, Huttner E, Kleinhofs A, Kilian A. Diversity arrays technology (DArT) for whole genome profiling of barley. Proc Natl Acad Sci USA. 2004;101:9915–20.

Wu YQ, Liu LX, Guo HJ, Zhao LZ, Zhao SR. Mapping QTL for salt tolerant traits in wheat. J Nuclear Agri Sci. 2007;21(6):545–9 (in Chinese with English abstract).

Xing YZ, Tan YF, Hua JP, Sun XL, Xu CG, Zhang QF. Characterization of the main effects, epistatic effects and their environmental interactions of QTLs on the genetic basis of yield traits in rice. Theor Appl Genet. 2002;105:248–57.

Xu SB. Construction of genetic map by SSR marker and location QTL for plant height and heading time in wheat. Master's thesis of Xinjiang Agricultural University; 2005 (in Chinese with English abstract).

Xu YF, An DG, Liu DC, Zhang AM, Xu HX, Li B. Mapping QTLs with epistatic effects and QTL×treatment interactions for salt tolerance at seedling stage of wheat. Euphytica. 2012;186:233–45.

Xue DW, Chen MC, Zhou MX, Chen S, Mao Y, Zhang GP. QTL analysis of flag leaf in barley (Hordeum vulgare L.) for morphological traits and chlorophyll content. J Zhejiang Univ Sci B. 2008;9(12):938–43.

Yan L, Helguera M, Kato K, Fukuyama S, Sherman J, Dubcovsky J. Allelic variation at the VRN-1 promoter region in polyploid wheat. Theor Appl Genet. 2004;109(8):1677–86.

Yang CF. Mapping QTL for salt tolerant traits in wheat seedling stage under different salt stress. Master's thesis of Agricultural University of Hebei; 2012 (in Chinese with English abstract).

Yang DL, Jing RL, Chang XP, Li W. Quantitative trait loci mapping for chlorophyll fluorescence and associated traits in wheat (*Triticum aestivum* L.). J Integ Plant Biol. 2007a;49:646–54.

Yang DL, Jing RL, Chang XP, Li W. Identification of quantitative trait loci and environmental interactions for accumulation and remobilization of water-soluble carbohydrates in Wheat (*Triticum aestivum* L.) Stems. Genetics. 2007b;176:571–84.

Yao Q, Zhou RH, Pan YM, Fu TH, Jia JZ. Construction of genetic linkage map and QTL analysis of agronomic important traits based on a RIL population derived from common wheat variety Yanzhan 1 and Zaosui 30. Sci Agricultura Sinica. 2010;43(20):4130–9 (in Chinese with English abstract).

Zhang KP. Construction of wheat (*Triticum aestivum* L.) molecular genetic map and QTL analysis. Doctoral thesis of Shandong Agricultural University; 2008 (in Chinese with English abstract).

Zhang Q. Genetic map construction and QTL mapping of important agronomic traits in common wheat. Master's thesis of Shandong Agricultural University; 2012 (in Chinese with English abstract).

Zhang ZB, Xu P. Reviewed on wheat genome. Hereditas. 2002;24(3):389–94 (in Chinese with English abstract).

Zhang KP, Xu XB, Tian JC. QTL mapping for grain yield and spike related traits in common wheat. Acta Agronomica Sinica. 2009;35(2):270–8 (in Chinese with English abstract).

Zhou XG, Jing RL, Hao ZF, Chang XP, Zhang ZB. Mapping QTL for seedling root traits in common wheat. Sci Agricultura Sinica. 2005;38(10):1951–7 (in Chinese with English abstract).